T2R2 東京科学大学 リサーチリポジトリ
Science Tokyo Research Repository

論文 / 著書情報
Article / Book Information

題目(和文)	協調認知を実現するためのSDNに基づくV2Xプラットフォームに関する研究
Title(English)	SDN-Based V2X Platform for Cooperative Perception
著者(和文)	李宗典
Author(English)	Zongdian Li
出典(和文)	学位:博士(学術), 学位授与機関:東京工業大学, 報告番号:甲第12588号, 授与年月日:2023年9月22日, 学位の種別:課程博士, 審査員:阪口 啓,廣川 二郎,岡田 健一,TRAN GIA KHANH,西尾 理志,原井 洋明
Citation(English)	Degree:Doctor (Academic), Conferring organization: Tokyo Institute of Technology, Report number:甲第12588号, Conferred date:2023/9/22, Degree Type:Course doctor, Examiner:,,,,,
学位種別(和文)	博士論文
Type(English)	Doctoral Thesis

Powered by T2R2 (Science Tokyo Research Repository)

Doctoral Dissertation

SDN-Based V2X Platform for Cooperative Perception

Supervisor Professor Kei Sakaguchi

Department of Electrical and Electronic Engineering
Graduate School of Engineering
Tokyo Institute of Technology

Zongdian Li

Contents

List of Figures

List of Tables

Acknowledgments

Since I came to Japan in 2018, five years have passed in the blink of an eye. Countless joys, passions, tears, and sweat have become indistinct in my memory. At the moment I stop writing, all that remains in my heart is gratitude and a profound sense of appreciation. I never imagined that I would become a doctoral candidate in engineering and the first doctorate in my family. My parents surely feel proud. To accomplish all of this, the person I am most grateful to is my supervisor, Prof. Sakaguchi. Without his selflessness, patience, and professional guidance, I would not have been able to successfully complete my doctoral research. His dedication to work and unwavering passion for academia inspired and influenced every aspiring young researcher, including myself. Prof. Sakaguchi provided me with all the necessary resources for my growth in research, including opportunities for exchange at RWTH Aachen University and collaborative research with top-tier companies like Denso. I have greatly benefited from these experiences.

I also extend my sincere gratitude to Prof. Hirogawa, Prof. Okada, Associate Prof. Tran, Associate Prof. Nishio, and Dr. Harai as the committee members of my defense. Throughout the entire defense, they provided numerous professional and invaluable insights, helping me refine the thesis and prompting profound reflection on the shortcomings that still linger within my works. I have gained clarity on the direction I need to dedicate myself in my future career. I am deeply grateful for the time and efforts they have devoted to me.

Furthermore, I appreciate Specially Associated Prof. Tao Yu for his commitment to fast and clear feedback on research problems I encounter. He treats every student as a kind brother and provides us with countless support in campus life. I am also grateful to Emeritus Prof. Araki for his valuable comments during my seminar presentations. I thank Ms. Minami and Ms. Funabashi for creating a comfortable lab environment for our easy study and research. I still remember the warm support from Associate Prof. Maruta during his stay at Sakaguchi Lab. His contribution to the SSS and smart mobility field paves the way for our good research

and publications. I'd like to express my sincere gratitude to him.

Lastly, I appreciate my parents, who give continuous support and understanding during my study abroad. They taught me the wisdom of living and fostered me to be a qualified adult. I thank the lab family, too. My outstanding seniors, Mr. Fukatsu, Ms. Yin, Project Assistant Prof. Nakazato, etc., taught me knowledge and research skills selflessly and showed me the way to become a good researcher. My talented juniors always assisted my experiments and created a relaxing atmosphere in the lab. I wish them a bright and enjoyable future.

Abstract

Automated driving represents one of the most attractive innovations in this century. Yet, we haven't seen the roll-out of fully safe and automated vehicles. Vehicles on markets claiming to have automated driving capabilities are inevitably entangled in various road accidents due to the limited or impaired visibility of local sensors. Cooperative perception has the potential to address such safety concerns by allowing automated vehicles to share perspectives obtained from local sensors through vehicle-to-everything (V2X) communication and gather perceived data from mounted sensors on roadside units (RSU). However, traditional V2X networks have difficulty meeting strict communication requirements posed by this safety-critical application.

In this dissertation, a novel V2X network architecture is proposed to support cooperative perception. The emerging network technology, software defined networking (SDN), is introduced and integrated with millimeter wave (mmWave) to establish a centralized mmWave V2X network with ultra-high data rate and ultra-low latency performances. Three key SDN functions are developed to arrange multi-hop V2X for cooperative perception. Proof-of-concept experiments have demonstrated the effectiveness of the proposed V2X network.

Next, in order to enhance the scalability of the previous network architecture, Het-SDVN, an evolved network that consists of hierarchical control planes, geographically distributed but logically centralized sub-SDVNs, and heterogeneous V2X, is introduced. The design of local SDVN controllers in RSUs, the division and collaboration between local and global SDVN controllers, and the utilization of heterogeneous V2X, are elaborated. The proposed Het-SDVN has been set up in Ookayama Capmus, Tokyo Institute of Technology. Based on this platform, a proof of concept that demonstrate the effectiveness of Het-SDVN in supporting CP has been carried out. The evaluation results are comprehensively discussed.

Finally, this dissertation presents the design, implementation, and field test of mobility-aware high-definition (HD) map distribution, which can be regarded as an extension of cooperative perception, based on the proposed centralized V2X network architecture.

Chapter 1

Introduction

1.1 Background

1.1.1 Position of V2X in ITS and automated driving

Intelligent transportation system (ITS) represents the grand vision of human society towards a road revolution. Cutting-edge technologies are exploited to modernize transportation systems in order to make commuting safer, more efficient, and more enjoyable. In this process, vehicle-to-everything (V2X) communication plays a fundamental role. According to the International Organization for Standardization (ISO) Technical Committees (TC)-204 [8], current efforts in developing ITS focus on enriching road functionalities and raising vehicle automation levels. V2X communication can contribute to road functionalities by delivering three-category V2X applications: (1) road safety; (2) traffic efficiency; (3) telematics and infotainment. The road safety applications include the electronic emergency brake light (EEBL), forward collision warning (FCW), blind spot warning/lane change warning (BSW/LCW), etc [9]. With pre-warning messages from these applications, human drivers can fine-tune their driving decisions to prevent potential accidents. The green light optimal speed advisory (GLOSA) and emergency vehicle warning (EVW) are two examples of traffic efficiency applications [10]. With real-time information about traffic status (volume, signal phase, construction, etc.), these applications can suggest human drivers with high-level route planning and fine-grained maneuvering, lowing down the probability of encountering traffic congestion and reducing harmful gas emission. Telematics and infotainment applications can bring considerable economic values. Their roll-out speed is therefore leading compared to other V2X applications.

For example, the vehicle near-field payment (VNFP) has been extensively used for electronic toll collection (ETC) in super markets, parking lots, petrol stations, etc., and the in-vehicle infotainment (IVI) system has become an integral part of commercialized vehicles to provide localization and navigation services, radio/video broadcasting, online games, etc.

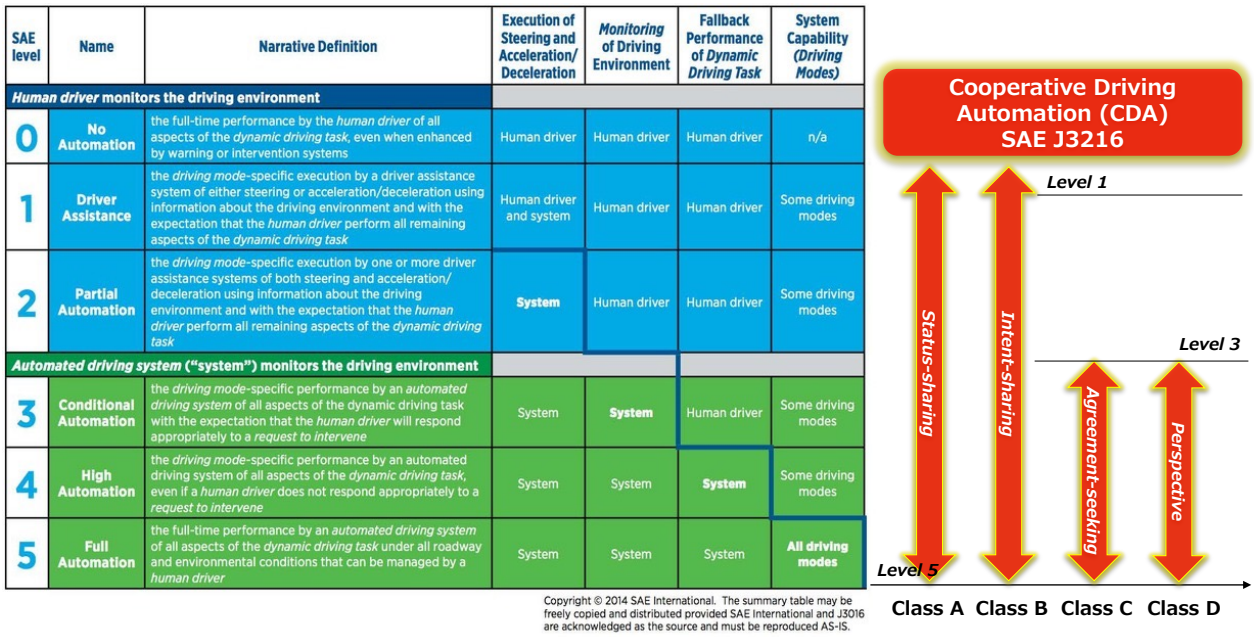

SAE level	Name	Narrative Definition	Execution of Steering and Acceleration/ Deceleration	*Monitoring* of Driving Environment	Fallback Performance of *Dynamic Driving Task*	System Capability *(Driving Modes)*
***Human driver* monitors the driving environment**						
0	No Automation	the full-time performance by the *human driver* of all aspects of the *dynamic driving task*, even when enhanced by warning or intervention systems	Human driver	Human driver	Human driver	n/a
1	Driver Assistance	the *driving mode*-specific execution by a driver assistance system of either steering or acceleration/deceleration using information about the driving environment and with the expectation that the *human driver* perform all remaining aspects of the *dynamic driving task*	Human driver and system	Human driver	Human driver	Some driving modes
2	Partial Automation	the *driving mode*-specific execution by one or more driver assistance systems of both steering and acceleration/ deceleration using information about the driving environment and with the expectation that the *human driver* perform all remaining aspects of the *dynamic driving task*	**System**	Human driver	Human driver	Some driving modes
***Automated driving system* ("system") monitors the driving environment**						
3	Conditional Automation	the *driving mode*-specific performance by an *automated driving system* of all aspects of the dynamic driving task with the expectation that the *human driver* will respond appropriately to a *request to intervene*	System	**System**	Human driver	Some driving modes
4	High Automation	the *driving mode*-specific performance by an automated driving system of all aspects of the *dynamic driving task*, even if a *human driver* does not respond appropriately to a *request to intervene*	System	System	**System**	Some driving modes
5	Full Automation	the full-time performance by an *automated driving system* of all aspects of the *dynamic driving task* under all roadway and environmental conditions that can be managed by a *human driver*	System	System	System	**All driving modes**

Copyright © 2014 SAE International. The summary table may be freely copied and distributed provided SAE International and J3016 are acknowledged as the source and must be reproduced AS-IS.

Figure 1.1: Taxonomy of driving automation and CDA [1] [2].

In recent years, automated driving technology has experienced a significant leap in development, driving the prosperity of the automotive industry. The original equipment manufacturers (OEMs), such as Tesla, Toyota, Honda, etc., roll out their new products with Level 3 automation in succession. The levels of automation are referred to the Society of Automotive Engineers (SAE) J3016 definitions [1], as shown in Fig. 1.1. From Level 3, automated systems dominate driving behaviors while requiring minimum intervention from human drivers in an emergency. So far, this level of automation has represented the highest level achievable solely through artificial intelligence (AI) equipped by a single vehicle. To realize fully automated driving (Level 4 - 5 automation), vehicles must overcome the well-known constraints of local sensors by their range, field of view (FOV), and vulnerability to occlusions, bad weather, and lighting conditions to meet high safety and reliability expectations. In this sense, V2X communication will be a key enabler for fully automated driving as it allows vehicles to exchange sensor information and be aware of road status, over multiple air interfaces, including vehicle-to-vehicle (V2V), vehicle-to-infrastructure (V2I), vehicle-to-pedestrian (V2P), and

vehicle-to-network (V2N) communications, when vehicles suffer catastrophic sensor degradation. With V2X capabilities, SAE J3216 has extended its definitions of automation levels into another dimension, called cooperative driving automation (CDA) [2], in which four classes of CDA are defined depending on cooperation degrees and types of exchanged information:

- Class A (status-sharing): Perception information about the traffic environment and information about the sensor (i.e., "Here I am, and here is what I see.")
- Class B (intent-sharing): Information about planned future actions of the sender (i.e., "This is what I plan to do.")
- Class C (agreement-seeking): A sequence of collaborative messages among specific vehicles intended to influence local planning of specific driving actions (i.e., "Let's do this together.")
- Class D (prescriptive): The direction of specific action(s) to specific traffic participants, provided by a prescribing entity (e.g., emergency vehicles) and adhered to by a receiving entity (i.e., "I will do as directed.")

Figure 1.1. draws the contribution scope of Class A - D to driving automation.

1.1.2 Advanced V2X applications

Together with earlier mentioned V2X applications, the European Telecommunications Standards Institute (ETSI) Technical Report (TR) 102 638 [11] and the Third Generation Partnership Project (3GPP) TR 22.885 [12] have introduced a richer set of V2X applications, including cooperative adaptive cruise control, curve speed warning, control loss warning, etc. These applications based on the first-generation V2X technologies are designed to assist human drivers, targeting Level 1 - 2 vehicle automation. With the rapid development of automated driving technologies and the commercialization of Level 3 automotive products, a novel set of V2X applications will be generated to serve both human and AI drivers. AI drivers feature stronger processing capabilities than human drivers, which in other words, require more detailed information for analysis or larger amounts of sensing data as input. This fact raises an increasing quality of service (QoS) requirement for those advanced (novel) V2X applications, which can overwhelm the capabilities of the first-generation V2X technologies.

3GPP TR 22.886 describes some advanced V2X applications and summarizes them into four groups: vehicle platooning, advanced driving, extended sensors, and remote driving [7].

- Vehicle platooning: This allows vehicles to dynamically form a group, traveling in close proximity. All the vehicles in the platoon receive periodic data from the leading vehicle to keep a meter-level distance between them. The platooning enhances traffic efficiency while reducing wind resistance and energy consumption.

- Advanced driving: This enables semi-automated or fully-automated driving. Each vehicle and/or RSU shares data obtained from its local sensors with vehicles in proximity, thus allowing vehicles to coordinate their trajectories or maneuvers. This results in safe traveling, collision avoidance, and enhanced traffic efficiency.

- Extended sensors: This allows the exchange of raw or processed data gathered through local sensors or live video data between vehicles, RSUs, pedestrian devices, and V2X application servers. The vehicles can enhance the perception of their environment beyond the local sensor range and gain a more comprehensive view of the local situation.

- Remote driving: This enables a remote driver or a V2X application to operate a remote vehicle, catering to those passengers who cannot drive themselves or a remote vehicle located in dangerous environments.

Table 1.1: QoS requirements for advanced V2X application groups [7].

Group name	Latency (ms)	Reliability (%)	Data rate (Mbps)	Communication Range (m)
Vehicle platooning	10 - 25	90 - 99.99	50 - 65	80 - 350
Advanced driving	3 - 100	99.99 - 99.999	10 - 53	360 - 700
Extended sensors	3 - 100	90 - 99.999	10 - 1000	50 - 1000
Remote driving	20	99.999	UL: 25 DL: 1	Ubiquitous

Due to the feature enhancements, the utilization of V2X messages with a higher payload, such as the maneuver coordination message (MCM) [13] and collective perception message (CPM) [14], and even the need for raw data transmission in extended sensors, a demanding V2X requirement is observed from Table 1.1, which includes a maximum data rate of 1000 Mbps, a minimum end-to-end latency of 3 ms, and a reliability of 99.999%. This requirement

far surpasses that of enabling basic V2X applications with the small cooperative awareness message (CAM) [15] or decentralized environmental notification message (DENM) [16].

Note that the definition of extended sensors in 3GPP aligns with the collective perception concept in ETSI. In this thesis, they will be collectively referred to as cooperative perception.

1.1.3 Overview of standardized V2X technologies

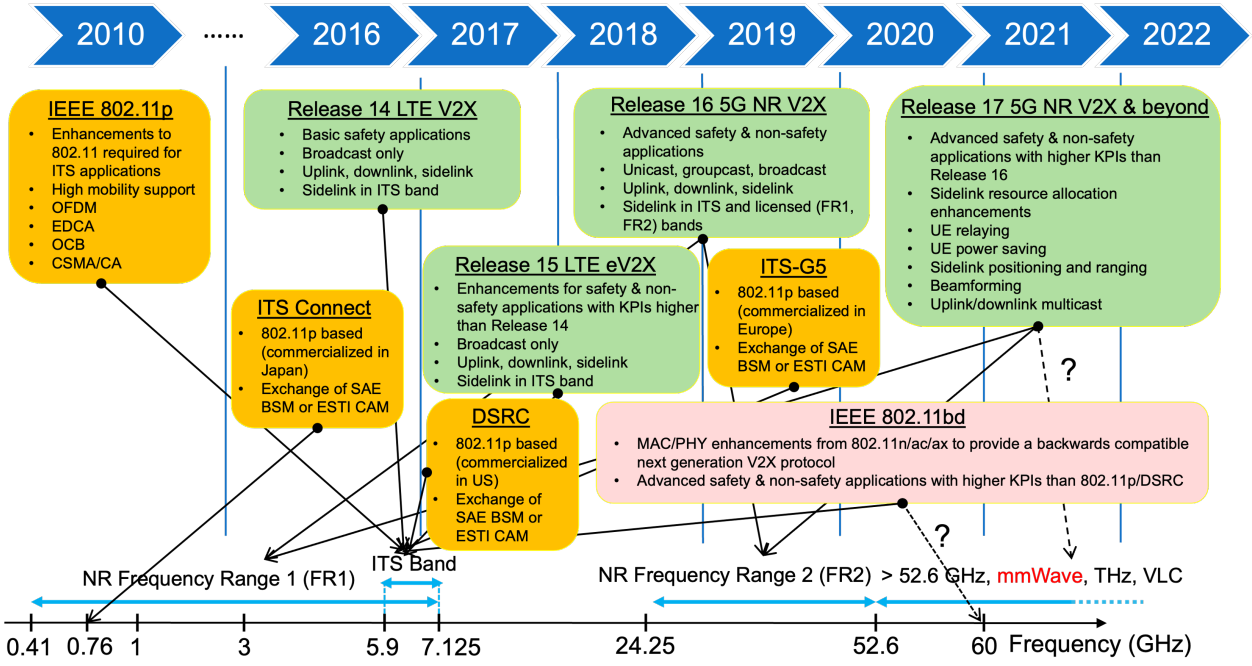

Figure 1.2: Standardization progress of IEEE and 3GPP on V2X.

The Institute of Electrical and Electronics Engineers (IEEE) and 3GPP are two main forces of V2X standardization. They have different road maps. Figure 1.2 draws the timeline of the standardization activities of IEEE and 3GPP for V2X. IEEE 802.11p and long-term evolution (LTE)-V2X are the first-generation V2X technologies, which were specified in 2010 and 2016, respectively. IEEE 802.11p enhances the PHY and MAC layers for Wireless Access in Vehicular Environments (WAVE) based on IEEE 802.11 series standards. At the physical layer, IEEE 802.11p operates in the 5.9 GHz band with a 10 MHz channel width. Orthogonal frequency division multiplexing (OFDM) with convolutional coding is employed. At the MAC layer, IEEE 802.11p simplifies the communication procedure to enable low latency by defining a new rule called "outside of the context of BSS (OCB)". To support prioritization and QoS

differentiation, enhanced distributed channel access (EDCA) is adopted. IEEE 802.11p is the basis of dedicated short-range communications (DSRC) in US, ITS-G5 in Europe, and ITS Connect in Japan. Their commercial deployment started in 2017, 2019, and 2015, respectively. IEEE is now standardizing the next-generation V2X (NGV) technology, i.e., IEEE 802.11bd, as a successor of IEEE 802.11p. It will leverage the newest Wi-Fi technologies and a mmWave band from 57 GHz to 71 GHz, thus providing higher QoS support than IEEE 802.11p.

3GPP announced the LTE-V2X in Release 14. Besides the legacy cellular interface Uu, a sidelink interface called PC5 was specified to support direct communications. LTE PC5 works in the 5.9 GHz band and supports two resource configuration modes inside/outside the eNodeB coverage. Release 15 mainly discussed the PC5 enhancements of LTE-V2X (64QAM, carrier aggregation, MIMO, etc.). Shortly after the commercialization of 5G new radio (NR), 3GPP standardized the first version of NR-V2X in Release 16 in Jun. 2020. Although the 5G NR utilizes two frequency bands (FR1: 410 MHz - 7.125 GHz; FR2: 24.25 GHz - 52.6 GHz), the main focus of NR-V2X in Release 16 and 17 is FR1. NR-V2X made extensive modifications to the channel structures, introduced advanced coding technologies (Polar/LDPC), supported adaptive operations on sidelinks (HARQ), etc. It also enabled the cross-radio access technology (RAT) scheduling mechanism (LTE sidelink controlled by NR Uu; NR sidelink controlled LTE Uu). Release 17 mainly studied the support to vulnerable road user (VRU) scenarios, the energy-saving mechanisms as well as the enhancements to resource allocation. Release 17 has been frozen in Jun. 2022, but future releases will continue to investigate the utilization of mmWave bands up to 100 GHz on top of the dedicated 5.9 GHz ITS band, as well as sidelink communication capability enabled in these frequency bands as well [17].

From the standardization overview, it can be noticed that most standardized V2X choose the sub-6 GHz band, but there is a clear trend that higher frequency bands will be utilized for V2X. Before the deployment, plenty of technical obstacles need to be overcome, such as the adverse propagation characteristics, limited coverage, and unpredictable reliability.

1.2 Research objectives and related works

This thesis presents the author's efforts to enable cooperative perception, one of the most challenging (advanced) V2X applications described in Sect. 1.1.2, by introducing novel RATs and network designs to enhance the performance of existing vehicular networks. The motivation for studying cooperative perception can be concluded into three points:

1. Cooperative perception is a safety-critical V2X application containing great economic and social values. It assists both human and AI drivers and contributes to all levels of driving automation (Class A of CDA). If this application can be installed on all commercialized vehicles and effectively supported by the vehicular network, road fatalities will become zero and fully automated driving will come true.

2. Many beyond 5G and 6G applications rely on the data from cooperative perception. For example, digital twin is a promising application that gathers sensor data from its physical systems to build a high-fidelity cyber world. To build a mobility digital twin, cooperative perception is necessary. In [18], the see-through application for drivers with augmented reality (AR) glasses utilizes RSU sensor data from cooperative perception.

3. As shown in Table 1.1, cooperative perception requires the most stringent QoS (1000 Mbps, 3 ms, 99.999%). If the vehicular network has the capability to support cooperative perception, other V2X applications will definitely be enabled.

However, existing V2X technologies and vehicular networks have considerable limitations. Cooperative perception cannot be naturally supported, thus requiring new designs.

1.2.1 Limitations of existing V2X technologies

Table 1.2: Performances of existing V2X technologies.

Features	IEEE 802.11p			Cellular V2X	
	DSRC in US	ITS-G5 in Europe	ITS Connect in Japan	LTE-V2X (Sidelink)	NR-V2X (Sidelink)
Frequency band	5.9 GHz	5.9 GHz	760 MHz	5.9 GHz	2.5 GHz, 5.9 GHz
Bandwidth	10 MHz	10 MHz	9 MHz	10, 20 MHz	10, 20, 30, 40 MHz
Supported data rate	3 - 27 Mbps	3 - 27 Mbps	$\leq$ 18 Mbps	R14: $\leq$ 31.7 Mbps R15: $\leq$ 73.5 Mbps	$\leq$ 400 Mbps
Range	1000 m	1000 m	200 m	R14: 320 m R15: 500 m	1000 m

As stated in Sect. 1.1.3, the standardized and commercialized V2X technologies today mainly operate in the sub-6 GHz band. Table 1.2 summarizes their performances. It can be observed that the first-generation V2X adopts a small bandwidth between 9 - 20 MHz. The IEEE 802.11p-based ITS Connect working in the 760 MHz band can only support a data rate of less than 18 Mbps. In the 5.9 GHz ITS band, IEEE 802.11p-based DSRC and ITS-G5 with 10 MHz bandwidth have the same supported data rate but limited to 27 Mbps. With a larger bandwidth of 20 MHz, the LTE-V2X achieves a higher data rate of 31.7 Mbps in Release 14 and 73.5 Mbps in Release 15. However, LTE-V2X can only enable advanced V2X applications at low automated driving levels. Even the NR-V2X has introduced a 40 MHz bandwidth and a higher-order modulation scheme (256QAM) for the sidelink, at the condition of a sing carrier, the peak data rate cannot exceed 400 Mbps. This performance is sufficient for most advanced V2X applications at high automated driving levels except cooperative perception.

The reason that the mmWave band (FR2) of NR-V2X is not mentioned here, is because this frequency band has not been specified for the sidelink. Currently, the FR2 is used by NR Uu. With the abundant spectrum resource, NR Uu has the potential to meet the data rate requirement of cooperative perception (1 Gbps), but is unlikely to satisfy the latency requirement (3 ms), since the data has to go through the core network of NR. The feasibility of exploiting mmWave for direct communications needs to be further evaluated.

1.2.2 Limitations of current vehicular networks

There are two types of vehicular networks. One is the vehicular ad-hoc network (VANET), the other is the cellular V2X network, as shown in Fig. 1.3 (a) and (b), respectively. The VANET is a fully distributed and self-roganized network. When the RAT is IEEE 802.11p, vehicles can easily and reliably form a network via broadcasting. In order to support cooperative perception in the VANET, mmWave has to be introduced. Constrained by the severe path loss and weak penetration capability of mmWave, multi-hop routing will become a dominant way to form the network. This poses great challenges to the VANET as the routing protocols such as GeoNetworking create topology information also via broadcasting [19]. Because of using directional antennas, mmWave is much more sensitive to the topology change than IEEE 802.11p. The time for topology generation in the VANET cannot be ignored by mmWave, otherwise an unexpected packet loss will occur.

In contrast, the C-V2X introduces centralized nodes (i.e., base stations) to manage the network. Topology information collection and resource allocation can be done efficiently through

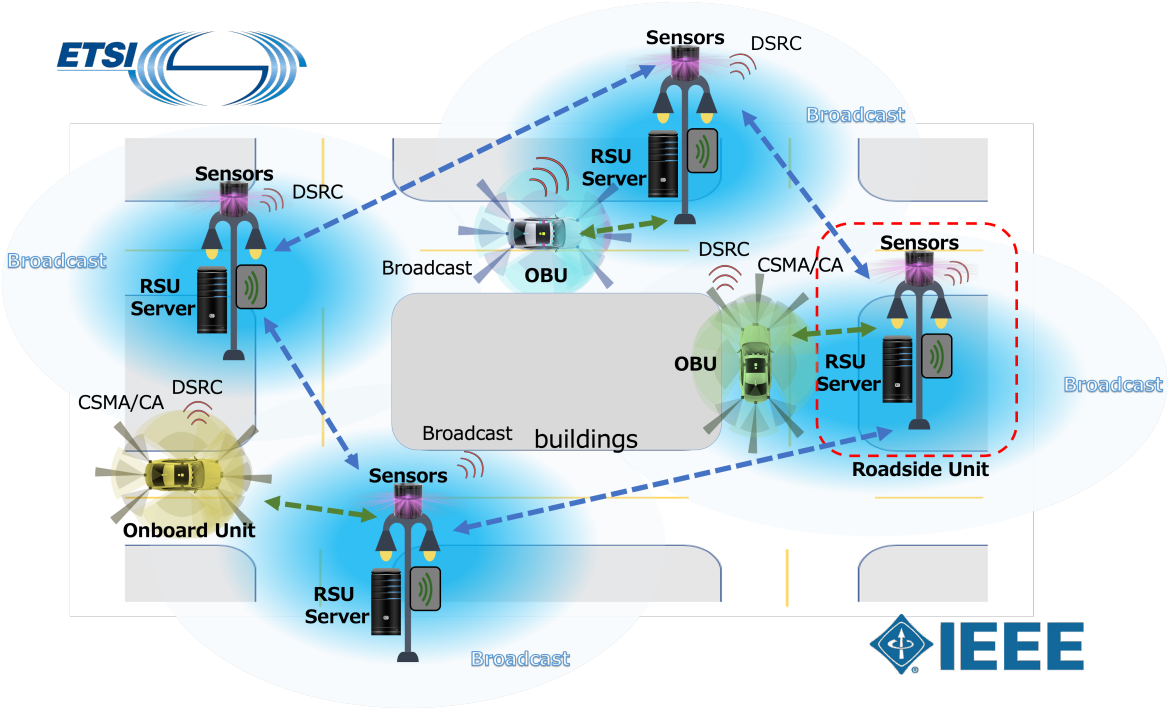

(a) Vehicular ad-hoc network (VANET)

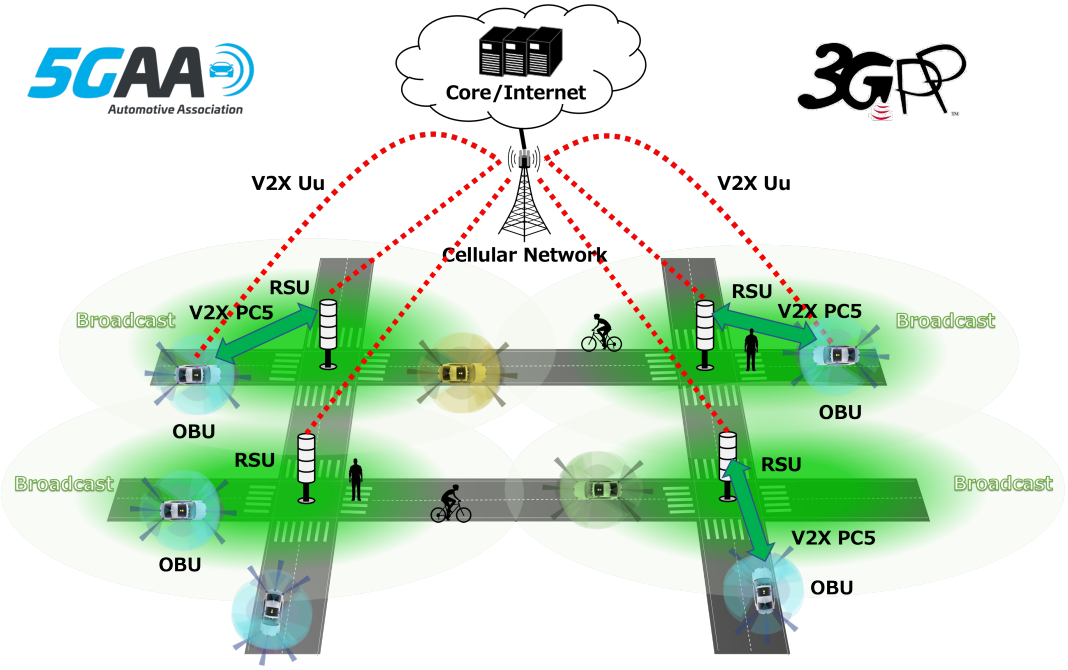

(b) Cellular V2X (C-V2X)

Figure 1.3: Current vehicular networks.

the control channel. This provide a chance to utilize mmWave. Nevertheless, since mmWave has not been specified for the sidelink, and in the current NR-V2X architecture, the network function (NF) for leveraging RATs from heterogeneous network (e.g., IEEE 802.11ad/WiGig working in the unlicensed 60 GHz band) has not been explored, mmWave V2X with ultra-low latency cannot be enabled for cooperative perception.

1.2.3 Related works

Table 1.3: Related works of mmWave V2X and SDVN.

Target	Reference	Contributions & Limitations
mmWave V2X	[20,21]	✓ Derive required data rates of cooperative perception ✓ Showcase the necessity of mmWave (30 GHz, 60 GHz) ✗ Only consider one V2V link (without multi-hop)
	[22]	✓ Design beamforming and blockage recovery schemes ✓ Construct a mmWave V2X testbed ✗ Only improve single-hop mmWave V2I performance
	[23]	✓ Build a remote driving system with 22.6 GHz NR mmWave ✗ Use a LOS link and not for cooperative perception
	[24]	✓ Mitigate interference in multi-hop mmWave V2V ✗ Under a distributed network architecture (VANETs)
SDVN Solutions	[25]	✓ Enumerate benefits and open challenges ✗ Theoretical works only
	[26]	✓ Evaluate the performances of 5G SDVN ✗ Theoretical and simulation works only
	[27]	✓ Investigate multi-hop routing with SDVN ✗ Theoretical and simulation works only
SDVN Testbeds	[28]	✓ Implement SDVN in Mininet-WiFi and test RAT handover ✗ Based on an emulator and no mmWave
	[29]	✓ Implement and test wireless access management in SDVN ✗ Data plane adopts Wi-Fi (no mmWave)
	[30]	✓ Implement and test mobility management in SDVN ✗ Data plane adopts Wi-Fi (no mmWave)

The motivation of utilizing mmWave for cooperative perception has been thoroughly confirmed. The researchers calculated the required data rate of cooperative perception for safe driving in specific traffic scenarios (overtaking [20], intersection crossing [21]). It showed that mmWave can support safe driving at a higher velocity than V2X technologies at 5 GHz. As the interests in mmWave increase, some researchers attempt to resolve the obstacles hindering its practical use. For example, the researchers in [22] optimize the codebook to accelerate beamforming and leverage non-light-of-sight (NLOS) paths to combat blockage. However, these PHY layer optimizations can only ensure the mmWave performance in one hop. Similarly, the researchers in [23] tested the remote driving with mmWave complied with NR standards. The QoS requirement was met but only one light-of-sight (LOS) link was employed. In mmWave scenarios, especially for cooperative perception, multi-hop links should be imagined. The researchers noticed that the inter-vehicle interference of mmWave in multi-hop cooperative perception degraded the achievable throughput, so they proposed ZigZag antenna configuration and dynamic bandwidth division to mitigate this impact [24]. However, their proposed schemes were based on a distributed network. The resource configuration status was notified to vehicles through broadcasting. Hence, their system will suffer from the same limitations of the VANET as explained above. So far, there is little research conducting practical evaluations on mmWave for cooperative perception under multi-hop scenarios.

In fact, centralized architectures for vehicular networks have been investigated in recent years. Software defined networking (SDN), due to its flexibility and capability to perform global management, draws growing attention. Due to the cost of building a test network, most studies stayed in theoretical and simulation levels [25,26,27]. The researchers in [28] implemented a software defined vehicular network (SDVN) with an emulator called Mininet-WiFi but only tested the handover management between Wi-Fi and LTE. A few group of researchers established prototypes to demonstrate the network capability. For instance, in [29], the group implemented and tested wireless access management in SDVN, and another group focused on mobility management [30]. However, their scenarios are less challenging as the management target is low-frequency Wi-Fi. There is still a lack of evaluations on the SDVN performance in managing mobility-sensitive mmWave V2X for cooperative perception.

Table 1.3 summarizes the above-mentioned related works as well as their respective contributions and limitations.

1.3 Summary of contributions

To enable advanced V2X applications, this thesis develops an SDN-based vehicular network architecture to satisfy their stringent QoS requirements in data rate, latency, and reliability. This thesis targets cooperative perception as it is the most challenging application to existing vehicular networks, and at the same time, it has significant value in realizing road safety and fully automated driving. Due to the high data rate requirement for exchanging raw sensor data, mmWave has to be introduced despite the well-known obstacles. Therefore, the first contribution of this thesis is the design and development of three key control functions (context manager, access manager, and routing manager) in the SDN/SDVN controller to orchestrate dynamic mmWave V2X networks for cooperative perception. Compared to the distributed management in VANETs, the centralized management by the SDN/SDVN controller can collect topology information in real-time and perform forward-looking operations, for example, selecting the beam index of mmWave access points (AP) based on the vehicle position and direction. In this way, the whole mmWave communication procedures, from the association to the routing, can be timely and adaptively adjusted under fast vehicle mobility and environment changes. The latency and reliability requirements of cooperative perception relying on multi-hop mmWave V2X are thus promised. Instead of discussing these benefits at theoretical and simulation levels, an outdoor deployment is carried out and demonstrates the network performance in real-life proofs of concept.

Next, to resolve the remaining challenges in the previously proposed architecture, including the network scalability, control plane availability in infrastructure-less areas, and the accommodation of heterogeneous V2X technologies, this thesis designs the evolved network architecture Het-SDVN, to achieve more comprehensive management of V2X resources for cooperative perception. Hierarchical control planes in Het-SDVN address the scalability and availability issues of fully centralized architectures. To deploy the local control plane to the RSUs, an SDVN framework for RSUs is developed. This framework also introduces sensor management which saves power and reduces deployment costs. In addition, the developed local SDVN controller can select the optimal RAT and transmission mode to support cooperative perception at different data-sharing levels. Through the real-life proof of concept with a full-fledged network and smart mobility testbed, the functionalities, mechanisms, and performances of the designed Het-SDVN are comprehensively evaluated.

Ultimately, with the demonstrated Het-SDVN architecture, this thesis explores its support

for other safety-critical or mission-critical V2X applications. Specifically, a mmWave-based mobility-aware high-definition (HD) map distribution application is developed, which benefits from the three-layer (MEC/Cloud - RSU - vehicle) cooperation enabled by Het-SDVN. This application is also demonstrated through a proof of concept.

The following parts of this thesis can be summarized as follows.

- Chapter 2: Cooperative Perception and SDVN

  1. Surveys the state of the art of cooperative perception and highlights the importance of raw sensor data sharing.
  2. Introduces general concepts and principles about SDN and numerates its benefits for the vehicular network as SDVN.

- Chapter 3: Software Defined Dynamic mmWave V2X Network for Cooperative Perception

  1. Designs the SDN-based vehicular network architecture to dynamically manage the mmWave V2X for cooperative perception. The core control functions and the RATs for each network plane are introduced.
  2. Conducts indoor and outdoor proofs of concept based on the established testbeds. The indoor tests verify the control of a single link (V2V and V2I), while the outdoor field trial demonstrates the muti-hop connectivity.
     - These works are published in
       * Z. Li, T. Yu, R. Fukatsu, G. K. Tran and K. Sakaguchi, "Proof-of-Concept of a SDN Based mmWave V2X Network for Safe Automated Driving," *2019 IEEE Global Communications Conference (GLOBECOM)*, Waikoloa, HI, USA, pp. 1-6, 2019.
       * Z. Li, T. Yu, R. Fukatsu, G. K. Tran and K. Sakaguchi, "Towards Safe Automated Driving: Design of Software-Defined Dynamic MmWave V2X Networks and PoC Implementation," in *IEEE Open Journal of Vehicular Technology*, vol. 2, pp. 78-93, 2021.

- Chapter 4: Het-SDVN: Software Defined Heterogeneous V2X Network for Cooperative Perception

1. Introduces the enhancements to the network architecture with hierarchical control planes and heterogeneous V2X to support cooperative perception.
2. Designs an SDVN framework for RSUs to manage their local networks. This framework is practically implemented and tested in a field trial with system evaluations.
3. Builds Het-SDVN and analyzes its performance when a test vehicle requests cooperative perception, which involves the collaboration between the local and global SDVN control planes for network scheduling.
   - These works are published in
     * Z. Li, T. Yu, T. Suzuki and K. Sakaguchi, "Building an SDVN Framework for RSU-Centric Cooperative Perception with Heterogeneous V2X," *2023 IEEE 20th Consumer Communications & Networking Conference (CCNC)*, Las Vegas, NV, USA, pp. 1-7, 2023.
     * Z. Li, K. Wang, T. Yu and K. Sakaguchi, "Het-SDVN: SDN-Based Radio Resource Management of Heterogeneous V2X for Cooperative Perception," in *IEEE Access*, vol. 11, pp. 76255-76268, 2023.

- Chapter 5: Orchestration of Mobility-Aware HD Map Distribution in Het-SDVN

1. Proposes a map partition strategy that reduces the size of overlap.
2. Implements the map distribution system and conducts field trials.
   - These works are published in
     * Z. Li, M. L. R. Lagahit, M. Matsuoka and K. Sakaguchi, "Design of Mobility-Aware Map Partition and Distribution System for Smooth Automated Driving," *2022 IEEE 33rd Annual International Symposium on Personal, Indoor and Mobile Radio Communications (PIMRC)*, Kyoto, Japan, pp. 628-634, 2022.

Figure 1.4. shows the organization of this thesis.

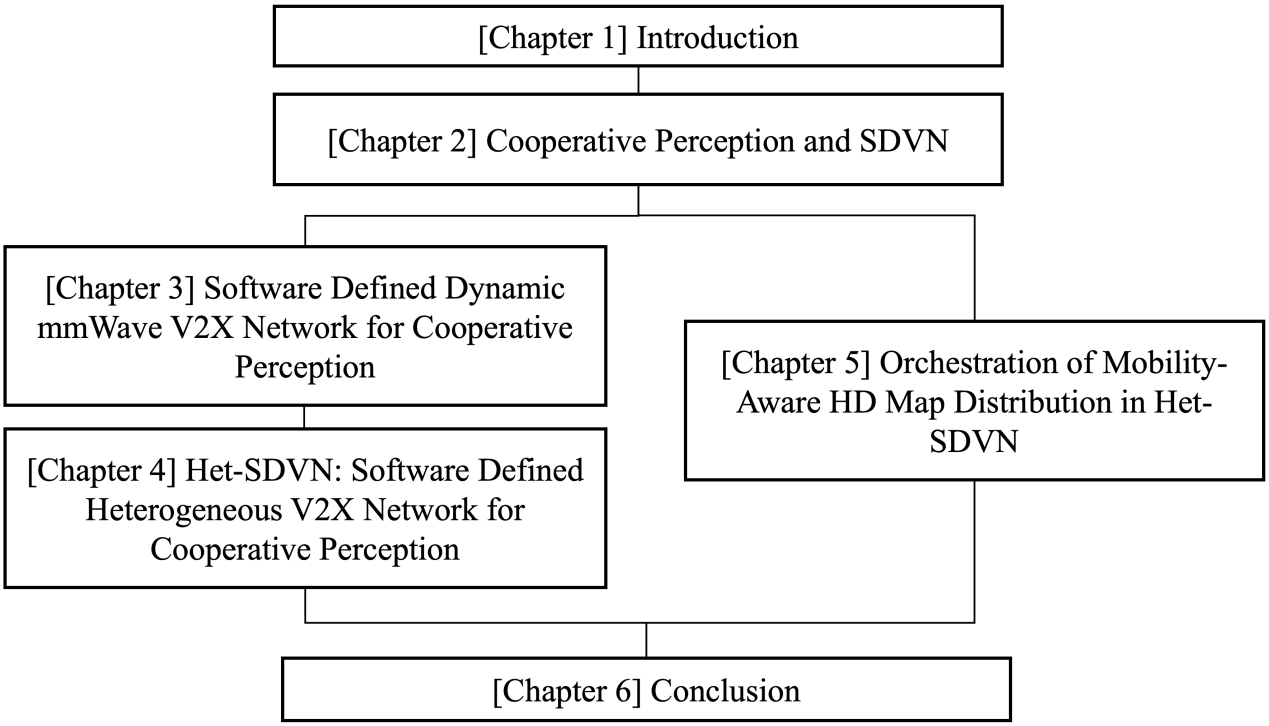

Figure 1.4: Thesis organization.

Chapter 2

Cooperative Perception and SDVN

2.1 Introduction

Enabling cooperative perception is the research target of this thesis. Chapter 1 hides some details about this advanced V2X application. One decade ago, commercialized vehicles have not equipped with as many sensors as they do today. The most commonly used vehicle sensor at that time was the global navigation satellite system (GNSS) in order to provide navigation service for human drivers. In this period, cooperative perception was at the stage of "share where I am." because the vehicle can only read its position from the GNSS. In recent years, the vehicle's level of automation rapidly grows with an increased number of sensors including cameras, light detection and rangings (LiDARs), radars, etc. Cooperative perception evolves to the new stage of "share what I see." Nevertheless, this evolution occurs so fast that the research, development, and standardization of V2X technologies are left behind. The transmission of raw images and raw pointcloud data among multiple vehicles remains a challenge in the current vehicular network. Some may question the necessity of sharing unprocessed sensor data, emphasizing the high bandwidth requirements. This chapter present the reasons why the exchange of raw sensor data is crucial in certain circumstances. Additionally, there is a viewpoint that believes introducing high-frequency V2X such as mmWave can resolve all limitations of the existing vehicular network in performances. However, this claim is also subject to scrutiny. In conjunction with the insights presented in Chapter 1, this chapter introduces the concept and principles of software-defined networking (SDN), an innovative communication architecture designed for the next-generation Internet. By comparing its advantages to the limitations of the current vehicular network, this chapter elucidates the

motivation behind adopting SDN as the primary platform to support cooperative perception. At the end of this chapter, the challenges that lie ahead for achieving the anticipated SDVN are uncovered. These challenges serve as the focal points of this thesis work.

2.2 Trade-offs in cooperative perception

2.2.1 Classification and state of the art

According to the definition of 3GPP, cooperative perception (referred to as extended sensors [7]) is an advanced V2X application for sharing sensor data to enhance the environmental perception of the vehicles. Based on the processing level of shared sensor data, a research team gives their insight on the classification of cooperative perception [31]:

- Raw/low-level cooperative perception: This means the raw data from local sensors are shared. Typically, the pointcloud data from the light detection and ranging (LiDAR) and the images from the cameras can be regarded as raw data.
- Feature/middle-level cooperative perception: This means the data after a series of pre-processing steps are shared. Redundant information has been removed, while the valuable information that can contribution to the final detection is maintained, such as the 3D profile of objects, the reflection intensity, the object mobility characteristics, etc.
- Object/track-level cooperative perception: This means the data have been fully processed before being shared to the vehicles over V2X. These data are highly abstracted, only preserving the semantic information about the classification results of objects or events, and the numerical information about the accurate/estimated positions.

Considering the diversity of sensors and the variation of products among manufacturers, the data format for the object/track-level cooperative perception is the easiest to be standardized because of the high-level abstraction. The cooperative awareness message (CAM) [15] is the first-generation V2X message, specified by ETSI, to share such highly abstracted sensor data. The CAM information includes the vehicle position, velocity, and heading derived from the global navigation satellite system (GNSS) and inertial measurement unit (IMU). In road safety applications, this message is broadcasted by vehicles periodically to notify their existence when locating at the blind spots of others (vehicles, pedestrians, cyclists, etc.). The decentralized environmental notification message (DENM) [16] is defined to alert road

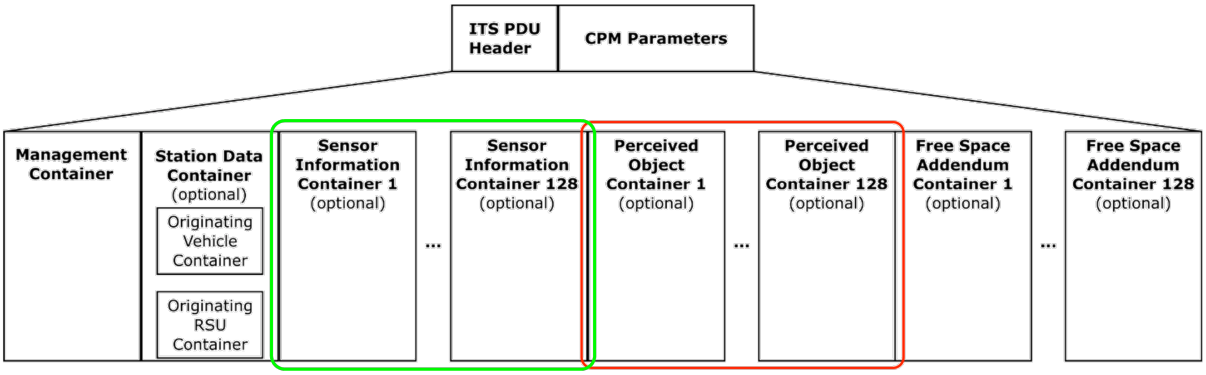

Figure 2.1: ETSI CPM format [3].

users of a detected event (accidents, constructions, temporary traffic controls, etc.), instead of detected objects, to improve safety and traffic efficiency. Therefore the broadcasting of DENM is event-triggered and targets the vehicles that plan to pass through the corresponding regions. Now, the ESTI is drafting a new specification for sharing detected objects in the collective perception message (CPM) [3]. Figure 2.1 shows the structure of CPM. One CPM message can contain information about up to 128 perceived objects and the sensors that captured these objects. Intensive discussions are still ongoing regarding the generation method of CPM and the type of objects which should be included into the list. Before it is finalized, the researchers have already tried to reuse the CAM as a proxy format to include the detected objects [32]. Although using the proxy-CAM is inefficient as it only contains one perceived object at one-time broadcasting and does not include sensor attributes, demonstrating such messages and systems is a critical step for the standardization of object/track level cooperative perception. Figure 2.2 provides an example of the visualization result from object/track-level cooperative perception.

The feature/middle-level cooperative perception recently gained considerable popularity from research attention. Compared to sharing object information from detection, sharing so-called features loses less amount of information from raw data and avoids generating excessive traffic volume in the V2X network, which is suitable for the vehicles to achieve cooperative perception in bandwidth-limited environments. Nevertheless, the definition of features is too diverse to be unified. It can vary in the methods and depth of data processing. For example, in [33], the researchers proposed to use feature maps in cooperative perception, which are generated from LiDAR pointcloud data by the convolutional layers in a neural network. By

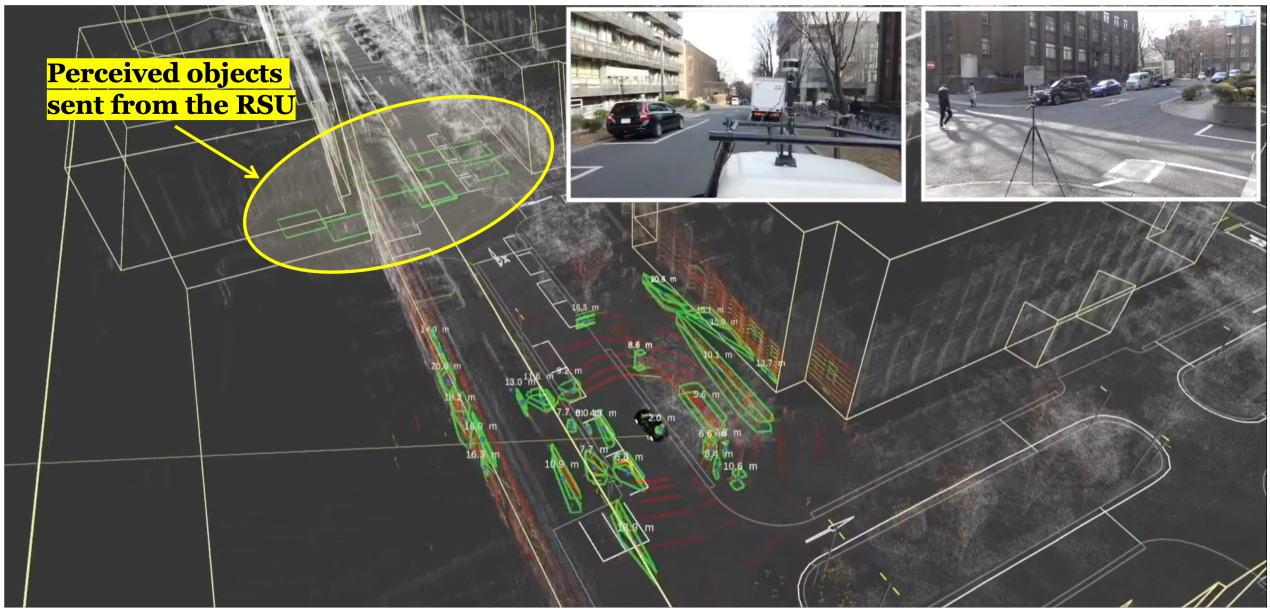

Figure 2.2: Example of object/track-level cooperative perception [4].

fusing these feature maps, they achieved around 10% improvement for detection within 20 m and 30% for further distances. Another group of researchers introduced the spatial confidence map as a feature [34]. The spatial confidence map was similar to the cost map usually used for navigation. It indicated the score/probability of object detection in each map grid. They used fewer communication resources and achieved higher perception performance by focusing on perceptually critical areas. Figure 2.3 gives our example of features, where the dynamic LiDAR points (blue in Fig. 2.3(b)) are extracted from one scan frame by the octree filter [x] as the feature. The permanently static points of trees, curbs, buildings, etc., do not contribute to the detection on roads so that they can be discarded.

It is also hard to form a unified data format for the raw/low-level cooperative perception, because various sensors can be used for detection, such as cameras, LiDARs, and mmWave radars, but the generated raw data are totally different (images, pointcloud frames, etc.). Even for the same type of sensors, due to the diversity in their specifications (for example, the number of lasers), the raw data may have distinct structures. Therefore, the drivers are designed individually to make the data readable. Figure 2.4 shows the LiDAR packet format of a 32-beam LiDAR (RS-LiDAR-32) manufactured by the company RoboSense. The packet payload is 1248 bytes, which is a common size in commercialized LiDAR products. With this

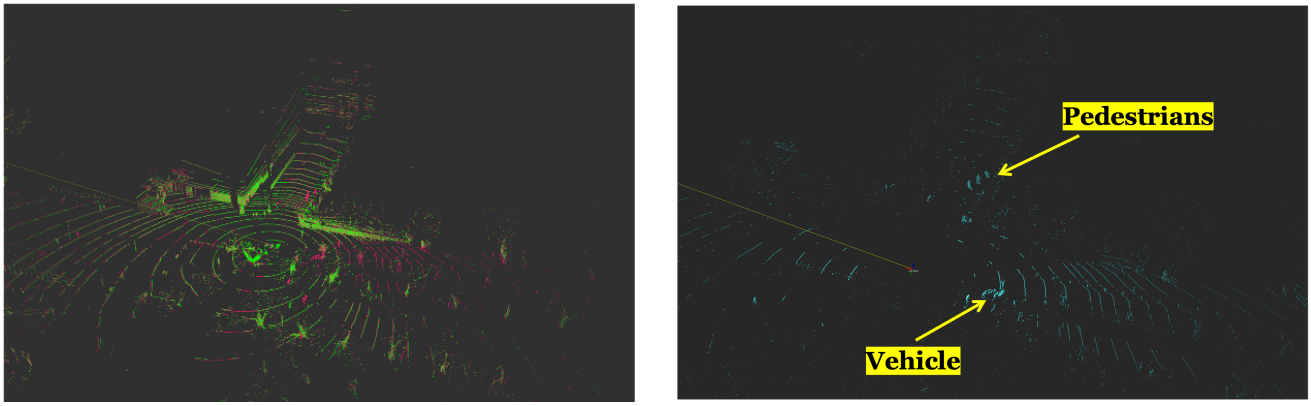

(a) Raw LiDAR scan frame. (b) Extracted dynamic LiDAR points.

Figure 2.3: Dynamic LiDAR points as the features for cooperative perception.

structure, the size of one LiDAR scan frame can be calculated by

$$N = 1248 \times 8 \times \frac{R \times \frac{60}{\omega}}{32 \times 4} \tag{2.1}$$

where R represents the size of the LiDAR point rate (pts/s) and ω indicates the rotation speed of the motor (rpm). Since the R in single return mode is 6×10^5 pts/s, and the maximum ω is 1200 rpm, one LiDAR frame at least occupies 2.34 Mbit.

2.2.2 Fusion techniques

For cooperative perception, fusion is the last step before the received data contribute to the detection and navigation of automated vehicles. With respect to the three types of cooperative perception in Sect. 2.2.1, the fusion can also be categorized into (1) raw/low-level data fusion; (2) feature/middle-level data fusion; and (3) object/track-level data fusion.

The fusion of the first and second types needs to take a trade-off between the detection accuracy, bandwidth limitations, and computational capabilities. To that end, the researchers in [35] proposed two fusion paradigms, as known as early fusion and late fusion, respectively. Figure 2.5 illustrates the difference between these two paradigms. In the case of raw LiDAR data, i.e., pointcloud frames, early fusion involves merging these frames as a whole and then feeding them into the detection model. On the other hand, late fusion entails performing detection on each frame individually and subsequently merging the final results (exactly the same as object-track-level fusion). Each paradigm offers its pros and cons. Early fusion has the potential to produce the optimal results as it preserves all information prior to detection.

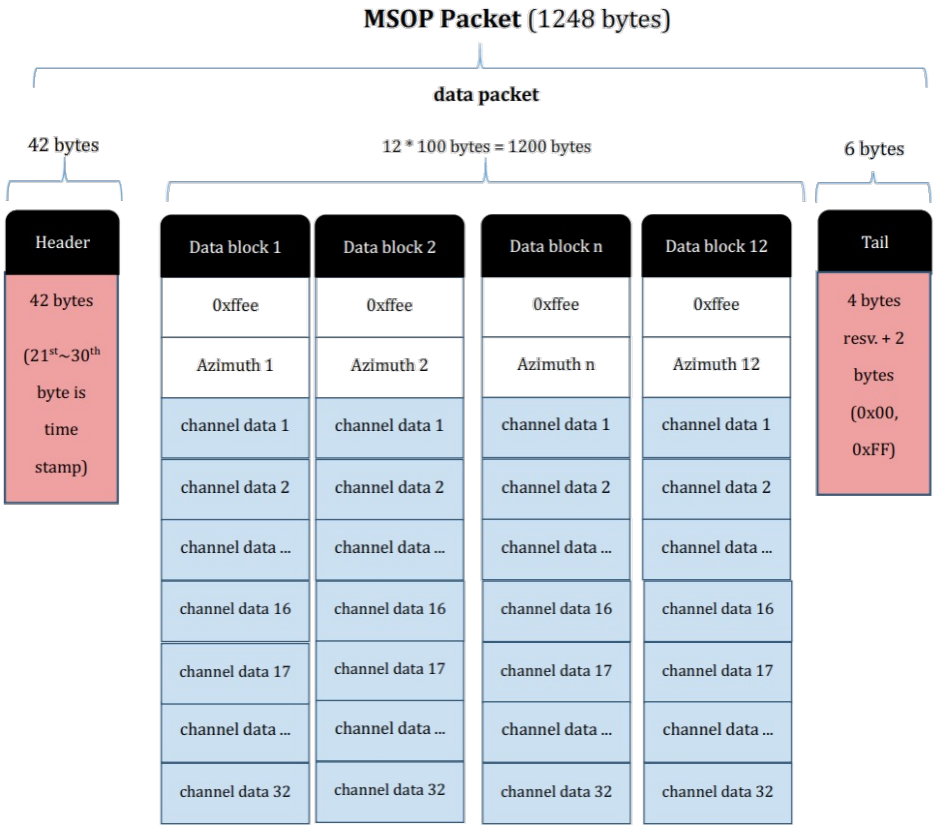

Figure 2.4: RS-LiDAR-32 packet structure [5].

However, it necessitates a strong computational capability that only edge servers can supply, as implemented in [36]. Otherwise, the detection latency will significantly increase. In contrast, late fusion mitigates the bandwidth requirement but compromises the accuracy. Given the uncertainty in data quality and sensor positions, late fusion may lead to detection failures or duplicate detections, thereby impacting vehicle operation and driving safety.

For all types of fusion, perspective transformation is the fundamental step to integrate cooperative perception data to the vehicle point of view [37]. The positional information from CAM, CPM, or other localization sensors will be useful to derive perspective (coordinate) relationships. As shown in Fig. 2.6, when an object is detected at the position $P_r = [x, y, z, 1]^T$ by RSU in the RSU perspective (r). To translate it into a position $P_v = [x^{'}, y^{'}, z^{'}, 1]^T$ in the vehicle perspective (v), perspective transformation should be done by

$$P_v = T_{rv}(t) * P_r \tag{2.2}$$

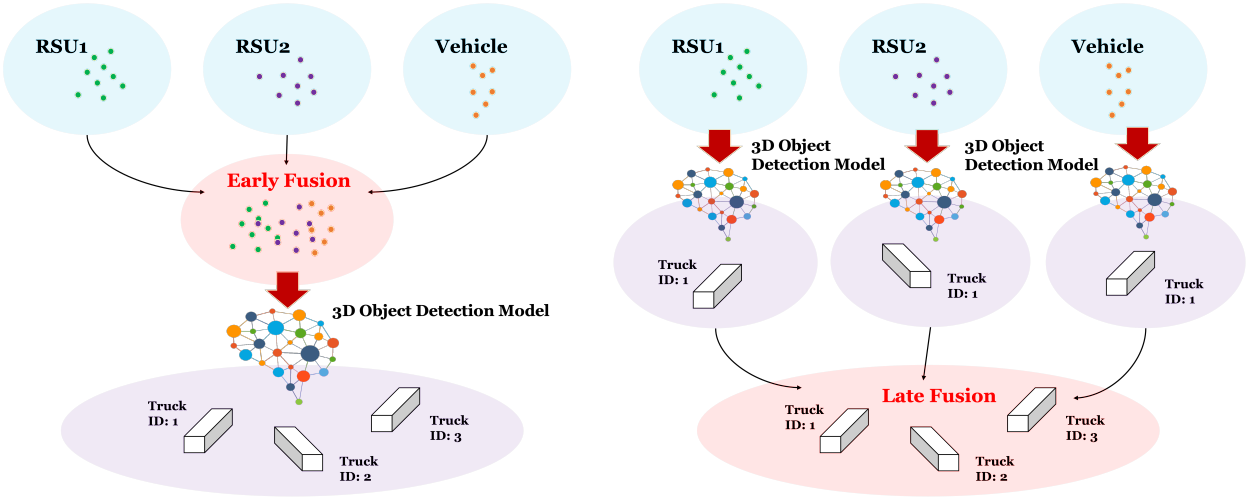

(a) Early fusion.

(b) Late fusion.

Figure 2.5: Two fusion paradigms for cooperative perception.

where $T_{rv}(t)$ is the transformation matrix from the RSU perspective to the vehicle perspective. $T_{rv}(t)$ is expressed by

$$T_{rv} = \begin{pmatrix} RotX.x & RotY.x & RotZ.x & Translation.x \\ RotX.y & RotY.y & RotZ.y & Translation.y \\ RotX.z & RotY.z & RotZ.z & Translation.z \\ 0 & 0 & 0 & 1 \end{pmatrix} \tag{2.3}$$

which dynamically changes with the vehicle movement.

2.2.3 Philosophy of data type selection

The object/track-level cooperative perception shares fully processed sensor data. The main benefits consist in three aspects. Firstly, it does not require high communication bandwidth as the sensing information has been highly abstracted and can be stored in a few bits. So legacy V2X technologies like IEEE 802.11p and LTE-V2X are capable of this application. Secondly, most standardization efforts up to now concentrate in the format for fully processed sensor data, like the CAM, DENM, and CPM mentioned before. This is convenient for third-party application suppliers because they do not need to consider what sensors are available and used for the detection in the environment to prepare multiple drivers. Thirdly, the emergence and commercialization of advanced computing technologies like cloud and multi-access edge

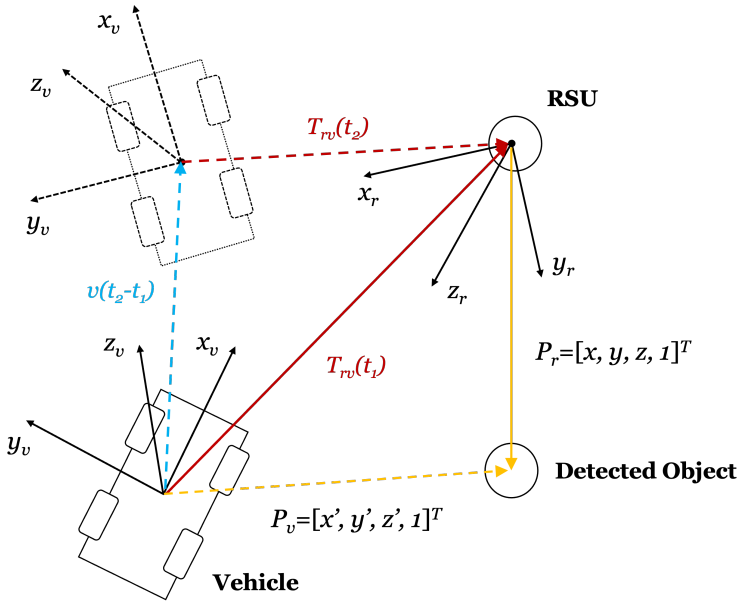

Figure 2.6: Illustration of perspective transformation (v: vehicle velocity).

computing (MEC) provide strong computing resources to deploy big models and process the sensor data with ultra-low latency. These resources will become cheaper and easier to access as the penetration rate increase. However, sharing fully processed data can bring some risks as the cooperative perception receiver has no idea about the sender's detection capability and accuracy. Purely believing in these detection results may cause wrong behaviors.

The feature/middle-level cooperative perception only involves preliminary abstractions on the raw sensor data, but by removing invaluable information, it has significantly reduced the data amount and relaxed the bandwidth requirement. On the other hand, the features preserve more environmental details than fully processed sensor data, which may produce a better accuracy. However, one serious shortcoming of this approach is complexity. It requires strict consistency between the cooperative perception sender and receiver (e.g., the design of the feature encoder/decoder). In addition, the definitions of features are too diverse to be generalized for all cooperative perception use cases.

The raw/low-level cooperative perception is underexplored. The major concern still lies in the bandwidth limitation. The existing V2X technologies cannot satisfy the QoS requirement. This issue will be addressed after introducing the mmWave. The opportunities from sharing raw sensor data are more than its challenges. Firstly, integrating raw sensor data can achieve the best detection accuracy due to the richness of information. Secondly, sharing raw

sensor data has the potential to resolve a highly controversial topic related to connected and automated vehicles (CAV), i.e., the liability in accidents. Imagine the cooperative perception scenario where a CAV receives fully processed sensor data from the RSU deployed by the government or telecom operators. If this CAV made detection errors and ran into an accident, it bears the highest liability. However, if the CAV ran into the accident due to believing in the detection results of RSUs, the government or telecom operator should share the liability. The shared raw data will be used as evidence. To prevent such accidents, the CAV can also double-check the received objects by performing detection on the raw data by itself.

It is worth noting that, all types of cooperative perception could be required according to specific circumstances. The V2X network should be adaptive to their QoS demands, thus motivating a powerful management architecture and functions.

2.3 Transition from SDN to SDVN

2.3.1 Concepts and principles of SDN

2.3.1.1 History overview

The software defined networking (SDN) technologies originate from the "Clean State" research program at Stanford University, aiming to redesign today's communication infrastructure and break the network's ossification. This program was directed by famous Prof. Nick McKeown. In 2008, their team introduced the concept of OpenFlow [38]. OpenFlow is a protocol that allows the separation of network control and forwarding functions. It provides a standardized interface between the control plane (C-plane: decides how to handle network traffic) and the data plane (D-plane: forwards traffic based on the instructions from the C-plane). Seeing the programmability brought by OpenFlow, Prof. Nick McKeown and his team further proposed the concept of SDN in 2019, using OpenFlow as a critical component so that network managers can to remotely control the behavior of the switch/router through a separate controller. Since then, SDN has been placed at the forefront of academia and industrial attentions. In 2011, the Open Networking Foundation (ONF) was established. This foundation aims to promote the development and standardization of SDN. Its core members include Google, Facebook, NTT, etc. In 2012, the ONF released the SDN whitebook [39], which marked a milestone that the three-layer SDN architecture had earned global recognition.

Today, SDN, together with the network functions virtualization (NFV) are expected to

transform the networking landscape of beyond 5G and 6G networks. The open, flexible, and efficient architecture of SDN enables rapid innovation and low cost for communication infrastructure deployment. Moreover, SDN has expanded beyond its initial scope of the backbone network and initial focus on separating control and data planes. The capabilities of SDN are largely enriched, encompassing new functions such as network automation, radio resource management (RRM), network slicing, etc. The author of this thesis believe that there are still a plenty of fields where SDN can contribute and make innovations.

2.3.1.2 Three-layer architecture of SDN

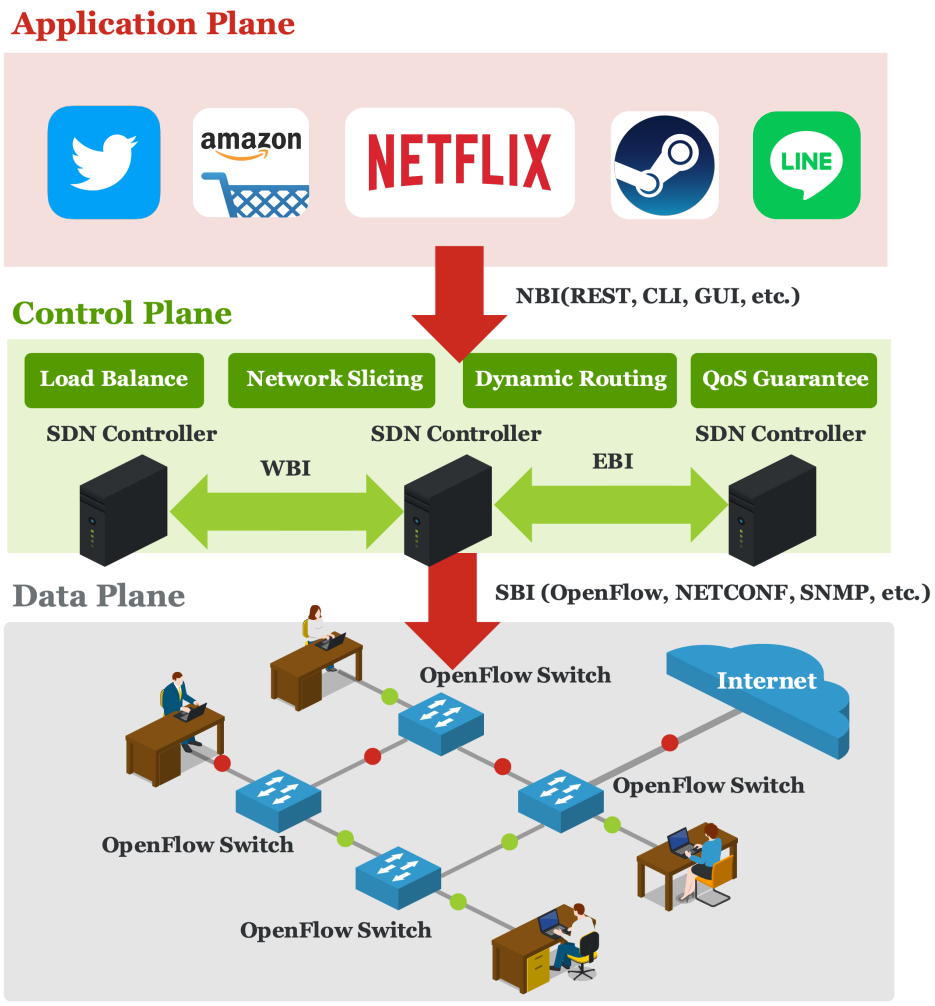

Figure 2.7: Three-layer architecture of SDN.

The most striking feature of SDN is the three-layer network architecture, as shown in Fig. 2.7. It consists of a data plane (D-plane), a control plane (C-plane), and an application plane from bottom to top. Each plane serves a specific function and has its own set of responsibilities.

- D-plane: The D-plane is also referred to as the user plane, forwarding plane or infrastructure plane. The D-plane devices, such as the physical switches, physical routers, and their virtualized counterparts, simply execute the forwarding actions as instructed by the C-plane. These devices are controllable and programmable by the SDN controller of the C-plane via the OpenFlow protocol. This plane takes care of the actual transmission and switching of user/application data packets over the network.

- C-plane: The C-plane is responsible for making high-level decisions about traffic forwarding and resource utilization. It relies on the SDN controller to manage and control the behavior of the network. On the one hand, the SDN controller listens to the instructions from the application plane through the northbound interface (NBI). On the other, hand, the SDN controller translates the network policies and requirements into low-level actions and injects to the D-plane devices through the southbound interface (SBI). The OpenFlow protocol is an implementation of the SBIs. Through the OpenFlow, the C-plane can obtain a global view of the network to make adaptive policies.

- Application plane: The application plane consists of software applications and services that interact with the network through the C-plane. The NBIs of SDN provides programmability and flexibility for the application plane to implement various network services. For instance, the multi-media application deployed by the third party can acquire the QoS support from the C-plane without dealing with the complicated D-plane network. The application layer works as an interface for network managers and developers to customize their own network policies and services.

The three-layer architecture for communication infrastructures will construct a logically centralized network, but it does not hinder the appearance of geographically distributed C-planes. When there are multiple peer C-planes, eastbound/westbound interfaces (EBI/WBI) between the SDN controllers and their collaboration mechanisms should be well-defined.

2.3.1.3 Benefits of introducing SDN

Attempting to restructure the traditional network that has existed vast communication infrastructures and users is not a task that can be accomplished solely with courage. It requires wisdom and the persuasive power of the new architecture. SDN offers irreplaceable cost and performance advantages, whether for telecom operators or application providers, although it may degrade the vendor's profit. These advantages are summarized as follows:

1. Improved network performance: SDN enables intelligent traffic management and optimization. The centralized C-plane collects global network information including topology, link status, resources, etc., for sophisticated algorithms (including today's prevalent AI models) to analyze and generate the globally optimized strategies for traffic routing, load balancing, or resource slicing. Compared to the distributed and competing-based networking, SDN provides an efficient and reliable network environment.

2. Increased flexibility and agility: SDN enables dynamic network reconfiguration adaptive to the changing requirements of applications. The convenient NBIs allow network managers or software applications to reshape the network environment according to their current needs. In addition, new services, policies, and functions can quickly function in the D-plane with the help of the centralized C-plane through the SBIs, avoiding unnecessary time consuming in on-site hardware configurations.

3. Cost efficiency: SDN offers cost efficiency from two aspects. Firstly, the D-plane consists of virtualized or generic forwarding devices. These devices remove proprietary C-planes and only needs to support SBI protocols so their prices will drop. The cost of scaling the network will become cheaper for telecom operators. Secondly, SDN increases the automation of network management with centralized intelligence. The tasks for network managers become fewer and easier so it can save human resources.

4. Enhanced security: A self-organized network is hidden with numerous security vulnerabilities in distributed devices. With the centralized C-plane of SDN, network managers can enforce security policies consistently across the network. They can implement firewalls, monitor traffic anomaly in real-time, and quickly eliminate security threats. Moreover, the applications can choose their preferred security policies through the C-plane, which enhances the overall network security.

5. Prosperous and innovative ecosystem: SDN provides an open and programmable platform with plentiful well-defined NBIs and SBIs to application developers and researchers to deploy and test cutting-edge services, functions, and protocols. This will promote rapid innovation, foster collaboration among academia, telecom operators, content suppliers, etc., and encourage the development of novel networking solutions.

2.3.2 Challenges towards SDVN

The concept of SDN was initially proposed for the next-generation Internet. Nowadays, it is also conceived as one of the key technologies for 5G and beyond networks. This means the telecommunication industry has noticed the great potential of SDN and planned to adapt it to the wireless/mobile network, for radio access network (RAN) management, backhaul network management, multi-access edge computing (MEC) resource management, etc. The software-defined wireless networks (SDWN) [40] or software-defined mobile networks (SDMN) [41] refer to the wireless/mobile networks which follow the SDN principles in their architectures. Before 5G commercialization, the researchers in [42] constructed a software-defined mmWave mesh backhaul network to realize dynamic MEC container migration and content delivery based on the mobile user's trajectory. This provided a great example for 5G network designers to see how they can leverage SDN to serve mobile users. The vehicular network is a special type of wireless/mobile network that features higher mobility. However, the software-defined vehicular networks (SDVN) have not drawn extensive discussions from academia and industries. From the author's point of view, it is due to some realistic challenges.

2.3.2.1 Resource abstraction

In the vehicular network, the roles of vehicles/onboard units (OBU), roadside units (RSUs), and base stations (eNodeB, gNodeB) are not only communication infrastructures but also computing and storage infrastructures. Managing these heterogeneous communication, computing, and storage resources requires a high-level abstraction in the SDVN C-plane. So far, there have been well-defined abstractions for the computing resources in MEC and Cloud owing to the fast development of NFV and NFV platforms such as Docker, Kubernetes, etc. Nevertheless, there is still a lack of methods and platforms for communication resource abstractions. This hinders the possibility of doing fine-grained radio resource allocation. As the heterogeneity of V2X technologies increases after introducing mmWave, THz, VLC, etc., and

the two sets of V2X communication standards (IEEE, 3GPP) develop in parallel, the SDVN must implement a standardized or consistent abstraction layer for them. Only then can SDN unleash its advantages of global resource management in the context of vehicular networks, while providing the flexibility and programmability required for V2X applications.

2.3.2.2 Mobility management

As mentioned above, the vehicular network features higher mobility, which indicates a highly dynamic node topology and frequent connection handovers. This poses a challenge to the traditional SDN and low-mobility SDWN/SDMN. They have stationary or semi-stationary topology, without the need to implement a real-time and accurate node tracking function in the C-plane. For the SDVN, the vehicle's position, velocity, direction, destination, etc., must be collected to the C-plane. Based on the information, the SDVN controller predicts the future topology and adapts the network behaviors, such as routing, association, service migration, etc., accordingly by issuing forward-looking policies or modifying OpenFlow tables. After introducing mmWave V2X, the requirements for mobility management further increase due to the use of directional antennas and the vulnerabilities to environmental changes. How to stably and accurately collect and synchronize vehicle mobility information becomes critical.

2.3.2.3 Interoperability

Interoperability is a non-negligible issue in the vehicular network due to the heterogeneity of V2X technologies. Resolving this issue needs efforts from vendors, standardization organizations, and network operators. Due to the support of a different set of V2X technologies (IEEE, 3GPP), some vehicles may not be able to join the network to obtain the service or be designated as a relay vehicle for multi-hop routing by the SDVN controller. To overcome this challenge, it needs to specify a new protocol of SBIs for exchanging information about the supported V2X technologies of vehicles, RSUs, and base stations between the SDVN D-plane and C-plane. With the V2X capability information from the D-plane, the SDVN controller can instruct the vehicles that share the same V2X technologies to form a network. On the other hand, the application plane can select the most appropriate QoS guarantee mechanism from the C-plane for vehicles considering the V2X interfaces they have.

2.3.2.4 Lack of proofs of concept

Similar to the initial situation of SDN practice, although Stanford University allowed the use of the campus network for SDN technology trials, for large-scale network tests, the operators became very cautious as there were a huge number of users, and any technical failure might lead to unpredictable economic loss. Hence, SDN deployment in real carrier networks was launched in recent years after demonstrating technical maturity and reliability. The SDVN components and test requirements are much more complex than that of SDN. Firstly, the experimental equipment is costly. Besides the communication infrastructures, the testbed needs to prepare vehicles. Secondly, due to vehicle mobility, a wide test field is required. Thirdly, safety issues are the primary concern in real traffic. Because of these reasons, most studies about SDVN were performed by simulations. Some researchers have established simplified testbeds [29,30], but such works are still insufficient. Proofs of concept are essential for researchers to develop SDVN frameworks compatible with commercial off-the-shelf equipment and to verify the network performance and C-plane algorithms in practical traffic scenarios.

It is worth noting the contributions of this thesis fully/partially cover the challenges described above, which shed light on SDN adoption to enhance traditional vehicular networks.

Chapter 3

Software Defined Dynamic mmWave V2X Network for Cooperative Perception

Chapter 2 has delivered a comprehensive introduction to cooperative perception in terms of the categories, fusion techniques, and required data rates. The significance of sharing raw sensor data has been highlighted, considering the benefits for high-level automated driving in reducing latency, enhancing detection accuracy, improving maneuvering reliability, and clarifying liability. To fulfill the demanding communication requirements (a data rate of over 1 Gbps, and a latency of less than 10 ms), millimeter wave (mmWave) technology operating in the 30 - 300 GHz band has to be utilized. Despite of mmWave's potential to enable ultra-high data rate and ultra-low latency communications, its severe path loss, weak penetration rate, and antenna directivity hinder the establishment of a reliable, scalable, and efficient mmWave vehicular network. Traditional broadcasting-dominated vehicle-to-everything (V2X) networks should be transformed into multi-hop V2X networks. In this chapter, the author decides to integrate the software defined networking (SDN) and mmWave technologies and proposes a novel architecture called software-defined dynamic mmWave V2X network. This architecture takes advantage of the centralization, flexibility, and programmability of SDN for resource management and the outstanding communication performance of mmWave for V2X. Hence, raw sensor data sharing can be effectively supported. This chapter also presents the prototyping process, in which the necessary hardware and software equipment are enumerated. Finally, this chapter gives a detailed introduction to the proofs of concept (PoCs).

3.1 Motivation

The primary public concern regarding automated driving is safety, especially after the first road death caused by a testing automated vehicle in 2018 [43]. V2X communication is now considered as a promising solution to addressing the safety limitation of the commercialized automated vehicles in non-line-of-sight (NLOS) perception, by allowing sensor data sharing among vehicles (vehicle-to-vehicle, V2V), with nearby RSUs (vehicle-to-infrastructure, V2I) or smart devices (phones, watches, etc.) taken by road users (vehicle-to-pedestrian, V2P) [44]. On the other hand, technology evolutions of V2X accommodate the growing demands in data rates (larger than assumed 1320% for machine-to-machine/internet of things (M2M/IoT) from 2016 to 2021) and latency reduction [45]. The IEEE 802.11p based ITS-G5 [46]/dedicated short-range communication (DSRC) [47], operating in the licensed ITS 5.9 GHz band, can hardly exceed 6 Mbps with high mobility, although it ensures low latency less than 10 ms. As an alternative, 3GPP-conducted cellular V2X (C-V2X) has concluded the design of long term evolution V2X (LTE-V2X) in Release 14. It supports higher throughputs using LTE radio interface (Uu) and side-link interface (PC5) [48]. However, the peak data rate is still lower than 28.8 Mbps and the end-to-end latency cannot go below 100 ms [49]. In order to fulfill the stringent quality of service (QoS) requirement of safety-critical V2X applications, especially the target cooperative perception in this thesis, which requires a data rate of over 1 Gbps, end-to-end latency of less than 10 ms, communication range of larger than 50 m and reliability of above 99.99%, evolutions for DSRC and C-V2X, known as 802.11bd and new radio (NR) V2X respectively, are underway, taking millimeter wave (mmWave) into account because of its abundant spectrum resources to enhance communication performances [50].

The massive multi-hop connections due to the introduction of mmWave and the huge traffic volume generated by raw sensor data sharing will definitely challenge the capability of traditional vehicular ad hoc networks (VANETs) in their capacity, support to high mobility, and resource management efficiency. In addition, the increasing penetration of automated vehicles and ITS infrastructures demands rapid protocol updates and application deployment. Software defined networking (SDN) emerges as a revolutionary network paradigm that breaks the inherent coupling of data plane (D-plane) and control plane (C-plane). This paradigm surpasses the conventional one in terms of flexibility, programmability, global awareness and centralized management. In order to diffuse its advantages into the vehicular networks, preliminary attempts have been made by some researchers in architecture design and performance

analysis. Nevertheless, most of the architecture works focus on the technical combination with other emerging technologies like fog computing [51] and multi-access edge computing (MEC) [52] to satisfy the general QoS requirements of V2X, rather than orienting a specific safety service like cooperative perception. Besides, nearly all the performance evaluations are based on network simulators (ns-2, ns-3) and emulation tools (Mininet, Mininet-WiFi) [53], thus lacking field trials with real testbeds.

The contributions of this chapter lie in two fronts. Firstly, in order to support raw sensor data-based cooperative perception and tackle the inevitable challenges using mmWave, the author proposes a software-defined dynamic mmWave V2X network, which not only achieves real-time context tracking in fast-changing network topologies, but also enables flexible radio resource management (RRM) for mmWave fronthaul/backhaul associations and transmissions. Secondly, the author conducts indoor verification and outdoor proof of concept that demonstrate the proposed network can serve the cooperative perception with a good performance. The testbeds are constructed by commercial off-the-shelf (COTS) equipment, and the functionalities are implemented by open-source and developer-friendly software frameworks.

3.2 Architecture design

3.2.1 Safety requirements

The common idea to improve the safety of automated vehicles is attaching multiple and multi-type sensors, e.g., cameras and light detection and rangings (LiDARs) on board, which however exerts much pressure on the processing capability of a single vehicle. The sensor detection performance is also highly constrained by frequent blockage and extreme weather. To ensure the reliability of information acquisition, delivering alarm messages via V2X then becomes a new safety demand. Either DSRC or LTE-V2X can support this application for use cases like pre-crash warning [12]. Nonetheless, alarm messages discard many environmental details due to the restricted message size. Complete safety is hard to meet with the limited context information. In this regard, raw sensor data retains full environmental details, but meanwhile its dissemination desires higher performances of vehicular networks. The requirements on three different network layers are summarized as follows:

1) High-speed V2X access layer: The high-definition (HD) dynamic maps composed by sensor data are crucial for the ADSs to safely maneuver vehicles, in particular as a means

to provide decimeter localization that consumer-grade GPS cannot achieve. For a LiDAR-generated HD map, the total data volume collected for the duration of one hour is about 1 TB, which corresponds to a 2.2 Gbps data output [54]. The required data rate for cooperative perception is analyzed based on an overtaking scenario, which reveals that over 1 Gbps LiDAR information per is needed on V2V links to ensure safety for vehicle velocities above 70 km/h [55]. Hence, an estimation of 1 Gbps can be reasonably considered as the typical data rate requirement for exchanging HD information via V2X links.

2) Low-latency and economical backhaul layer: Vehicular backhaul refers to the associations from the source OBU to the destination OBU or RSU. The backhaul carries huge amounts of user traffic and should guarantee the QoS correspondingly, of which the latency is the most significant metric for safety-related services. For example, an end-to-end latency of less than 20 ms is tolerable for remote driving [7]. But HD map exchanging requires a more strict latency of less than 10 ms [54]. Besides, since a considerable number of RSU are being deployed to facilitate the penetration of automated vehicles, cost-efficient alternatives for optical fibers are much preferred to reduce the budget of vast backhaul construction.

3) Ubiquitous and reliable control layer: Inadequate challenges are posed to the vehicular network when transmitting alarm and other context information embedded in the cooperative awareness message (CAM) [15] and the decentralized environmental notification message (DENM) [16]. However, the dissemination of raw sensor data or HD map can cause traffic congestion, load imbalance, etc that degrade the network performances. Therefore, a control layer with wide coverage should be supplied to manage global network resources and coordinate multi-hop flow transmission. Moreover, it is necessary to monitor the real-time vehicle status reliably in high dynamic contexts for safe automated driving.

3.2.2 Architecture description

Figure 3.1 gives an overview of the software-defined dynamic mmWave V2X network where cooperative perception is performing at urban intersections. In a mixed traffic environment, legacy vehicles and vehicles with OBUs coexist. For driving safety, alarm messages are broadcasted by OBUs and RSUs via LTE-V2X and DSRC. The contexts of legacy vehicles are captured by nearby RSUs which then send proxy notifications. As is mentioned above, HD dynamic maps measured by versatile sensors (e.g., LiDAR) are critical for automated vehicles to ensure safety. They can be basically divided into two types: the local dynamic map and the global dynamic map. The former indicates the single HD map captured by self-sensors

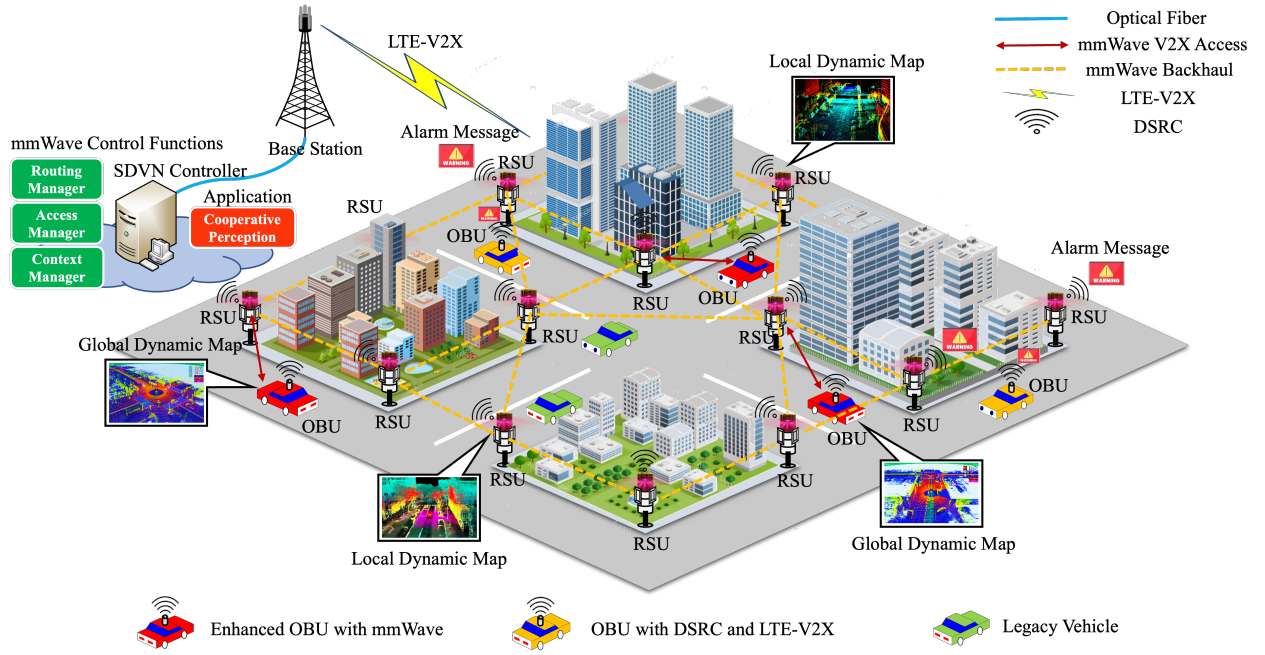

Figure 3.1: Software-defined dynamic mmWave V2X network for cooperative perception.

connected with an OBU or a RSU. This sort of maps can provide the context information of surroundings, but it only covers LOS regions and is subject to the visual range of equipped sensors. In other words, the local dynamic map only helps with local environmental perception, which is inadequate for 100% driving safety. The latter indicates the merged multi-source HD map. Besides its own HD map, a certain automated vehicle can acquire more than one local dynamic maps from vehicles ahead or fixed RSUs that monitor particular areas at high views. The received maps is then merged into a global dynamic map that provides extra information of NLOS regions and enables proactive risk awareness and reaction.

The proposed architecture is intended to ensure global HD dynamic maps available for each OBU in demand. Cooperative perception of HD dynamic maps is running on the application plane. It utilizes the functions of SDN controller in the C-plane via the northbound interface (NBI) to distribute local dynamic maps according to the context information (velocity, location, destination, etc) collected from the participants, i.e., OBUs and RSUs via the southbound interface (SBI). The role of three major elements in this architecture is described in detail:

- SDVN RSU: Existing infrastructures like street lamps or traffic lights can be easily retrofitted into RSUs by mounting sensing, computing and communication modules. A RSU

can directly share its raw/processed HD map with vehicular OBUs via V2I communications or simply forward map data via the backhaul network as relays. In the SDVN, RSUs belong to the D-plane, handling network traffic according to the decisions made by the C-plane and performing resource/mobility management (e.g., power allocation, channel/RAT handover, etc) under the instruction of SDVN controller.

• SDVN OBU: The OBU is commonly used to represent the automated vehicle but originally it refers to the platform of automated driving system, which takes raw sensing data coming from various on-board sensors (LiDAR, camera, GPS, IMU, etc) as input, develops dynamic path planning as intermediate results and finally maps to the appropriate action of the vehicular engine system as output. For the compatibility of cooperative perception, V2X module is added to receive external information. Multi-source data fusion is implemented before the path planning. In the SDVN, OBUs also belong to the D-plane and are controllable by the SDVN controller in terms of network selection, data relay and handoff.

• SDVN controller: As the core of the proposed architecture, SDVN controller locates at the C-plane and is responsible for tracking the network status including the dynamic topology and the resource distribution. It also accepts control edicts from the applications and applies them to the environment using specific protocols (OpenFlow, NetConf, SNMP, etc). In the scenario of cooperative perception, SDVN controller implements corresponding NBIs and SBIs for three key function components, i.e., context manager, access manager, and routing manager. The context manager periodically requests the D-plane elements to upload their context information to the C-plane. Based on the context information, the access manager associates OBUs with the most appropriate RSUs. And then the routing manager pushes flows to promote the data sharing.

In contrast to the geographically static network topology owned by traditional SDN controllers, with periodically collected context information from vehicles and a static HD map, the SDVN controller in the proposed architecture establishes a geographically dynamic network topology, which not only reflects the node and link status but also presents the obstacle information (e.g., buildings, trees, non-connected vehicles) that is critical to control mmWave V2X communications. The access and routing managers can utilize the topology information to reduce the blocking probability of mmWave caused by unconnected obstacles appearing between a certain V2X link. Vehicles and RSUs with sensors capture these unconnected obstacles and upload them as context information using collective perception message (CPM). Figure 3.2 illustrates the topology creation. Figure 3.3 shows the visualization of the topology.

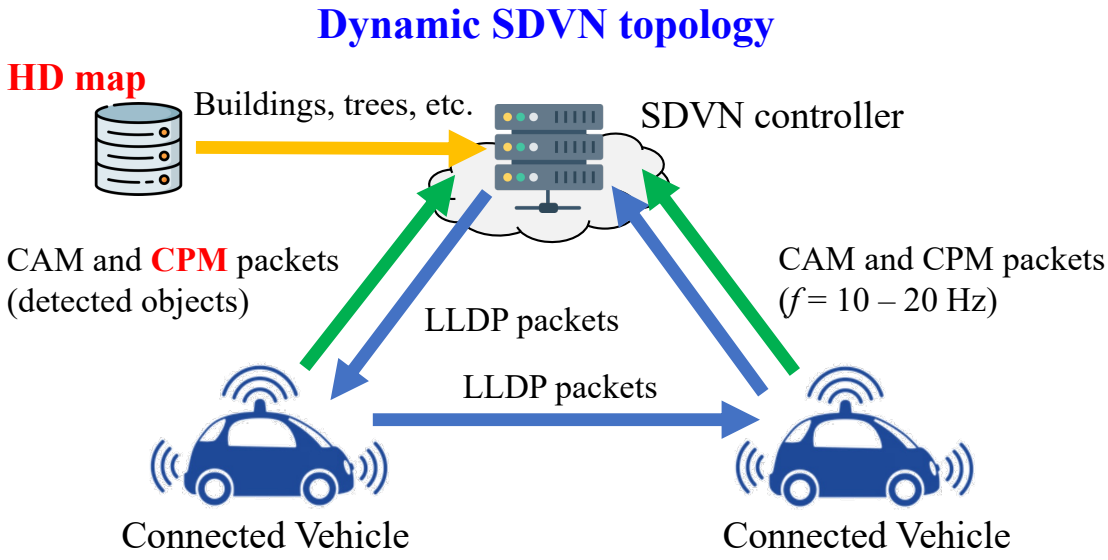

Figure 3.2: Creation of SDVN topology (LLDP: link layer discovery protocol, CAM: cooperative awareness message, CPM: collective perception message).

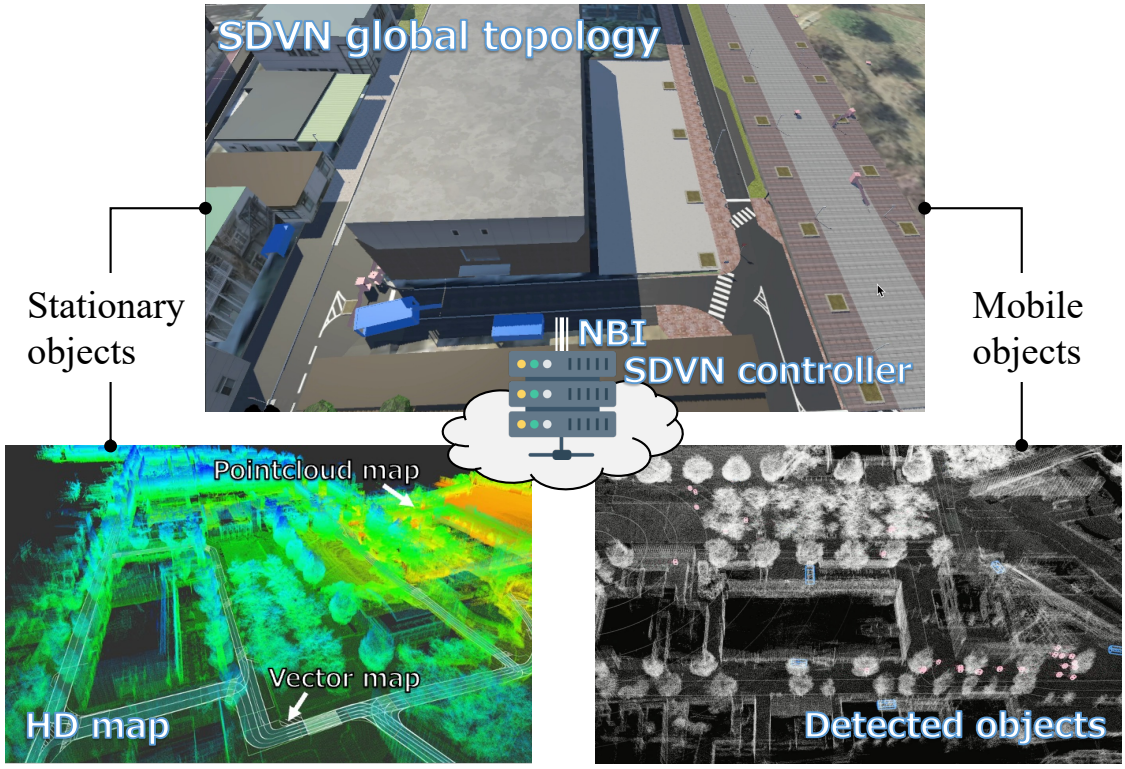

Figure 3.3: Visualization of the SDVN topology.

In order to meet the safety requirements from the aspect of vehicular network performances, mmWave as well as legacy V2X technologies are exploited:

1) MmWave V2X access layer: The broadband mmWave is the only means to support cooperative perception of HD maps, because the conventional V2X technologies, i.e., DSRC and LTE-V2X can not provide multi-gigabit data rates due to the limited bandwidth. In the proposed architecture, the access of mmWave V2X is under the coordination of SDN controller. With a global network view, the SDN controller can monitor the V2X status (e.g link stability) and help vehicles create dynamic V2X accordingly. Therefore, the negative impacts of severe path loss, blockage and fast fading on mmWave V2X can be timely noticed and minimized.

2) MmWave backhaul layer: The mmWave meshed network is a cost-efficient architecture that can be adopted to compose the vehicular backhaul. It can make full use of the network capacity enhanced by mmWave V2X. With SDN, the backhaul can be dynamically constructed in adaptation to the context information of the OBUs (e.g., position). Moreover, the QoS requirements such as optimum latency or bandwidth can be flexibly met by implementing various routing algorithms on the C-plane. Fast failover is another feature of such backhaul networks, since the SDN controller monitors the global link status in real time and can quickly handle any network failure.

3) LTE-V2X/DSRC control layer: Though the legacy V2X technologies cannot support the safety information (e.g., HD map) exchange which requires gigabit data rates and millisecond latency, they have demonstrated their adaptability and reliability of supporting a number of V2X services (e.g., pre-crash warning) in highly mobile environments. Hence, they are qualified to provide stable control signals for the SDVN C-plane. Since the LTE base station has a high penetration rate both in urban and rural areas, it can provide extensive user coverage. Meanwhile, free control resources will be usable as more and more DSRC modules are deployed in smart cities.

3.3 Prototype system and indoor verification

3.3.1 Prototype system

The deployment of the software-defined dynamic mmWave V2X network is initiated by the indoor implementation based on a prototype system. Table 3.1 lists the hardware components.

Table 3.1: Indoor Prototype Hardware

Hardware Name	**Specifications**
2D LiDAR	Model: Hokuyo UST-10LX Scan angle: 270° Resolution: 0.25° Rotation rate: 40 Hz Accuracy: ± 40 mm
3D LiDAR	Model: Velodyne Lidar VLP-16 Scan angle: 30° (vertical), 360° (horizontal) Resolution: 2° (vertical), 0.1°-0.4° (horizontal) Rotation rate: 5-20 Hz Accuracy: ± 30 cm
Wi-Fi AP	Model: Cisco Aironet 1850 Series Standards: IEEE 802.11n, 802.11ac MIMO: 4×4 Antenna: 2.4 GHz/3 dBi, 5 GHz/5 dBi, omni
Wigig Antenna (Type A)	Model: Intel Lens Antenna Scan angle: ±4.5° (vertical), ±17° (horizontal) 3 dB bandwidth: 7° (vertical), 3.5° (horizontal) Gain: 25.97 dBi
Wigig Antenna (Type B)	Model: Intel Lens Antenna Scan angle: ±7° (vertical), ±13.5° (horizontal) 3 dB bandwidth: 6.4° (vertical), 2.9° (horizontal) Gain: 25.4 dBi
Mobile Robot	Model: Kobuki Turtlebot II Maximum translational velocity: 70 cm/s Payload: 5 kg (hard floor), 4 kg (carpet)
PC/Laptop	OS: Ubuntu 16.04 Wireless LAN: IEEE 802.11a/b/g/n/ac

The OBU consists of one 2D/3D LiDAR, a pair of WiGig antennas and one control PC. And it is built on the Kobuki Turtlebot II, a low-cost mobile robot for education and research. The equipped 2D/3D LiDARs are used to create dynamic HD maps for automated driving. And the WiGig antennas enable ultra-high rate mmWave V2X communications for map sharing. As the brain of the OBU, the control PC processes the input data, plans the navigation route and interacts with the engine of the robot based on the ROS, an open-source robotics software project that commonly utilized by application developers of automated driving. The RSU is composed of one 3D LiDAR, a pair of WiGig antennas and one management PC. One of the WiGig antenna is used for mmWave access, the other is used for mmWave backhaul. The management PC deploys application agents for C-plane registration and map merging, or simply forwards raw sensor data to the next hop through the OVS, an open-source implementation of a distributed virtual multilayer switch that supports OpenFlow protocols. The SDN controller is running on a PC with the ODL framework, which is the most pervasive open-source SDN controller that provides abundant native features and well-defined APIs for network monitoring and traffic management. In addition, ODL supports flexible deployments of customized applications or protocols, which contributes to the extension of control functions for the software-defined vehicular network.

Figure 3.4(a) and Fig. 3.4(b) present the architecture of the prototype system from the perspective of hardware configuration and software platform respectively. Since Wi-Fi is widely used indoors, it can replace DRSC and LTE-V2X in the PoC. As seen in Fig. 3.4(a), wireless C-plane is constructed by a cluster of Wi-Fi APs that are deployed on the corridor roof. Basically, the out-band control channel carries two types of messages. One is the context messages collected from D-plane elements (OBUs, RSUs) periodically. The other is the control messages (access control, routing control) sent from the SDN controller once cooperative perception is activated. WiGig antennas establish mmWave V2X links for D-plane, where big LiDAR traffic is transmitted through the organized path to the target OBU. According to the specifications, on the one hand, 2D LiDARs have shorter detection range but higher accuracy comparing with 3D LiDARs, so they are preferred to be used for the indoor PoC. On the other hand, 3D LiDARs generate more data volumes, which is suitable to highlight the performances of mmWave V2X transmission. Therefore in this PoC, 2D LiDAR maps will only be utilized for self-navigation while 3D LiDAR maps are shared to ensure better safety.

Open-source software also plays an important role in this prototype system. The three

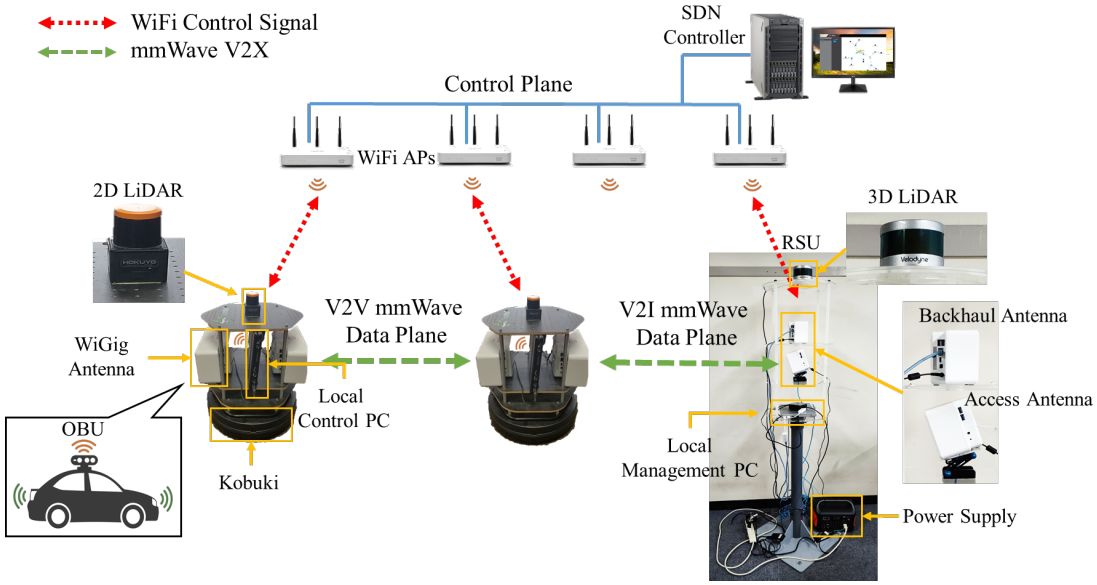

(a) Hardware configuration.

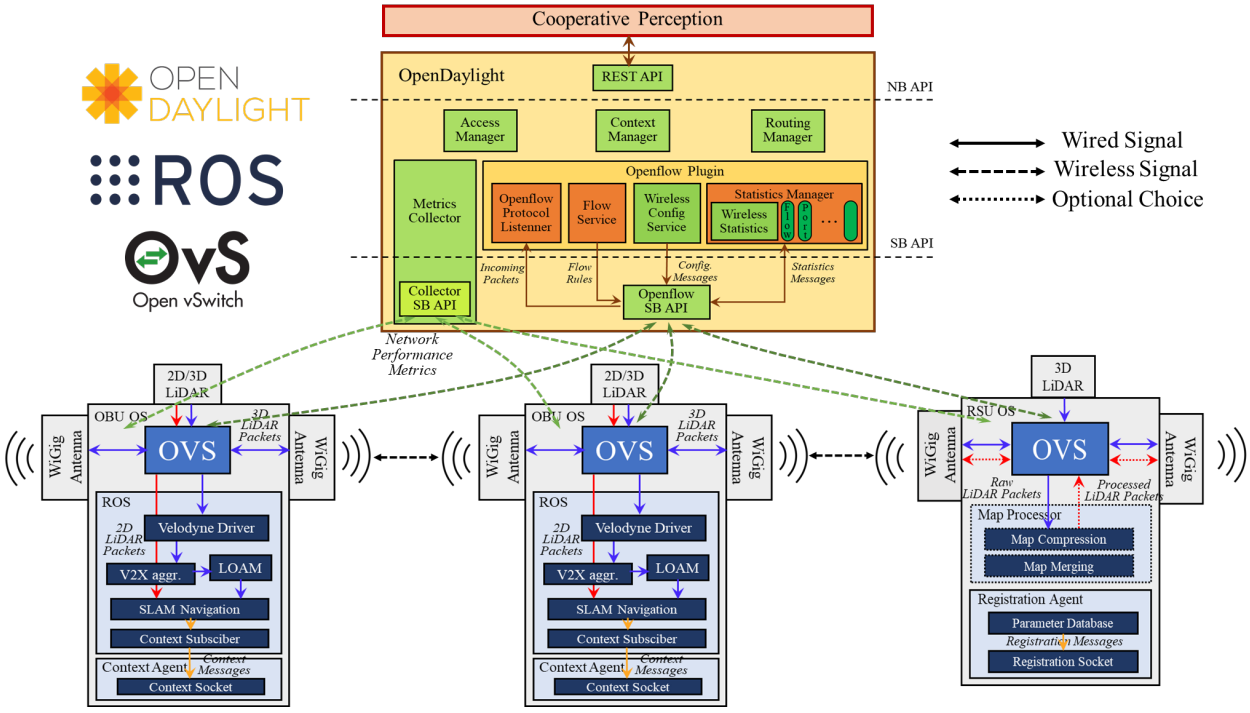

(b) Software framework.

Figure 3.4: Prototype details of indoor proof-of-concept.

representatives are ODL, ROS and OVS, as shown in Fig. 3.4(b). SDN control relies on the ODL platform, in which both native and customized components are implemented. Native components such as the metrics collector and OpenFlow plugins provide basic network information and configuration tools. Upon them, customized components, i.e., context manager, access manager and routing manager in this case, achieve extensive functions for cooperative perception in the mmWave V2X networks. Automated driving of OBUs depends on the ROS, which provides hardware abstraction for robotics motion control by applications or algorithms, and device drivers for 2D/3D LiDARs. Based on these fundamentals, simultaneous localization and mapping (SLAM) is implemented to create static and dynamic maps for automated navigation. In addition, OVS enables the map sharing among D-plane elements. Through the OpenFlow SBI, OVS updates flow tables that decide the data forwarding according to the dynamic routing decisions made by SDN controller.

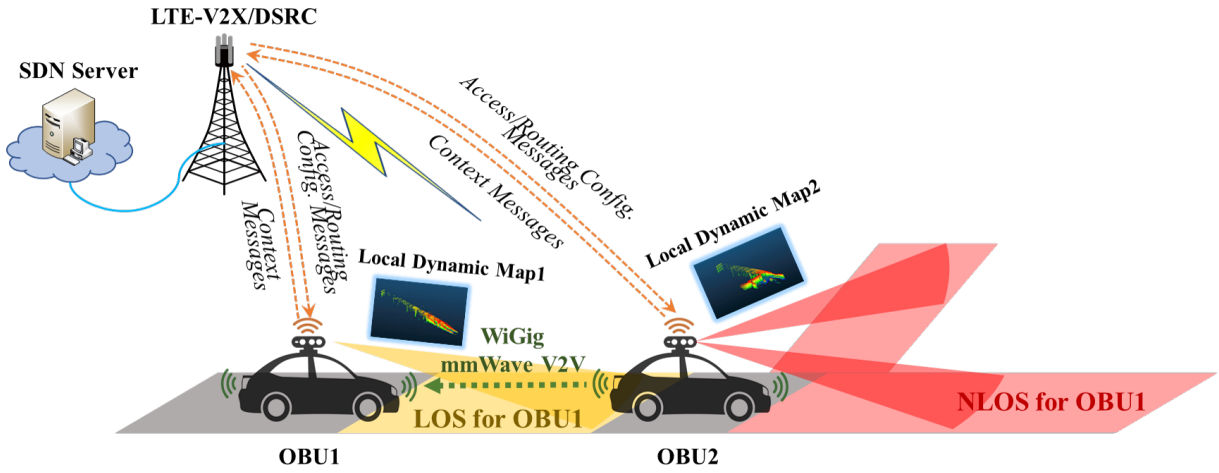

Figure 3.5: Scenario of cooperative perception over mmWave V2V.

3.3.2 Cooperative perception over mmWave V2V

Although on-board sensors are replacing human drivers' eyes, the vision of automated vehicles can still be blocked by obstacles while driving. For example, when inter-vehicle distance becomes too short, the front vehicle may decrease the LOS area of the behind vehicle, as shown in Fig. 3.5. This will lead to potential traffic hazards if the behind vehicle tries to overtake without the notification of oncoming vehicles or passes through a busy intersection without the information of both sides. Therefore, in order to acquire a boarder view for safe

driving, cooperative perception is necessary between the front vehicle and the behind vehicle over mmWave V2V. Under the proposed architecture, SDN controller periodically collects the context information of the two vehicles. Context information such as vehicle position, received signal strength indicator (RSSI), and etc can be the reference for mmWave access configuration. As soon as the V2V link is established, routing configuration messages are distributed to both vehicles to direct the data flows from OBUs.

To demonstrate the performance of our prototype system in above-mentioned scenario, an indoor PoC [1] is carried out. The test field is a long corridor over 50 m with a single fork. Two OBUs are deployed to represent the vehicle front and the vehicle behind. Since the corridor width is narrow, about 2 m, it is hard for the OBU to detect the region behind the fork before the OBU comes very close. Therefore, the OBU front will take responsibility to transmit its 3D LiDAR map which contains the information of this NLOS area for the OBU behind. As Fig. 3.6(a) indicates, the Wi-Fi APs on the roof provide wireless C-plane. SDN controller activates cooperative perception via mmWave V2V according to the vehicle's relative distance (e.g., 5 m), which can be determined by different safety requirements based

[1] https://www.youtube.com/watch?v=a5fd5oXv4qI

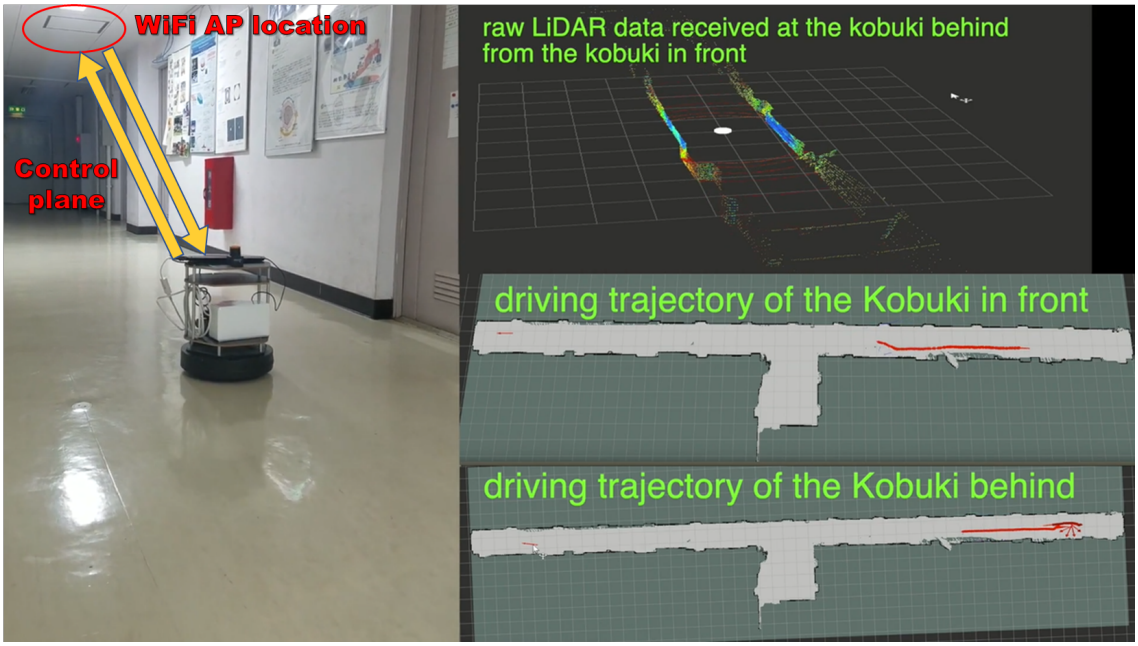

(a) SDN control through Wi-Fi signal.

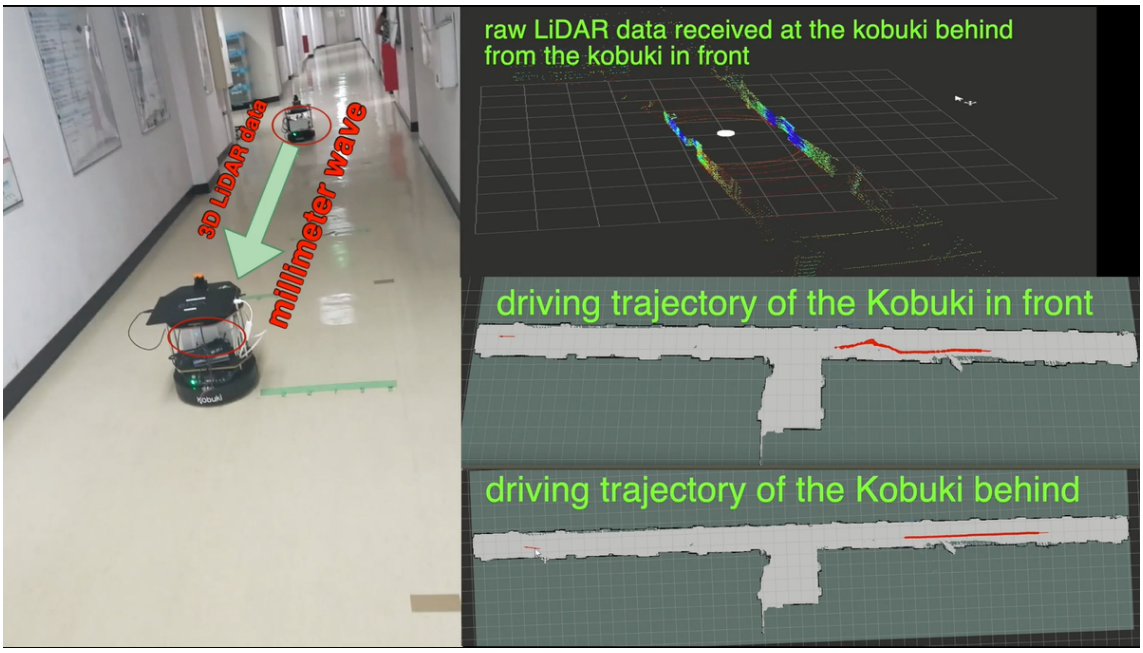

(b) Cooperative perception via mmWave V2V.

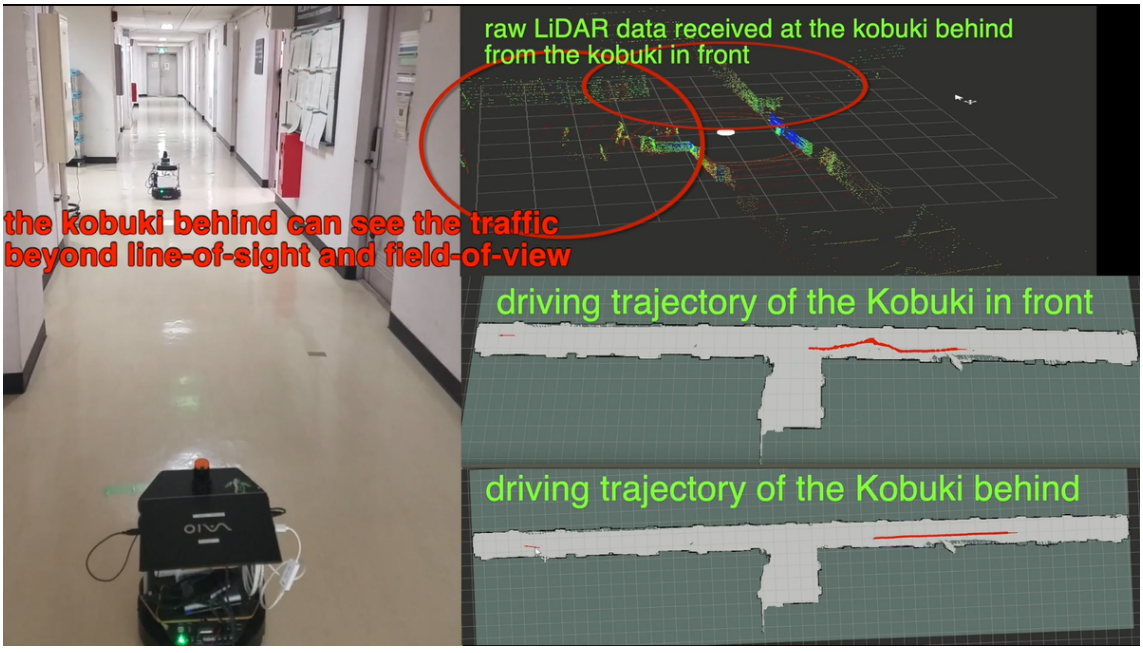

(c) Enhanced driving safety.

Figure 3.6: Scenario and demonstration for software-defined mmWave V2V.

on the speed or the degree of visual obstruction. Fig. 3.6(b) shows the map transmission process. The received 3D LiDAR map is presented at the top right of the figure. Apparently, the perception of the OBU behind is greatly enhanced that it can touch the field beyond LOS, as circled in Fig. 3.6(c), which highlights the benefit of mmWave V2V for large LiDAR data transmission. Besides, with software-defined mmWave V2V communications, the timing for cooperative perception can be flexibly modified by applications depending on specific safety requirements.

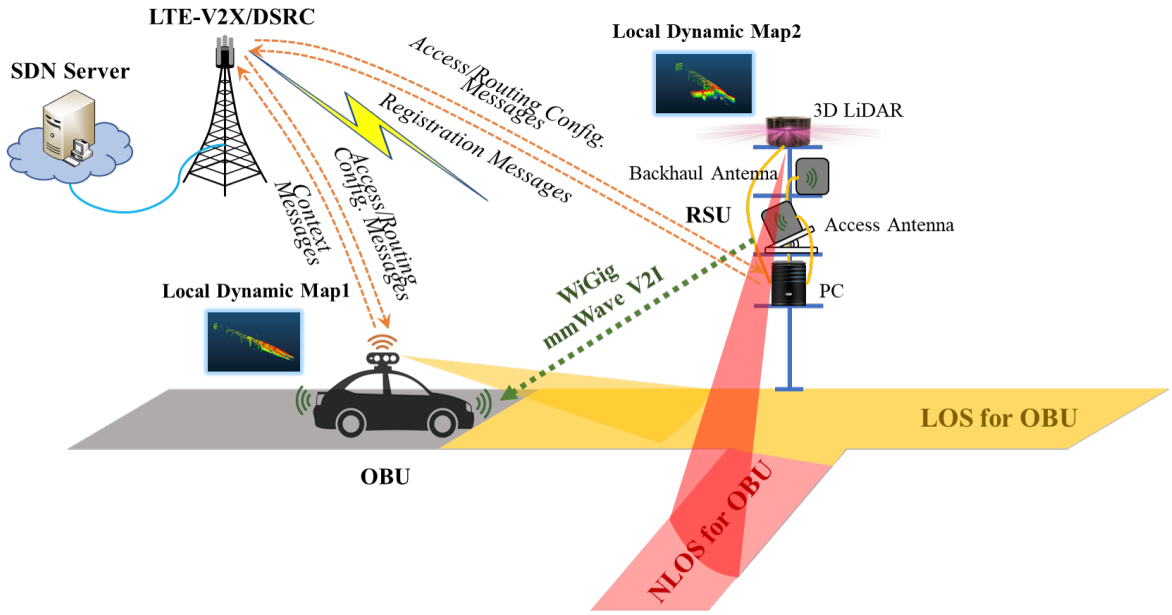

Figure 3.7: Scenario of cooperative perception over mmWave V2I.

3.3.3 Cooperative perception over mmWave V2I

Besides V2V communications, another sensible method to improve the driving safety is to communicate with RSUs, of which wider deployments can be envisioned in the future ITS. To save costs, RSUs are probably installed on the existing road infrastructures like street lamps and traffic lights. Meanwhile, their higher altitude than OBUs' brings them bird's eye views for broader monitoring. This contributes to the early warning in blind areas when a vehicle tries to pass the intersection with heavy traffic, as shown in Fig. 3.7. By cooperative perception over mmWave V2I, dynamic HD maps from the RSU can be exploited to compensate for the loss of vehicle perception in NLOS regions. Under the proposed archi-

tecture, this process is also managed by SDN controller. Once a RSU is built, its location and coverage will be record to the global topology. When vehicles move towards the RSU, their real-time positions are collected and used for control. If the relative distance is within the coverage, SDN controller starts mmWave access and routing configurations to perform cooperative perception.

To demonstrate our prototype system also adapts to this scenario, an indoor PoC is implemented. The test field keeps the same as previous mmWave V2V demonstration, where a fork of the corridor results in a NLOS region for upcoming vehicles. In this case, one OBU is deployed on the Kobuki robot and one RSU is installed on a multilayer bracket. The bracket is placed near the fork, but at the opposite side for global LiDAR monitoring. The communication coverage of RSU is an importance parameter that should be predefined and registered to the SDN controller. Although transmission throughput suffers from severe reflections in indoors, it remains higher than 1 Gbps up to 35 m. Moreover, transmission latency fluctuates slightly within the whole distance of the corridor (approximately 2.5 ms/packet). Considering the NLOS distance from the fork, the coverage value is set to 5 m. Fig. 3.8(a) shows the scenario when the OBU is moving out of the coverage. In the top right of the figure, the merged LiDAR map only contains the static map (grey points) and the OBU map (red points), which means the cooperative perception is still off. Since the indicated NLOS region is uncovered with dynamic point clouds, automated driving is under risks. Instead, Fig. 3.8(b) shows the scenario when the OBU moves into the coverage. At this moment, cooperative perception is initiated by SDN controller. In the top right of the figure, the RSU map (green points) appears in the merged LiDAR map and its dynamic point clouds already cover the NLOS region before the OBU arrives at the fork. Hence, with software-defined mmWave V2I communications, the driving safety is greatly improved.

3.4 Outdoor proof of concept

3.4.1 Prototype hardware

The indoor prototype system has achieved the network functions for software-defined mmWave V2X, and the indoor PoC has demonstrated its effectiveness for safety enhancement under two typical modes of cooperative perception, i.e., mmWave V2V and mmWave V2I communications. In order to test the robustness and reliability of our network in real environments,

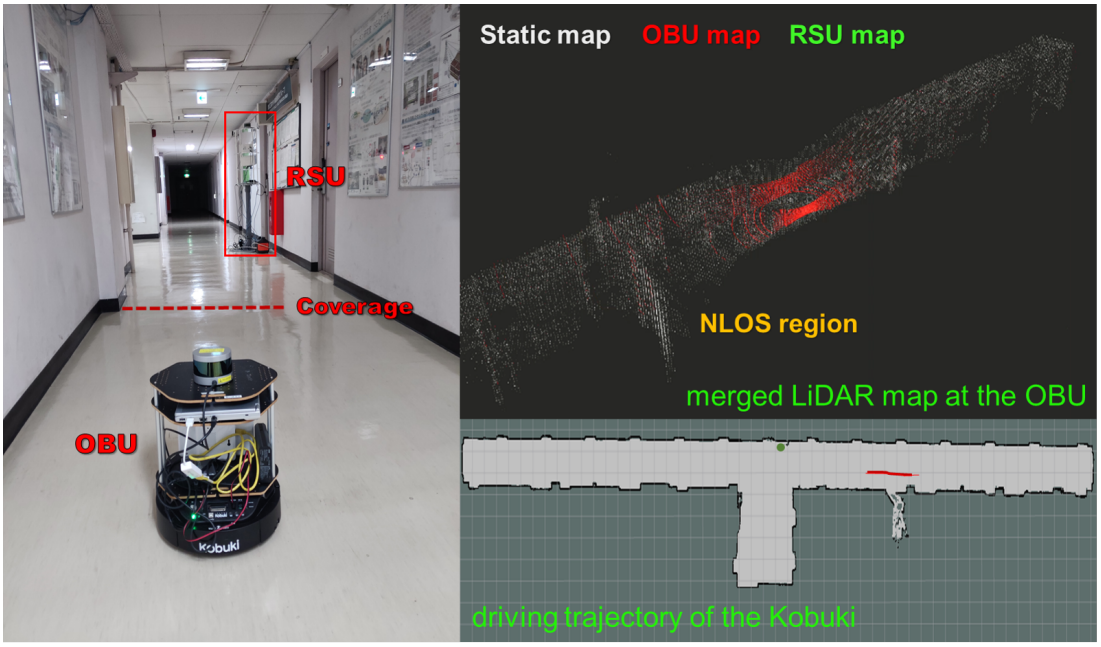

(a) Driving without cooperative perception.

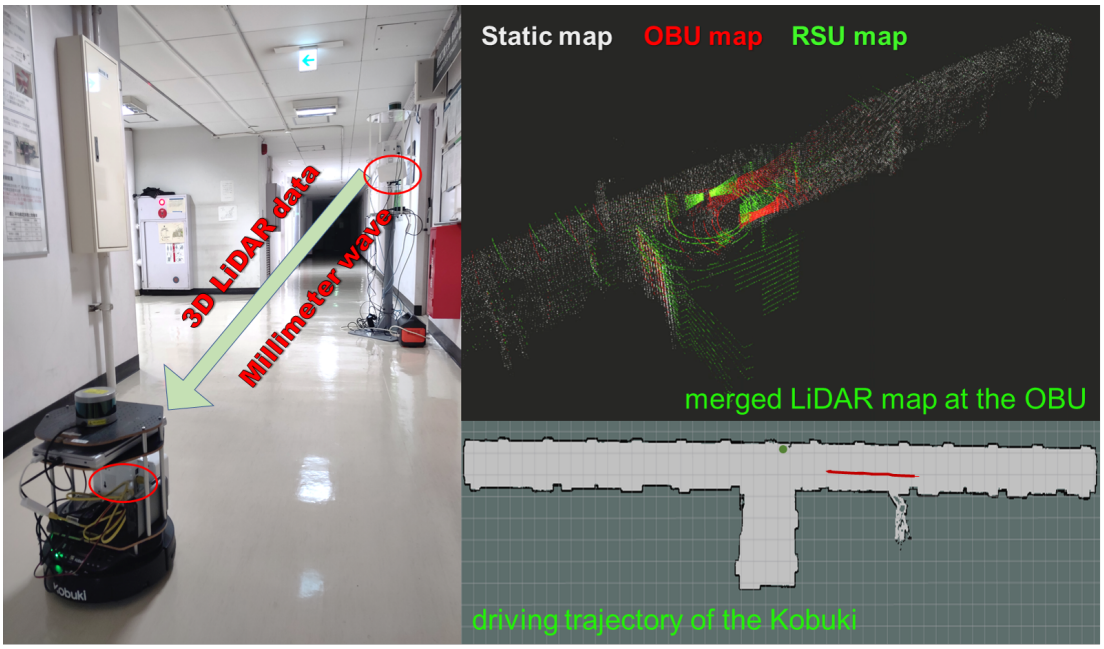

(b) Cooperative perception via mmWave V2I.

Figure 3.8: Scenario and demonstration for software-defined mmWave V2I.

Table 3.2: Outdoor Prototype Hardware

Hardware Name	**Specifications**
WiGig AP	Model: NETGEAR X10 R9000 Standards: IEEE 802.11ac, 802.11ad Bands: 800 Mbps @ 2.4 GHz, 1733 Mbps @ 5 GHz, 4600 Mbps @ 60 GHz
WiMAX Card	WAN interface: WiMAX 2+ @ 2.5 GHz Speed: Uplink $\leqslant$ 30 Mbps, Downlink $\leqslant$ 440 Mbps Size: 111×62×13.3 mm
PC/Laptop	Model: Acer TravelMate Series OS: Ubuntu 16.04 USB ports: 4 WLAN interface: 802.11ac, 802.11ad, Bluetooth
Vehicle	Model_1: Toyota Estima (grey) w OBU Model_2: Toyota Ractis (blue) w/o OBU

an outdoor PoC [2] will proceed by replacing or adding some hardware for the new outdoor prototype system. Table 3.2 lists the additional hardware. In this case, the OBU is directly deployed to a real vehicle rather than the mobile robot. A 3D LiDAR with the same type as indoors is fixed on the top of the vehicle. The model of the control PC is substituted by Acer, which builds in 802.11ad chipsets. It comes with the 32-element phased antenna array. Therefore, it's not necessary for the OBU to equip another WiGig antenna as indoors so the volume can be more compact and the power consumption can be less. As for the RSU, one of its antennas that serves for mmWave access is replaced by NETGEAR X10 R9000, which uses 802.11ad module and can switch to the AP mode. Saha *et al.* completed a review of the connection performances between Acer and NETGEAR X10 R9000 using WiGig, showing that the maximum transmission range in outdoors is about 20 m when the average throughput is above 1 Gbps, and the Gbps communication is possible for client angles in $[-60°, 75°]$ or AP angles in $[-45°, 30°]$ [56]. Since the outdoor field is too wide to be covered by Wi-Fi signals, WiMAX cards are utilized to provide wireless C-plane at 2.5 GHz, performing the same roles

[2] https://www.youtube.com/watch?v=di1GUaA5Q4I

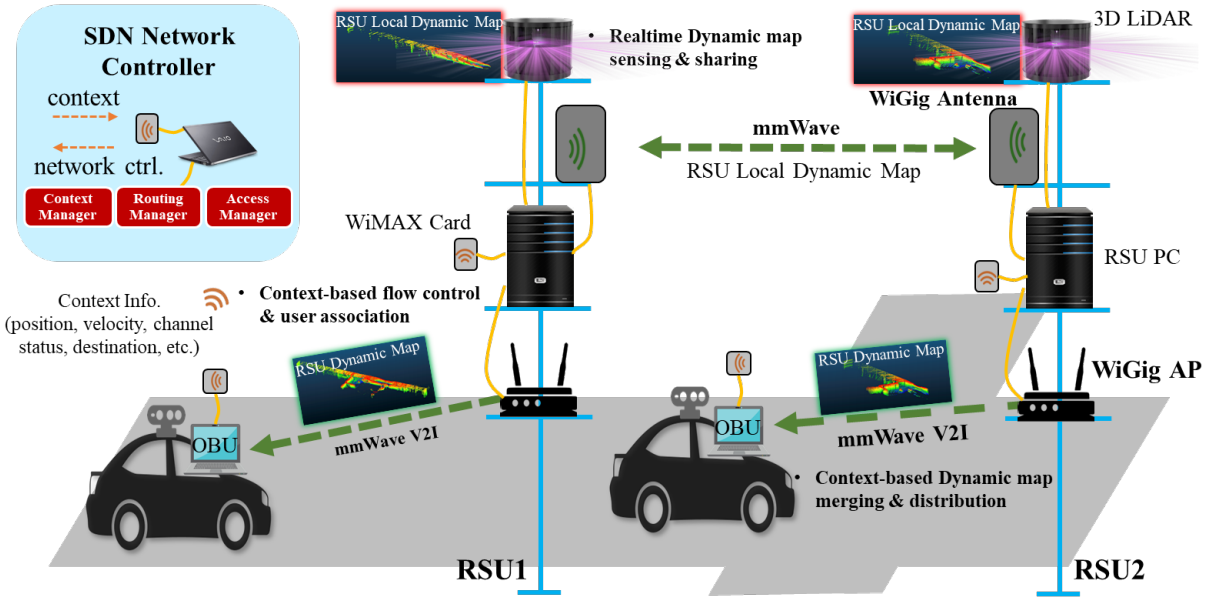

Figure 3.9: Hardware configuration for the outdoor prototype system.

of DSRC and LTE-V2X as the system design. The supported speeds for uplink and downlink transmission are adequate because the context messages and control messages won't occupy so much bandwidth.

Figure 3.9 gives an overview of the hardware configuration for the outdoor prototype system, which includes one OBU, two RSUs and one SDN control server. Since the demonstrations of indoor prototype system doesn't take mmWave backhaul capacity into account, the new prototype system will incorporate one mmWave backhaul link between the RSUs for dynamic map routing. Therefore, the network performances of mmWave V2X access, mmWave backhaul and SDN management can be all confirmed in the outdoors. Note that each D-plane and C-plane element is equipped with a WiMAX card for stable interconnections. And the only OBU appears twice in Fig. 3.9 just in order to highlight the association handover with RSU1 and RSU2. Considering the limited perception range of 2D LiDARs, they will not be used in the outdoor PoC.

3.4.2 Scenario description

The test field is selected at a L-shaped bend. In addition to the test vehicle with OBU, non-test vehicles in the lane are also passing normally. The driving route of the OBU has been marked on the photo of Fig. 3.10. To set up a dangerous scene artificially, a blue

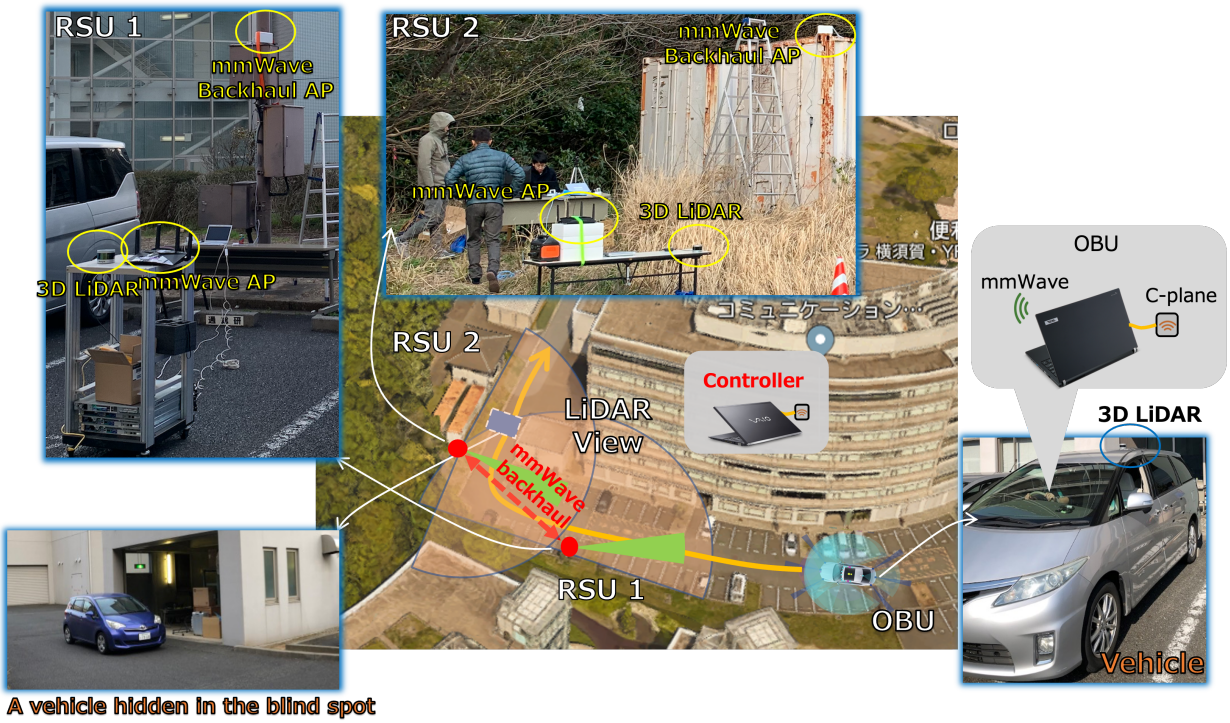

Figure 3.10: Photos of field trial.

vehicle without OBU is hidden as an oncoming vehicle at the other end of the L-shaped bend, which belongs to the NLOS region of the OBU. In Fig. 3.10, the locations of the two RSUs are indicated by red points. They are deployed at each side of the bend, so their LiDAR views can fully cover the dynamic environments of the whole area. Because the WiMAX base station has very wide coverage, the SDN controller can be placed even miles away. In order to test cooperative perception through the software-defined dynamic mmWave V2X network, along the driving route, network functions will be implemented by four steps. ① Leave the start point: When the test vehicle begins to move from the start point, the OBU is still out of the communication coverage of any RSU, which is set to 20 m in outdoors. At the moment, SDN controller will not activate cooperative perception but continuously collects and judges the context information (i.e., position) from the OBU via WiMAX C-plane. ② Associate with RSU1: When the test vehicle approaches RSU1. As soon as it enters the communication coverage, SDN controller will send configuration messages for V2X access and backhaul routing, by which the local dynamic maps from RSU1 and RSU2 are simultaneously forwarded to the OBU via mmWave D-plane. Then the OBU can create a global dynamic map using map merging techniques. ③ Handover to RSU2: After the test

vehicle passes RSU1, for the OBU, its dynamic map will not benefit the driving safety any more. When the OBU enters the coverage of RSU2, SDN controller will send configuration messages for mmWave V2X handover. In this case, only the dynamic map of RSU2 will be forwarded to the OBU without utilizing the mmWave backhaul. ④ Pass the bend: With cooperative perception, the test vehicle is expected to drive through the bend safely. After it leaves the coverage of RSU2. SDN controller will deactivate cooperative perception.

As a matter of fact, it is the interactions of C-plane and D-plane that achieves the SDN control in above mentioned scenario. The details are described in Fig. 3.11. The process starts from the registration of RSUs as soon as they are deployed. The registration information includes ID numbers, locations, AP parameters and etc. This information is integrated on the C-plane and used to generate a backhaul network topology for V2X. From the SLAM, the OBU subscribes the context information (vehicle position) and uploads to SDN controller almost in real time. When the trigger condition is reached, i.e., within the communication coverage, SDN controller will activate cooperative perception by firstly distributing new flow tables to all D-plane elements for map data routing. Secondly, mmWave V2X access will be established or handover under the coordination of SDN controller. Note that the MEH which indicates the mobile edge host plays a role of map merging and can be located both in RSU and OBU.

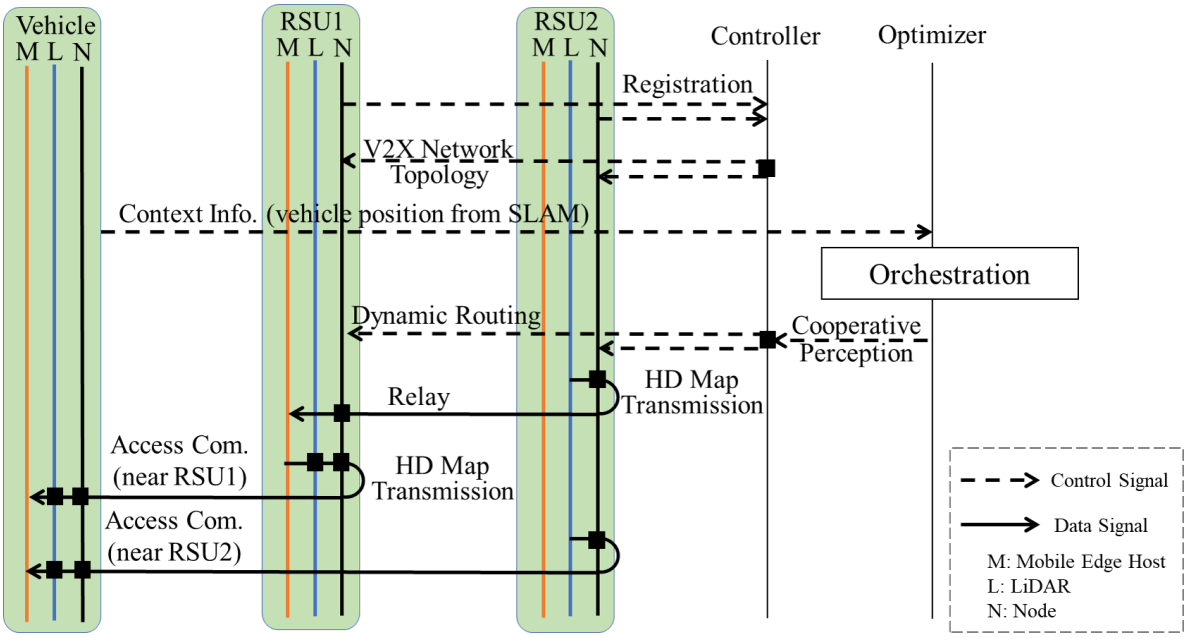

Figure 3.11: Interactions between C-plane and D-plane.

3.4.3 Results of field trials

The graphical user interface (GUI) of OBU presents the received and merged LiDAR point clouds from dynamic cooperative perception, which are important resources for SLAM-based navigation. In Fig. 3.12, the three sub-figures correspond to the three critical steps of safe automated driving mentioned in the last subsection. Fig. 3.12(a) shows the dynamic HD map of OBU when it starts to move. In the map, the white point clouds form the static map and will be updated in a long period. Besides, the green point clouds from the OBU LiDAR compose the dynamic vehicle map. Except the static map and the vehicle map, no RSU maps appear in the GUI since cooperative perception is not activated yet, i.e., the OBU has not reached the communication coverage of RSU1. In this case, the perception range of OBU is too limited to detect the potential risk at the other side of the bend.

Figure 3.12(b) and Fig. 3.12(c) show the dynamic HD maps of OBU when mmWave V2X association and handover are implemented by dynamic cooperative perception. In Fig. 3.12(b), RSU1 map (red point clouds) and RSU2 map (yellow point clouds) both appear. This is in accordance with the mechanism, that all local dynamic maps of RSUs will be forwarded to the OBU through the mmWave backhaul and V2X links under SDN control. The merged global dynamic map greatly extends the perception range of OBU as it can detect an oncoming vehicle in the NLOS region (56.86 m away, 5.12 s in advance when vehicle velocity equals 40 km/h), and then take earlier measures (e.g., emergency brake) to avoid the collision. If there is no terrain restriction, this perception performance can be further enhanced. The deployed mmWave backhaul antennas support a communication range over 200 m, thus a vehicle at 80 km/h will get more than 10 s to respond. Furthermore, Fig. 3.12(c) presents the handover scene, in which the mmWave V2X switches to the RSU2 since the RSU1 map no longer provides safety-related information. At the moment, the global map only consists of the static map, the vehicle map and the RSU2 map. Although the red point clouds remain in the GUI, they already became static. On the contrary, the yellow point clouds fully cover the moving vehicle, which indicates that the RSU2 map is dynamically transmitting to the OBU.

Figure 3.13 presents critical network performance indicators measured while the vehicle is staying within the RSU coverage (i.e., 20 m). As Fig. 3.13(a) shows, with mmWave V2X, both of the transmission control protocol (TCP) and user datagram protocol (UDP) throughputs exceed 1 Gbps. A peak value of 2.01 Gbps appears when using TCP and keeping the LOS distance of 5 m between RSU and OBU. Even at the coverage edge, the throughputs of TCP

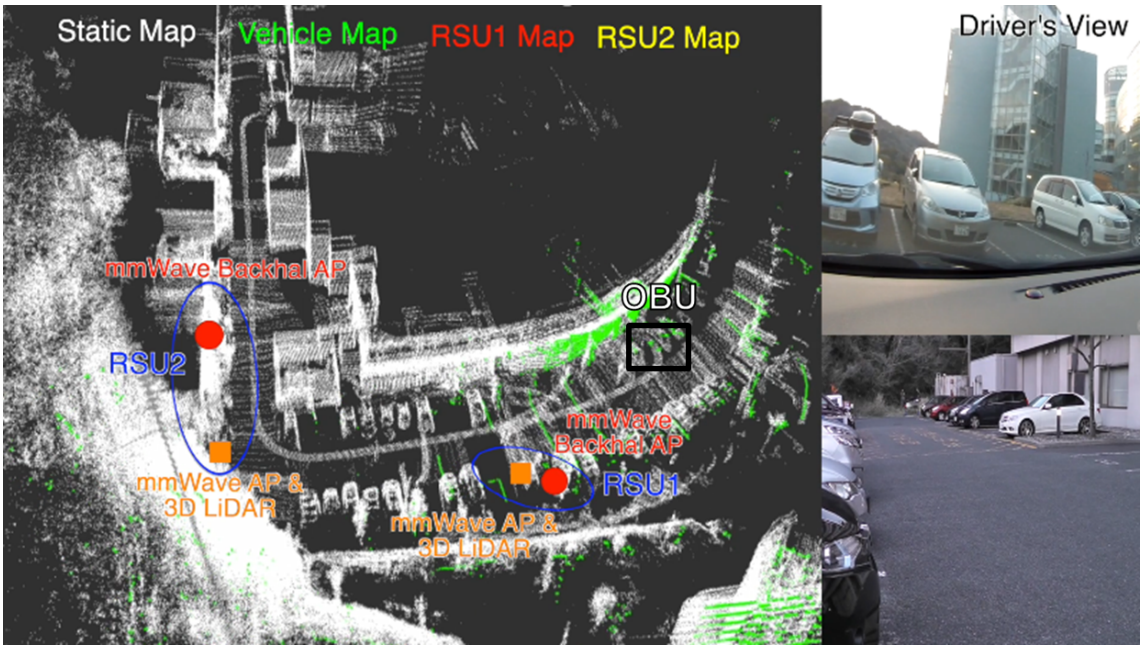

(a) Leave the start point.

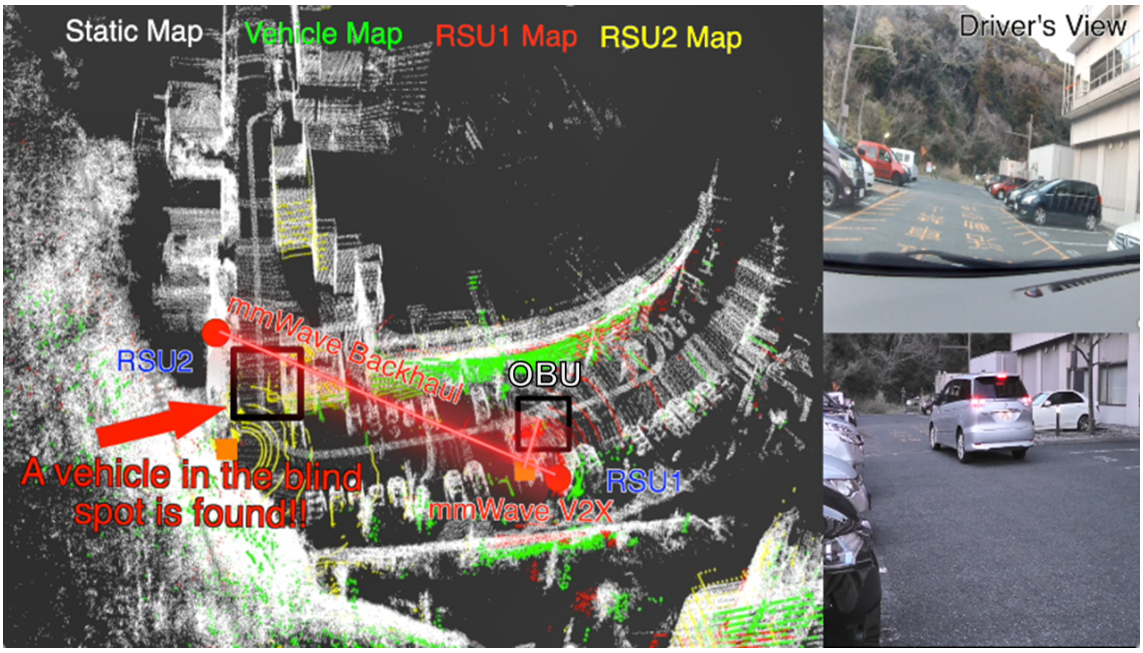

(b) Associate with RSU1.

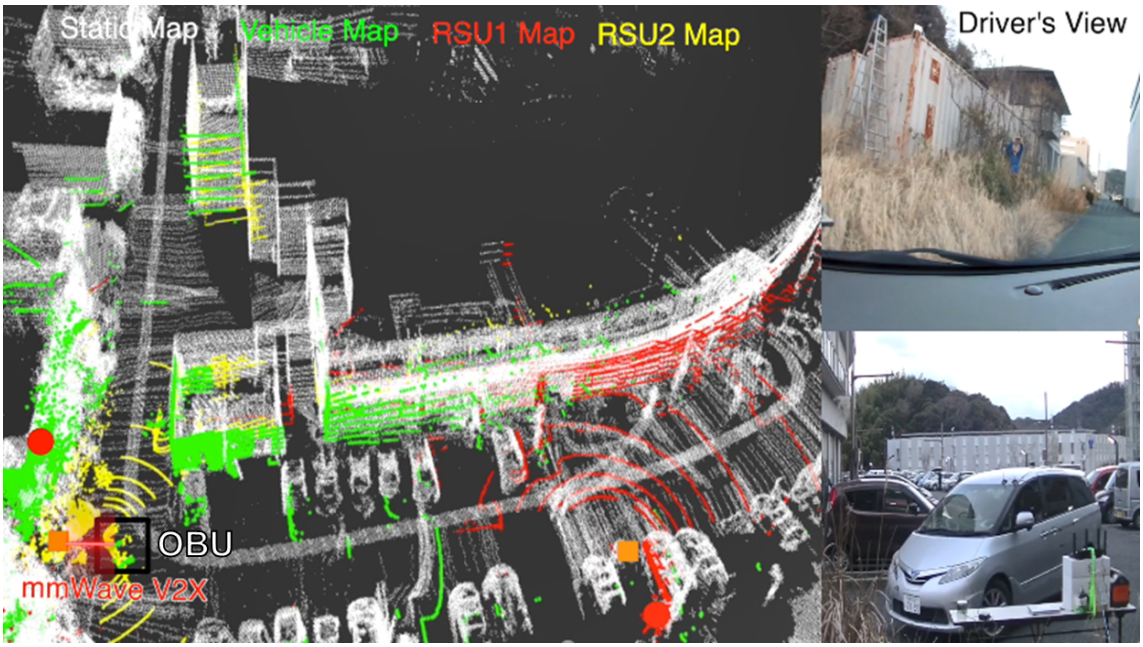

(c) Handover to RSU2.

Figure 3.12: Point clouds of OBU from dynamic cooperative perception.

and UDP still sustain at a relatively high level, i.e., 1.65 Gbps and 1.52 Gbps, respectively, which far surpass the maximum theoretical values of legacy V2X (e.g., 27 Mbps of DSRC and 28.8 Mbps of LTE PC5). Since the LiDAR utilized in the field trial generates UDP packets with a size of 1248 bytes, the latency performance of mmWave V2X for one LiDAR packet transmission is evaluated. As shown in Fig. 3.13(b), the average round-trip time (RTT) at 5 m and 20 m are 1.116 ms and 1.048 ms, respectively. It does not reveal any appreciable performance degradation as the LOS distance increases. Besides, all measured latency within the RSU coverage is less than 3 ms which is already the toughest latency requirement for sensor information sharing claimed in the 3GPP Technical Specification (TS) 22.186 [57]. In addition, the packet loss rate of UDP transmission via mmWave V2X is recorded to characterize its reliability. As Fig. 3.13(c) shows, although the packet loss rate slightly grows as the LOS distance increases, the highest value is 0.043% at 20 m. It keeps below 0.05%. Therefore in this network, mmWave V2X can ensure the reliability of at least 99.95% for LiDAR map transmission within the RSU coverage.

Throughout the entire process of automated driving, SDN management does endow efficiency and flexibility to mmWave association and backhaul routing, and also provides re-

markable safety enhancements to the OBU, which demonstrates the benefits of our proposed network architecture.

3.4.4 Discussions on scalability

It is worth emphasizing that the proposed network system has sufficient scalability, although the PoCs were conducted with a limited number of RSUs and vehicles. It can be illustrated from three aspects: 1) C-plane capacity, 2) D-plane capacity, and 3) SDN controller performance variation under an increasing number of D-plane elements. Specifically, in the outdoor testbed, the WiMAX router used for the C-plane can support an uplink data rate of 75 Mbps. The C-plane periodically collects the context information of vehicles at 10 Hz, which occupies the largest portion of the C-plane bandwidth. The common V2X message that includes such context information is the CAM, of which the packet size ranges from 200 to 800 bytes. Therefore, the C-plane has enough capacity to collect CAMs from at least 1171 vehicles. On the other hand, the D-plane deploys the 60 GHz WiGig. The WiGig modules in the testbed have an achievable data rate of 2.5 Gbps (MCS 2-9). Since the 3D LiDAR (VLP-16) generates packets at a speed of 7.52 Mbps, if each vehicle or RSU equips only one 3D LiDAR, the D-plane can support cooperative perception among 332 vehicles or RSUs. Indeed, the SDN controller's processing capability may degrade as the number of associated D-plane elements grows. A prior study has investigated the variation of flow installation latency of some commonly used SDN controller frameworks when the OpenFlow switch number increased from 2 to 128 [58]. However, no significant latency increase (0.78 - 4.68 ms) was observed for the ODL controller, exactly the one adopted in the testbed. Hence, it can be concluded the proposed system has scalability for large-scale V2X networks and extensive cooperative perception.

3.5 Conclusion

The commercial roll-out of 5G will create a new era for ITS. As two key technologies of 5G, SDN and mmWave communications have many use cases in vehicular networks to promote safe automated driving. The benefits of mmWave V2X and SDVN have been revealed by plenty of state-of-the-art works, respectively. However, the research concerning their integration is still vacant, especially lacking full-fledged prototype systems for PoCs. This chapter discussed the performance requirements of vehicular networks to enable safe automated driving. Based

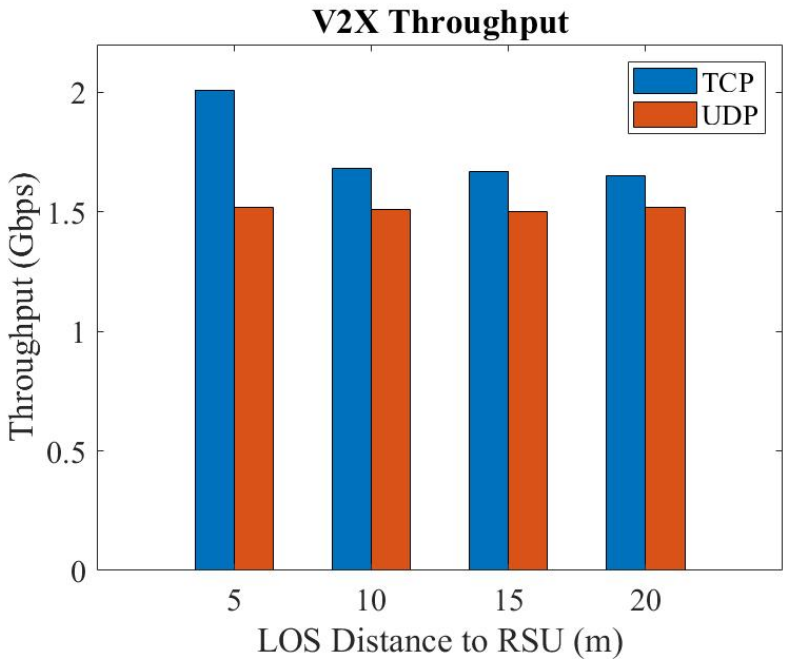

(a) Transmission throughput between RSU and OBU within the coverage.

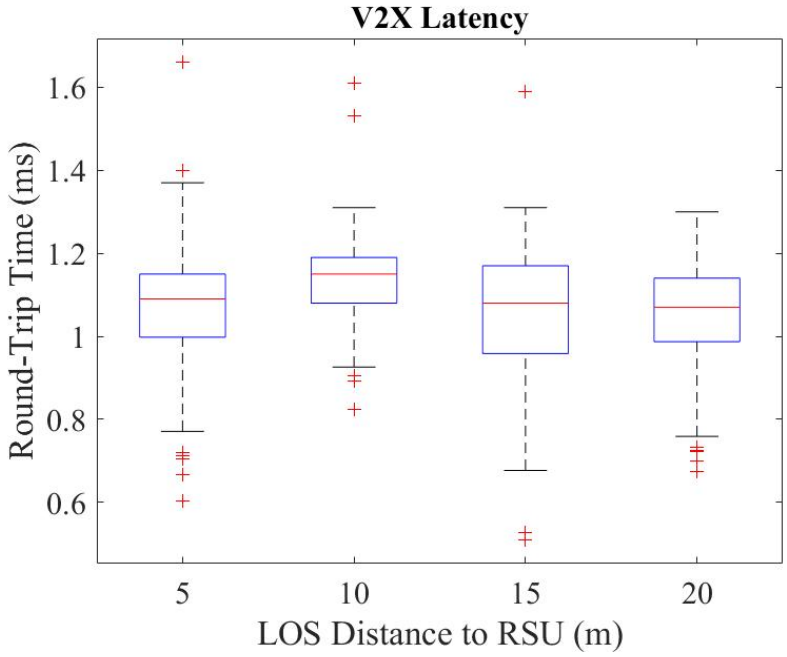

(b) Transmission latency for one LiDAR packet of 1248 bytes.

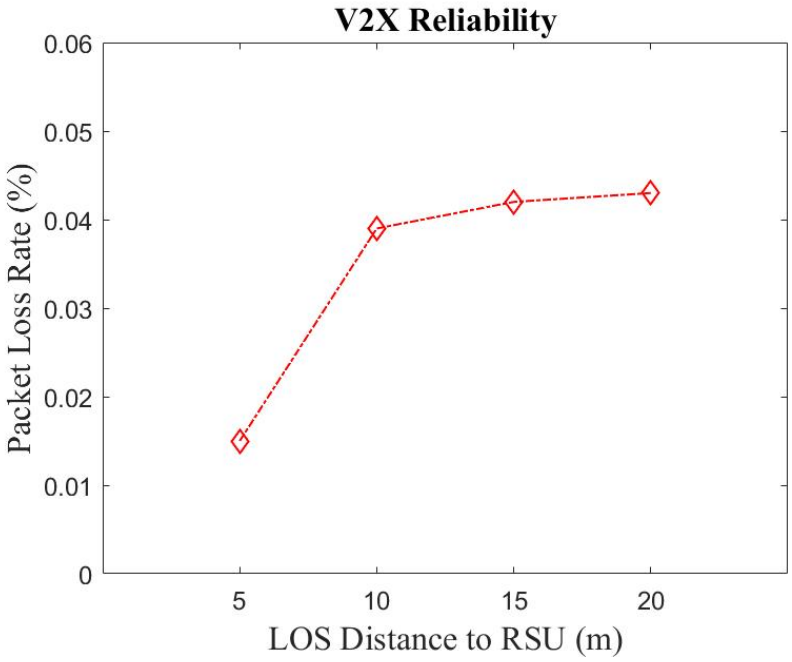

(c) Packet loss rate of UDP transmission.

Figure 3.13: Network performance with mmWave V2X.

on the discussion, a software-defined dynamic mmWave V2X network was proposed for cooperative perception. Beyond that, this chapter introduced the necessary hardware equipment and software frameworks to build prototype systems for indoor and outdoor PoCs. In the indoor PoC, the two modes of software-defined cooperative perception were implemented over mmWave V2V/V2I communications, showing that the indoor prototype system can achieve the network functions of the proposed architecture. Furthermore, with additional hardware, the outdoor PoC was carried out in real road environments. Under the dynamic management of SDN controller, the cooperative perception, which distributed raw LiDAR pointcloud data from RSUs to the vehicle over mmWave in a challenging U-bend driving scenario, was successfully performed, which verified mmWave performance, the feasibility of the proposed network architecture, and the safety benefit of cooperative perception to vehicles.

Chapter 4

Het-SDVN: Software Defined Heterogeneous V2X Network for Cooperative Perception

In order to cater to customer and automotive industry desires for advanced V2X applications and deal with their soaring QoS demands, academia, standardization organizations, and telecom operators start to throw their attention to the underexploited higher frequency bands, such as the mmWave band (30 - 300 GHz), terahertz band (100 GHz - 10 THz), and the visible light communication (VLC) band (400 - 800 THz). It is practical to envision such a future, where these high-frequency radio access technologies (RATs) and the traditional V2X technologies in the low-frequency bands (5.9 GHz, 2.5 GHz, 760 MHz, etc.) coexist and provide fundamental support to the smart mobility ecosystem. More specifically, they will be dynamically assigned to help different applications or enable the same application for different use cases or driving automation levels. As the V2X network becomes more and more heterogeneous, two main bottlenecks have been exposed:

1. Complexity of network management: As pointed out, low-frequency and high-frequency V2X will coexist in the network. They feature different characteristics in propagation (path loss, penetration capability, etc.). The network management must be adaptive to cooperative perception requirements and selected V2X. For example, broadcasting that used to be applied in IEEE 802.11p is not effective for mmWave. Multi-hop transmission is required by mmWave V2X, so the routing topology needs to be determined efficiently.

2. Interoperability between diverse networks: Currently, vehicular ad-hoc networks (VANETs) led by the European Telecommunications Standards Institute (ETSI) and cellular V2X (C-V2X) led by the 3rd Generation Partnership Project (3GPP) are independent networks. They possess their own V2X technical stacks. IEEE 802.11p and its successor IEEE 802.11bd are used for VANETs, while LTE and NR are adopted by C-V2X. The interaction and handover among these technologies have not been clearly specified.

4.1 Motivation

In the previous chapter 3, the author has designed an SDN-based mmWave V2X network and carried out extensive proofs of concept, in which both the 3GPP network (LTE) and IEEE network (IEEE 802.11ad) were involved. Their interoperability was achieved by serving different planes in SDVN (LTE as C-plane, IEEE 802.11ad as D-plane). To the best of the authors' knowledge, it was the first prototype of mmWave SDVN and the first demonstration of SDVN supporting cooperative perception. Nevertheless, it left some defects for improvement. One was at the D-plane. Only mmWave was exploited, so the management focused on multi-hops, which was inefficient for cooperative perception with processed sensor data that could be broadcasted. The other was at C-plane. The whole network only relied on a single C-plane. The scalability and stability were questionable. It may fail to meet the required latency when the network gets huge and crowded.

Therefore, in this chapter, additional contributions are achieved in four aspects:

- A hierarchical SDVN architecture is designed. By dividing the roles and scopes of local and global C-planes, the global SDVN controller will only focus on cross-network operations and extreme scenarios. The local SDVN controllers will handle the networking within sub-SDVN networks. In this way, control overhead can be diluted, and latency can be promised.

- Heterogeneous V2X is considered in this new hierarchical SDVN (Het-SDVN). After presenting a survey on the existing and emerging V2X technologies, the applicability of IEEE-based V2X, 3GPP-based V2X, and even satellite networks, to the Het-SDVN C/D-planes is comprehensively discussed.

- A local SDVN framework suitable for RSUs is developed. This framework adds sensor management, which leverages the legacy V2X messages over DSRC to control the

ON/OFF of RSU sensors for cooperative perception. The system shows good performance in application initiation delay and energy consumption after deployment.

- A full-fledged Het-SDVN testbed is set up. The testbed incorporates major ITS components, such as vehicles with OBUs, RSUs, and multi-access edge computing (MEC) servers. Based on the testbed, a proof of concept is carried out to demonstrate Het-SDVN's capability to provide cooperative perception within and across sub-SDVN networks. The holistic system performances of C-planes and D-planes are evaluated.

4.2 Design of Het-SDVN architecture

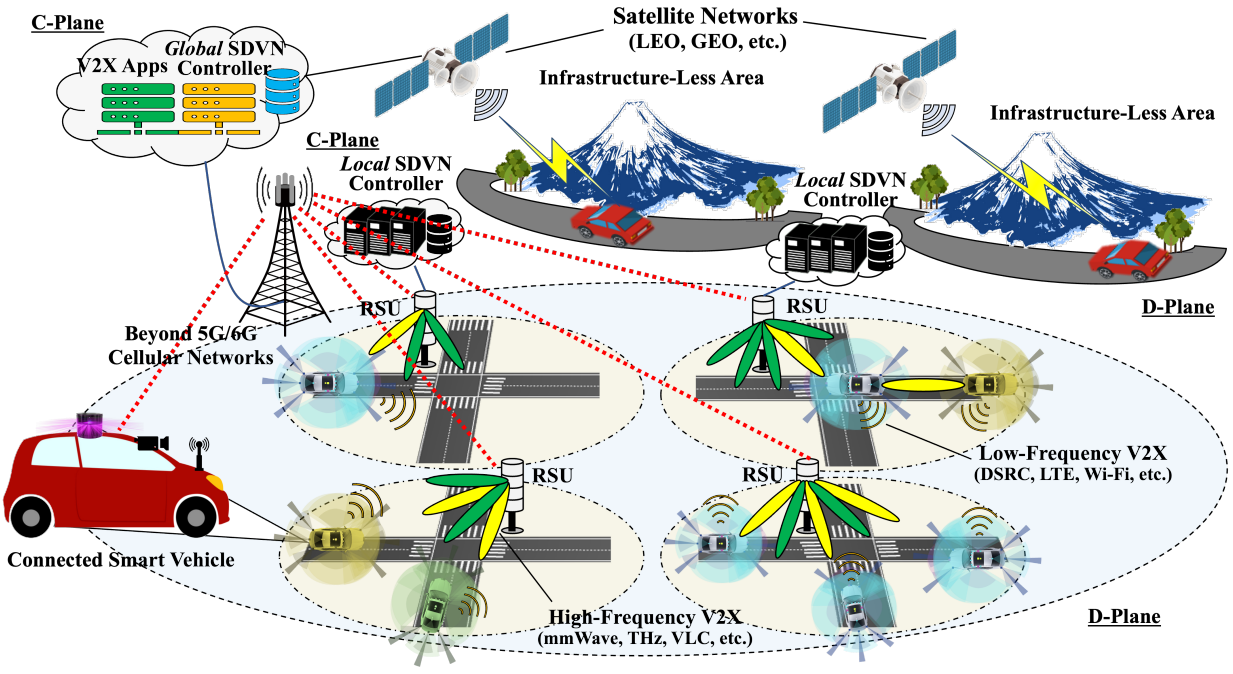

Figure 4.1: Overview of the Het-SDVN architecture (hierarchical C-plane and heterogeneous V2X D-plane).

4.2.1 Architecture description

The primary goal of the proposed Het-SDVN architecture is to effectively fulfill the stringent and diverse QoS requirements of V2X applications, specifically those pertaining to cooperative

perception. To that end, it is crucial to have global optimization on network decisions and minimize control overhead. Extensive studies have exposed that a fully centralized control architecture exhibits remarkable efficiency in adapting to highly dynamic vehicular networks [27]. However, these architectures encounter significant performance degradation when the service range of the SDVN controller expands substantially. In order to retain the benefits of centralization while simultaneously mitigating excessive overhead, a two-layer hierarchical SDVN C-plane is introduced and illustrated in Fig. 4.1.

1) Local SDVN C-plane: This C-plane manages one sub-SDVN network, where the central node is an RSU. The RSU hosts C-plane functions and orchestrates communication resources for D-plane applications. The local SDVN controller processes the requests sent by the on-board units (OBU) of connected vehicles and dynamically controls V2X networks (typically, V2V and V2I) to transfer the contents.

2) Global SDVN C-plane: Global C-plane manages geographically decentralized sub-SDVN networks. This C-plane takes advantage of MEC or Cloud resources and wide-area communication systems such as cellular networks and satellite networks. The global SDVN controller holds an extended network view by synthesizing the context information (e.g., topology, resource distribution, and traffic information) from the underlying local SDVN controllers. If vehicles send requests that exceed the capabilities of local SDVN controllers, or vehicles move to infrastructure-less areas, it hands over to the global SDVN controller to control the network.

3) RSU and OBU D-plane: The Het-SDVN D-plane consists of stationary RSUs and mobile OBUs. There have been a variety of wireless interfaces that support data transfer in this D-plane. IEEE-based interface technologies (IEEE 802.11p, 802.11n/ac, 802.11ad/ay, etc.) and their 3GPP-based counterparts (LTE and NR sidelinks) are two significant representatives. Application data, for example, raw or processed sensor data for cooperative perception, is routed over a relay network of RSUs and OBUs, which is configured by SDVN controllers using southbound interfaces like OpenFlow. The vehicle density, channel conditions, QoS requirements, etc., may affect the selection of heterogeneous V2X interfaces at each hop.

4.2.2 Utilization of heterogeneous V2X

Table 4.1 summarizes the legacy and emerging radio access technologies (RATs) that are used or potentially to be used for V2X.

Table 4.1: List of heterogeneous V2X technologies and characteristics.

Technology	Data Rate	Coverage	D-plane	C-plane
Low-frequency V2X				
Wi-Fi (2.4/5/6 GHz)	★★☆	★★☆	Local	Local
IEEE 802.11p (5.9 GHz)	★☆☆	★★☆	Local	Local
LTE-V2X (5.9 GHz)	★☆☆	★★☆	Local	Local
NR-V2X (FR1)	★★☆	★★☆	Local	Local
High-frequency V2X				
NR-V2X (FR2)	★★★	★☆☆	Local	N/A
IEEE 802.11ad (60 GHz)	★★★	★☆☆	Local	N/A
THz (0.1 - 10 THz)	★★★	★☆☆	Local	N/A
VLC (400 - 800 THz)	★★☆	★☆☆	Local	N/A
Other V2X				
IEEE 802.11bd (5.9/60 GHz)	★★★	★★☆	Local	Local
Starlink (Ku, Ka)	★★☆	★★★	Global	Global

4.2.2.1 Low-frequency V2X technologies

Low-frequency V2X mostly operates in the sub-6 GHz band. IEEE 802.11p is a representative of the first-generation V2X technologies, which becomes the basis of DRSC in America, ITS-G5 in Europe, and ITS-Connect in Japan. IEEE 802.11p performs at 5.9 GHz and provides a data rate of up to 28.8 Mbps to support basic V2X applications as defined in ESTI technical report (TR) 102 638 [11]. Then, the 3GPP launches formal discussions on enhancing cellular networks for V2X since Release 14 (Rel-14). In 2016, LTE-V2X was finalized. Further enhancements to LTE-V2X sidelink (PC5) for direct communications, and the legacy air interface (Uu), were studied under Rel-15. In addition, NR-V2X was developed since Rel-16, which was frozen in 2020, while the discussions on its enhancements now continue in Rel-17 and Rel-18. NR-V2X targets two frequency bands (FR1: 410 MHz - 7.125 GHz, FR2: 24.25 GHz - 52.6 GHz), but the primary focus for the first-generation NR-V2X design is in FR1 to enable low-latency reliable sidelink communications at 5.9 GHz. Cellular technology-based V2X (C-V2X) outperforms IEEE 802.11p in terms of data rates, latency, and reliability. However, IEEE 802.11p won't be obsolete owing to its successful mass-market applications

over the last decades and economy. Their coexistence and interoperability should be one of the major focuses of the newly designed V2X architecture.

Other than the IEEE 802.11p and C-V2X, Wi-Fi based on the IEEE 802.11 family of standards, which works in the unlicensed 2.4/5/6 GHz bands, can be potentially used for V2X due to its low cost and ease of deployment. Wi-Fi has become ubiquitous in urban areas and its performance is improving drastically as the generation evolves. In Wi-Fi 6 (802.11ax), a data rate of over 1 Gbps is supported under the single-carrier and single-stream settings. However, one of the well-known drawbacks of Wi-Fi is the catastrophic interference which heavily degrades its practical performance.

Since the aforementioned technologies all operate in low frequency bands, they suffer from trivial path loss and penetration loss, thus earning a good coverage. In this Het-SDVN, they can serve as C-planes in different layers. For example, Wi-Fi, DSRC, PC5-based LTE, and NR (FR1) provide local C-planes, while Uu-based LTE provides global C-planes as it can reach several kilometers. Apparently, low-frequency V2X can contribute to C-planes and D-planes simultaneously (in-band mode) or separately (out-band mode), because they have fully met the QoS requirements of basic V2X applications (including detected object-based and feature-based cooperative perception).

4.2.2.2 High-frequency V2X technologies

V2X operating in higher-frequency bands now attracts great interest due to the vast unexploited spectrum resources. The mmWave, terahertz (THz), and visible light communication (VLC) are promising technologies to be used for V2X. NR-V2X has to fulfill the peak data rate of 20 Gbps as required by IMT-2020, thus introducing the mmWave band (FR2). In a field trial of remote driving [23], the NR-V2X system deployed at FR2 demonstrates its ability to provide broadband, reliable and low-latency communications. At the same time, the applicability of IEEE 802.11ad to V2X is being evaluated by many projects [17]. IEEE 802.11ad, also known as WiGig, is an earlier, commercialized mmWave technology working in the unlicensed 60 GHz band. It enables the peak data rate of 6.75 Gbps with 2.16 GHz bandwidth.

Although THz and VLC were not included in the design of NR-V2X, they have been identified as key 6G-V2X technologies [59]. Of course, their utilization still faces serious challenges, such as the propagation measurement and channel modeling for THz communications, and the interference management for VLC. An indoor THz system measurement validates a

104 Gbps wireless link performance [60], which shows THz's potential to enable immersive V2X applications with AR/VR/XR. In [61], an automotive VLC system using light-emitting diode (LED) transmitters and camera receivers achieves a system performance of 45 Mbps without bit errors. These preliminary evaluations pave the way for their future adaptation to more challenging V2X scenarios.

Owing to abundant bandwidth allocation, high-frequency V2X enables ultra-high data rate and ultra-low latency communications, so that raw data-based cooperative perception is supported. However, the coverage is sacrificed as the frequency increases. In addition to severe path loss, antenna directivity and weakened penetration capability make broadcast-based communication infeasible. Hence, in this Het-SDVN, high-frequency V2X is only suitable for D-plane transmission. The SDVN controllers should manage their multi-hop communications and select appropriate D-plane nodes as relays.

4.2.2.3 Other V2X technologies

Other V2X technologies target both low- and high-frequency communications. In March 2018, a new task group, TGbd, was established by IEEE for next generation V2X (NGV). The task is to develop IEEE 802.11bd as the successor to IEEE 802.11p. IEEE 802.11bd will work in the 5.9 GHz band and optionally in the mmWave band from 57 GHz to 71 GHz. In addition to having interoperability, coexistence, backward compatibility, and fairness with IEEE 802.11p, IEEE 802.11bd will inherit advanced PHY and MAC techniques implemented in the latest Wi-Fi standards (IEEE 802.11/n/ac/ax) to enhance the 5.9 GHz performance for at least two times higher throughput and communication range. As for the mmWave band, it is proposed to reuse portions of the PHY and MAC layers from IEEE 802.11ad/ay [50]. However, detailed specifications are ongoing. Considering the coverage, for this Het-SDVN, 5.9 GHz IEEE 802.11bd can play roles in the local C-plane and D-plane, while its mmWave version should serve the D-plane.

In February 2021, SpaceX, the US company, launched its commercial low Earth orbit (LEO) satellite communication service, known as Starlink. This system comprises over 4000 small satellites in LEO and operates within the Ku (12 - 18 GHz) and Ka (27 - 40 GHz) frequency bands, as authorized by the Federal Communications Commission (FCC). According to the disclosed specification [62], it offers impressive mobile user performance, with up to 250 Mbps downlink and 30 Mbps uplink speeds, comparable to LTE systems. Notably, Starlink ensures ubiquitous coverage, enabling internet access even in rural and infrastructure-less ar-

eas. This unique capability makes it an exceptional choice for the global C-plane and D-plane of Het-SDVN, except the LTE-V2X.

4.2.3 Profits to cooperative perception

The proposed Het-SDVN resolves the connectivity and scalability issues of existing SDVN architectures. With reliable C-plane associations, local/global SDVN controllers master real-time context information in D-plane and respond quickly to application requests from vehicles.

Regarding cooperative perception, this Het-SDVN provides support from two aspects. Firstly, the local SDVN provides cooperative perception for road/driving safety. This type of cooperative perception requires the exchange of sensing data focused on the immediate regions. Typical scenarios include safe overtaking and safe ramp merging, where an RSU with local SDVN controller manages the transmission of raw or processed sensing data over V2I and V2V links, allowing for the notification or assistance in detecting the presence of vehicles that pose a risk of collision. Secondly, the global SDVN provides cooperative perception for traffic efficiency. Along the planned route that an automated vehicle will take, congestion and accident information perceived by sensors in other sub-SDVNs are useful for route re-planning. The global SDVN controller manages the distribution of the above information over backhauls according to requests. There is a special case of cooperative perception where the global SDVN guarantees safety. It is on roads with harsh driving conditions (lighting, surface quality, etc) and without infrastructure support (usually in rural or mountainous areas). Vehicles can get the latest sensing information from passing vehicles for safety by sending requests to the global SDVN controller, which establishes V2N2V connections using wide-area communication systems.

4.3 Local SDVN framework for RSU and evaluation

4.3.1 Framework composition

The proposed framework is established by integrating Ryu and Robot Operating System (ROS), two popular open-source projects in SDN and robotics, respectively. The Ryu is specialized in network traffic management and is capable of centralized and dynamic routing policy enforcement depending on (network) environmental changes. On the other hand, the ROS community has developed a plethora of robotics applications (nodes) for sensing and

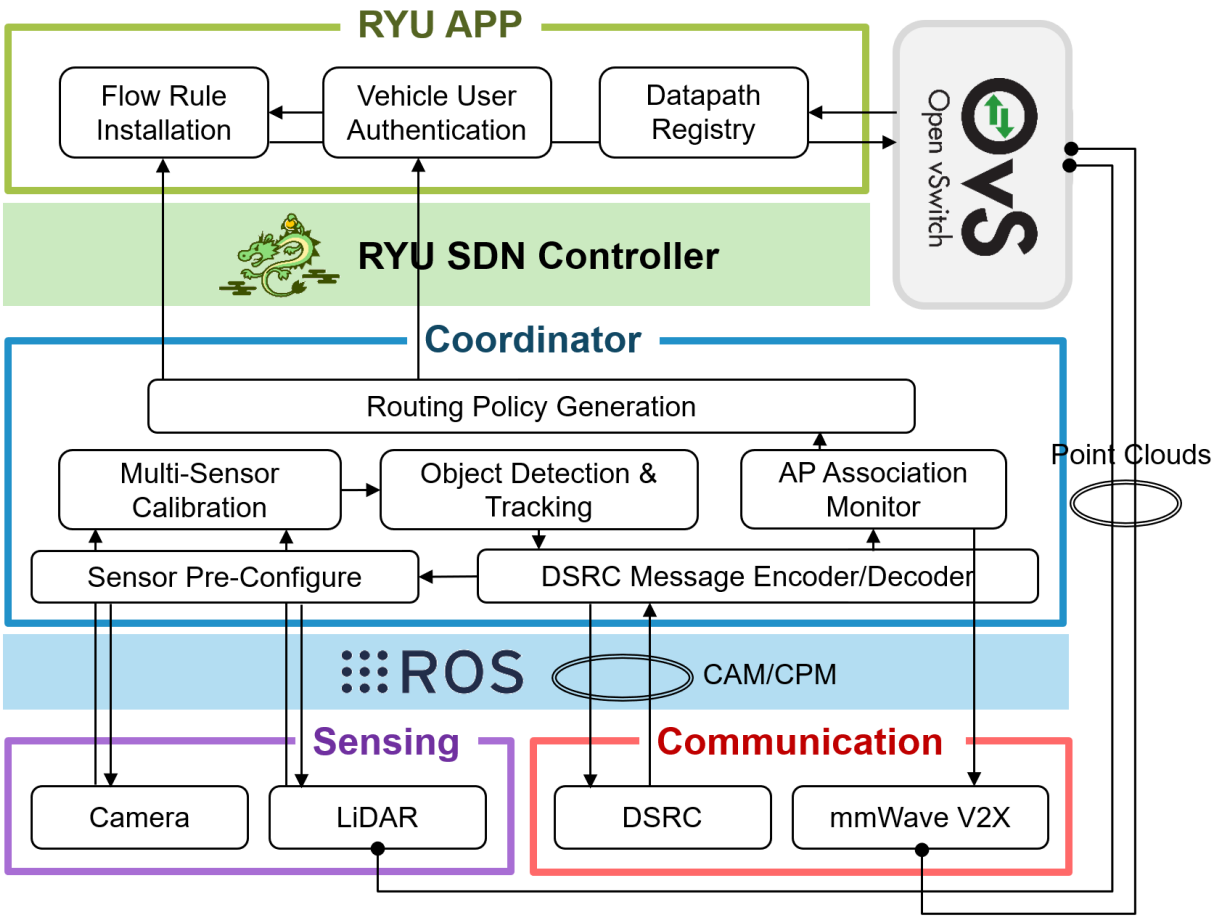

Figure 4.2: SDVN-based framework for cooperative perception.

communications. The drivers for most commercial-off-the-shelf sensors are available in ROS. Therefore, ROS can work as the major platform to provide perception capabilities and sensor management.

Figure 4.2 shows the framework composition. The boxes in the figure represent the fundamental hardware and software components. As of now, vision cameras and LiDARs have become the standard equipment of RSUs for comprehensive monitoring of surrounding environments. In addition, to supply V2X connectivity in different situations, RSUs will leverage two different V2X interface technologies. One is the classical DSRC interface at 5.9 GHz for small message broadcasting. There are already commercialized DSRC products for RSUs (e.g., Cohda Wireless MK6 [63]). The other is the promising mmWave interface for directional raw sensing data transmission. The technical candidates include 5G-NR V2X at FR2 (24.25-52.6 GHz), IEEE 802.11ad/ay and IEEE 802.11bd at 60 GHz. In some areas, streetlamps have been equipped with mmWave V2X for highly accurate positioning and enhanced perception [17]. Hence, the coexistence of DSRC and mmWave V2X interfaces on RSUs will soon be a trend.

The software components for service coordination are functioning in ROS. The `DSRC Message Encoder/Decoder` is a ROS driver for DSRC interfaces which parses incoming CAM messages and publishes corresponding vehicle information. The `Sensor Pre-Configure` is a ROS node for sensor management, in which a suite of sensor communication APIs is defined to control sensor status (e.g., the ON/OFF switching of cameras or LiDARs, the speed of laser motor rotation, etc.). The trigger of this node is the message from `DSRC Message Encoder/Decoder` that indicates the emergence of connected automated vehicle (CAV) users. Once cooperative perception is triggered, the `Multi-Sensor Calibration` and `Object Detection & Tracking` will handle the recognition tasks and generate an object list to format CPM messages. The `AP Association Monitor` waits for the access of mmWave V2X and reports the status to the `Routing Policy Generation` which summarizes associated vehicle contexts and creates an optimal (delay or bandwidth-based) routing policy.

The Ryu controller can map the routing policy to specific forwarding tables compatible with OpenFlow v1.3. The flow entries will be issued to the datapaths, i.e., Open Virtual Switch (OVS) bridges, of RSU and authenticated vehicles. Then, the point cloud data flows can be shared with specified targets.

4.3.2 Inherent mechanisms

4.3.2.1 Energy-efficient dynamic sensor ON/OFF strategy

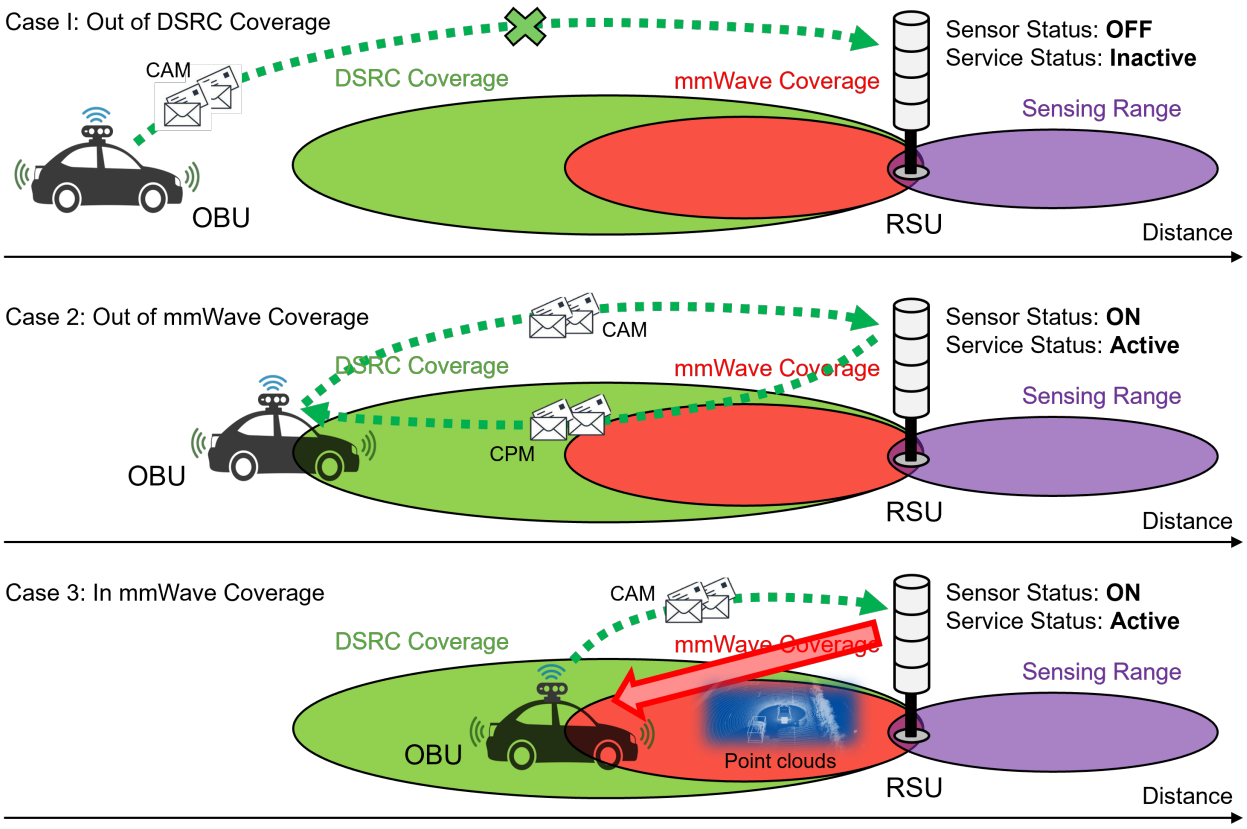

Figure 4.3: DSRC message-triggered dynamic sensor ON/OFF.

The energy consumption of RSUs depends on the number and capability of equipped sensors, which is not negligible. Take RoboSense LiDARs as an example. The average power consumptions for the 16, 32, and 80-beam series are 12 W, 13.5 W, and 38 W, respectively. On the other hand, turning RSU sensors ON all the time is neither energy-efficient nor judicious since there are periods when no CAVs appear in the service range. Empirical information can be leveraged to switch the ON/OFF of sensors. In [64], the authors predict vehicle traffic based on prior traffic information and employ reinforcement learning (Deep Q-learning) to decide whether to turn RSU ON/OFF. However, machine learning approaches incur more system complexity and additional requirements on computational abilities. Instead, we propose an intuitive strategy, i.e., to exploit existing and broadcasted DSRC messages as a trigger for dynamic sensor ON/OFF, as depicted in Fig. 4.3.

The switching of sensor ON/OFF is based on the reception of DSRC messages, mainly CAM messages, which indicate the incoming CAVs. When CAVs are out of DSRC coverage (hundreds of meters away), RSU sensors are turned OFF for energy-saving. When CAVs enter the range of DSRC but not mmWave (150 - 200 m), RSU sensors will be turned ON, and cooperative perception will be activated firstly to share CPM messages via DSRC interfaces. Further, as soon as mmWave V2X is associated, shared information will become raw sensor data like LiDAR point clouds and be steered by the SDN controller to CAVs for more fine-grained perception.

Likewise, when CAVs depart, RSU sensors will be switched OFF. Note that it is worthy of an in-depth discussion on the exact timing of sensor OFF after completing the service to avoid unnecessary energy consumption.

4.3.2.2 Multi-RSUs service scheduling

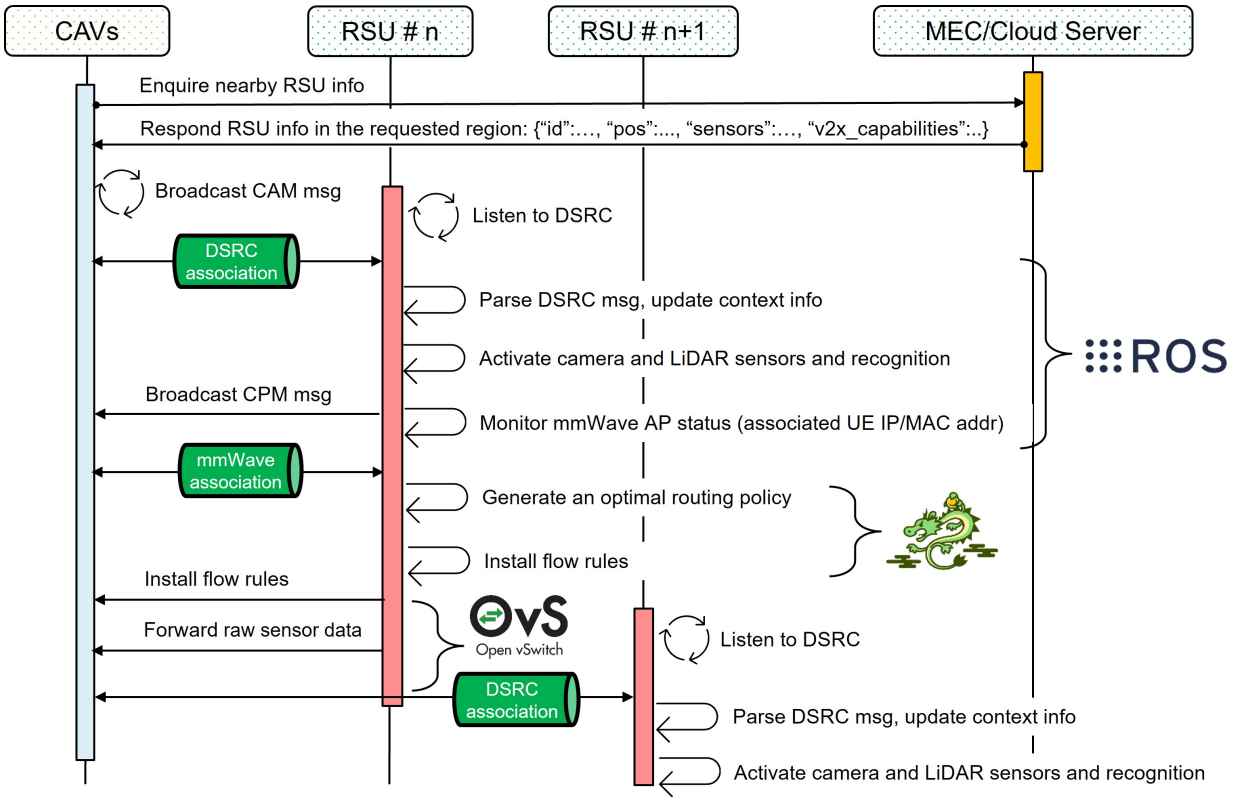

Figure 4.4: Sequence of RSU-centric cooperative perception.

Along the traveling course of CAVs, multiple RSUs provide cooperative perception subse-

quently. The service consistency is one of our pursuing features in this RSU system. Figure 4.4 explains the entire sequence of cooperative perception, from the sensor initiation and sensing data provision to the subsequent RSU handover. The DSRC association and mmWave association are of milestone significance in the described procedures. The former represents the wake-up of RSU sensors and the startup of CPM message broadcasting, and the latter triggers raw sensing data sharing and SDN fine-grained flow control. When the RSUs are deployed geographically close to each other (in urban scenarios), owing to the wide coverage of DSRC, CAVs are able to activate the service preparation in the subsequent RSU while enjoying cooperative perception in the current RSU. When the RSUs are deployed far apart (in rural or highway scenarios), CAVs can either trigger each RSUs' service independently or request the coordination of primary SDVN controller which will proactively activate the RSUs along the traveling course by driving intention sharing and route the point clouds of multiple RSUs through backhaul.

4.3.3 Implementation and Evaluation

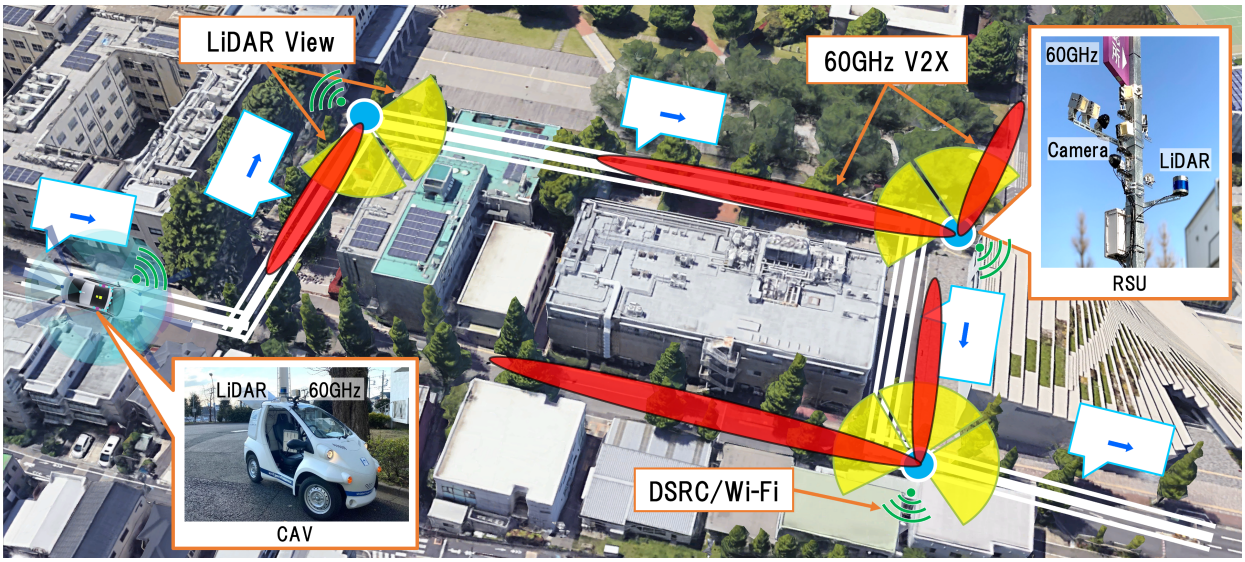

Figure 4.5: Experiment overview of Tokyo Tech smart mobility test field (three RSUs deployed, one Robocar used as CAV, cameras and LiDARs installed for contextual awareness, Wi-Fi and WiGig antennas providing V2X connectivity, and Intel NUCs empowering computing capability at RSUs; the test CAV drives along the 360 m course (blue arrows) at a velocity of 10 km/h) [6].

4.3.3.1 Implementation

Figure 4.5 gives an overview of the experimental environment. This smart mobility test field is located on the Ookayama Campus of Tokyo Institute of Technology, Japan. There have been three well-equipped RSUs deployed. Each of the RSUs has camera and LiDAR sensors, as well as V2X capabilities compliant with IEEE 802.11p/DSRC and IEEE 802.11ad/WiGig. Due to Japanese outdoor wireless regulations, we abandon DSRC and substitute it with 5.6 GHz Wi-Fi. The Wi-Fi routers belong to the Buffalo WAPM-1266WDPR Series. They can maintain connectivity up to 300 m outdoors [65]. In contrast, the WiGig antennas made by Panasonic can only reach around 150 m for line-of-sight (LOS) communications. Inside the waterproof box, Intel NUC PCs are embedded as RSU control units where we deploy developed functionalities according to the framework design presented in Section II. Note that to enable ETSI-defined V2X messages (CAM, CPM), we utilize OpenC2X [66]. It is an open-sourced prototyping platform that completely implements ETSI ITS-G5 protocol stack.

The tested CAV model is ZMP Robocar MV2 [67]. Except for a more powerful control PC for autonomous driving-related functions (provided by Autoware.ai [68]), the CAV's hardware configuration is almost the same as RSUs, including a 32-beam LiDAR on the rooftop, front cameras, Wi-Fi and WiGig antennas for V2X communications. Besides the OpenC2X, we installed OVS in the CAV control PC. The WiGig interface is logically attached to an internal OVS bridge, which will communicate with the Ryu controller in RSUs automatically after entering the mmWave coverage and then download the routing policy for raw sensor data sharing. In this experiment, the shared data is LiDAR point clouds.

When the CAV receives point clouds from RSUs, it will either forward or utilize the data itself. After mutli-hop relays, the received data will be merged together with the CAV's own observations (so-called sensor fusion process). This process can be implemented by a coordination transformation. Specifically, if $V_m = [x, y, z, 1]^T$ is a LiDAR point from a certain RSU in the static map (m) domain, we need to apply $T_{mc} * V_m$ to translate it into a point $V_c = [x^{'}, y^{'}, z^{'}, 1]^T$ in the CAV (c) domain, where

$$T_{mc} = \begin{pmatrix} RotX.x & RotY.x & RotZ.x & Translation.x \\ RotX.y & RotY.y & RotZ.y & Translation.y \\ RotX.z & RotY.z & RotZ.z & Translation.z \\ 0 & 0 & 0 & 1 \end{pmatrix} \tag{4.1}$$

T_{mc} is a dynamic transformation matrix from the static map coordinate frame to the moving

CAV coordinate frame. Using ROS `TF/TF2` packages, this matrix can be easily derived.

4.3.3.2 Evaluation

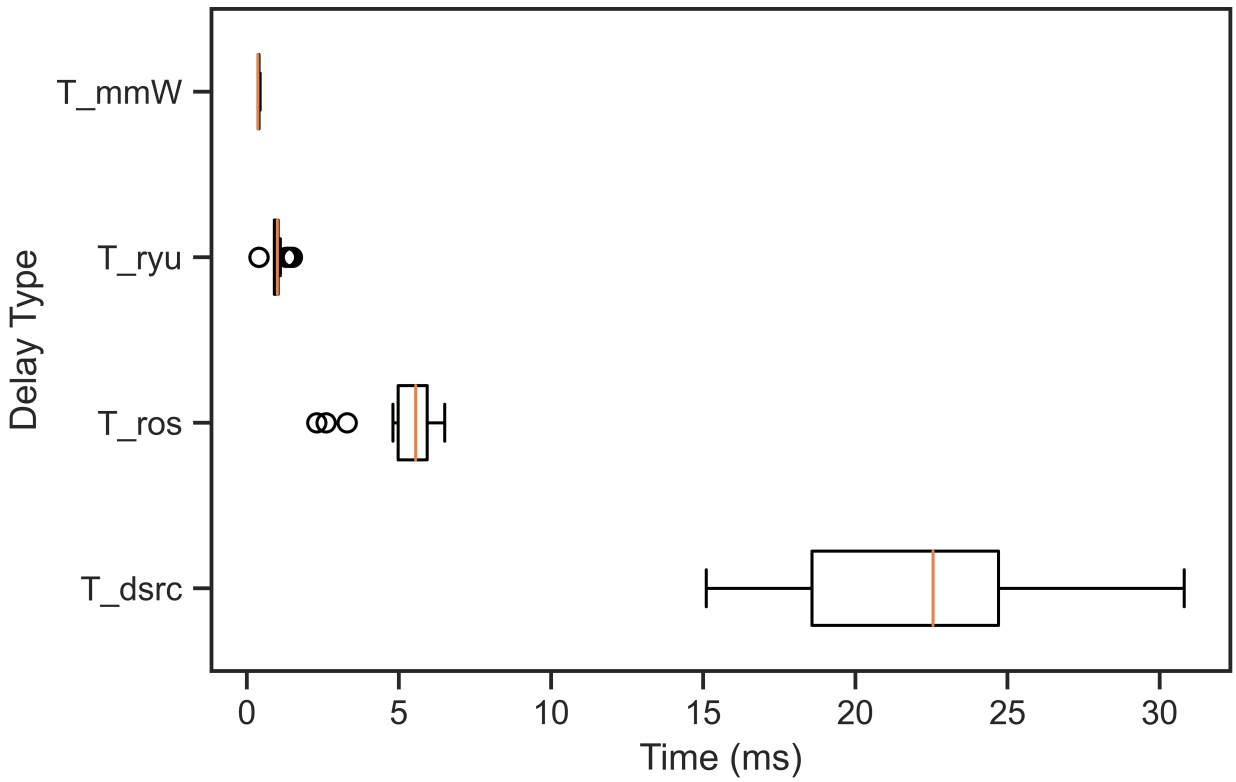

Figure 4.6: Total delay and the breakdown.

Time consumption: In a previous study [4], the necessary time consumption for CPM message delivery has been measured. Including the processing delay in Autoware, $\leq$ 100 ms can be achieved in the worst case. In our evaluation, we pay more attention to the time consumed throughout the handover from CPM-based cooperative perception to LiDAR point cloud-based cooperative perception. The total time consumption can be expressed as

$$T_{total} = T_{dsrc} + T_{ros} + T_{ryu} + T_{mmW} \tag{4.2}$$

where T_{dsrc} indicates the delay for trigger message (CAM) delivery, including the reading delay from GPS to OpenC2X sender and the transmission delay from OpenC2X sender to OpenC2X receiver via 5.6 GHz Wi-Fi; T_{ros} and T_{ryu} represent the processing delay in ROS

coordinator and Ryu SDN controller, respectively; T_{mmW} is the one-hop V2I transmission delay for one-scan LiDAR point clouds via 60 GHz WiGig.

Figure 4.6 reflects the breakdown of delay measurements. The total time consumption T_{total} is around 30 ms. Some of the delay, such as T_{ros} and T_{ryu}, will certainly increase as the serving CAV number increases. For one CAV, activating the LiDAR sensor, computing the routing policy and issuing flow tables just consume less than 10 ms in total. However, T_{dsrc} costs more than 20 ms (83% of T_{total}). We speculate that most time of T_{dsrc} is spent in the codec of DSRC messages. As for the mmWave transmission time T_{mmW}, a superior performance is found, as only 0.5 ms are needed for one-scan LiDAR point clouds transmission. In the case of the RSU LiDAR (RS-LiDAR-32) with a rotation speed of 600 rpm, one-scan data size equals 94036.8 bytes, which implies that the mmWave data rate is over 1.5 Gbps during the experiment.

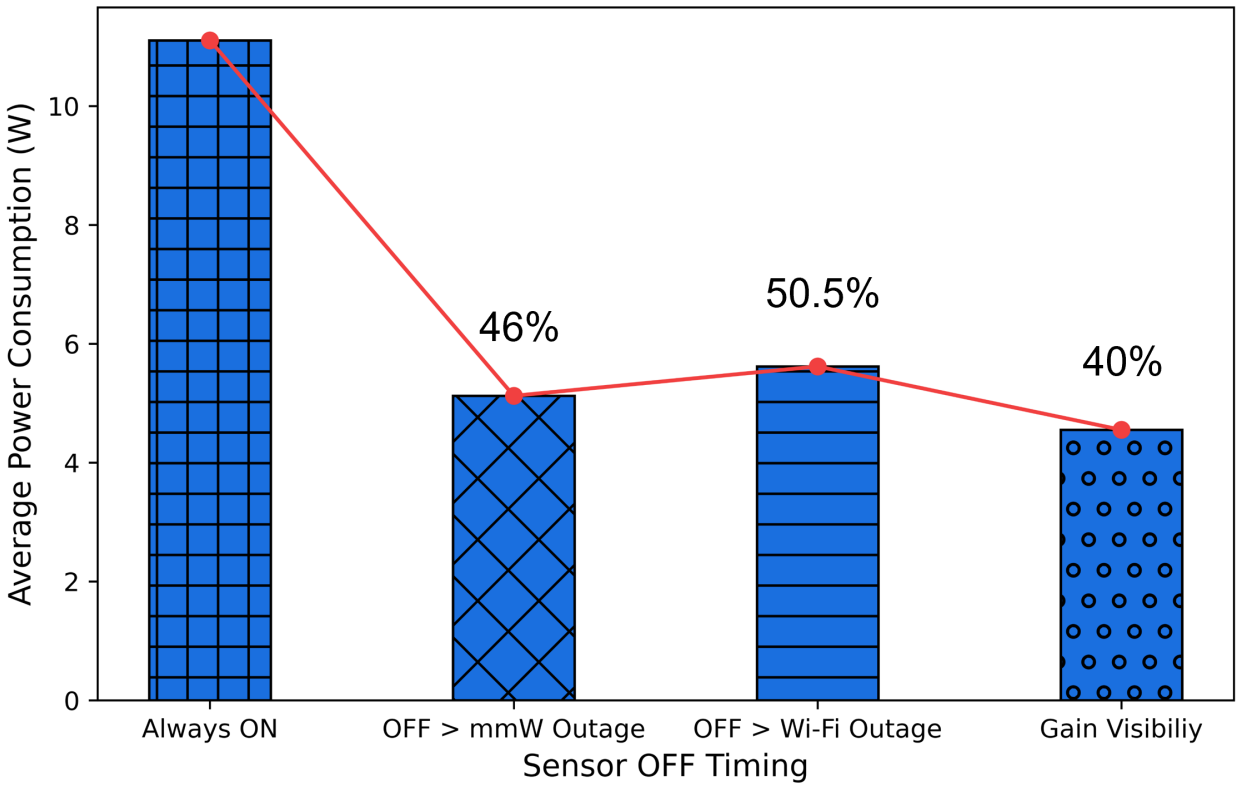

Figure 4.7: Power consumption under different sensor OFF timing.

Power consumption: As we mentioned in Section II. C, the exact timing of sensor OFF after completing cooperative perception is worth discussing because it can avoid unnecessary

energy consumption. We examine the power consumption in three cases: OFF after losing mmWave, OFF after losing Wi-Fi, OFF after gaining visibility of blind spots, and compare them to the case when the LiDAR sensor is always turned ON. The average power consumption, P_{avg} can be expressed as

$$P_{avg} = \frac{P_{sensor} \times V_{cav} \times T_{ON}}{L_{course}} \tag{4.3}$$

where P_{sensor} indicates the sensor power in its specification (13.5 W for RS-LiDAR-32 we deployed); V_{cav} is the CAV's average velocity; T_{ON} is the duration of sensor ON along the driving course; L_{course} represents the length of the course.

Figure 4.7 shows the results of average power consumption of RSU sensors when the test CAV moves along the course (white). The power reduction percentages for the three examined cases are 54%, 49.5% and 60%, respectively. This implies that, if an RSU can

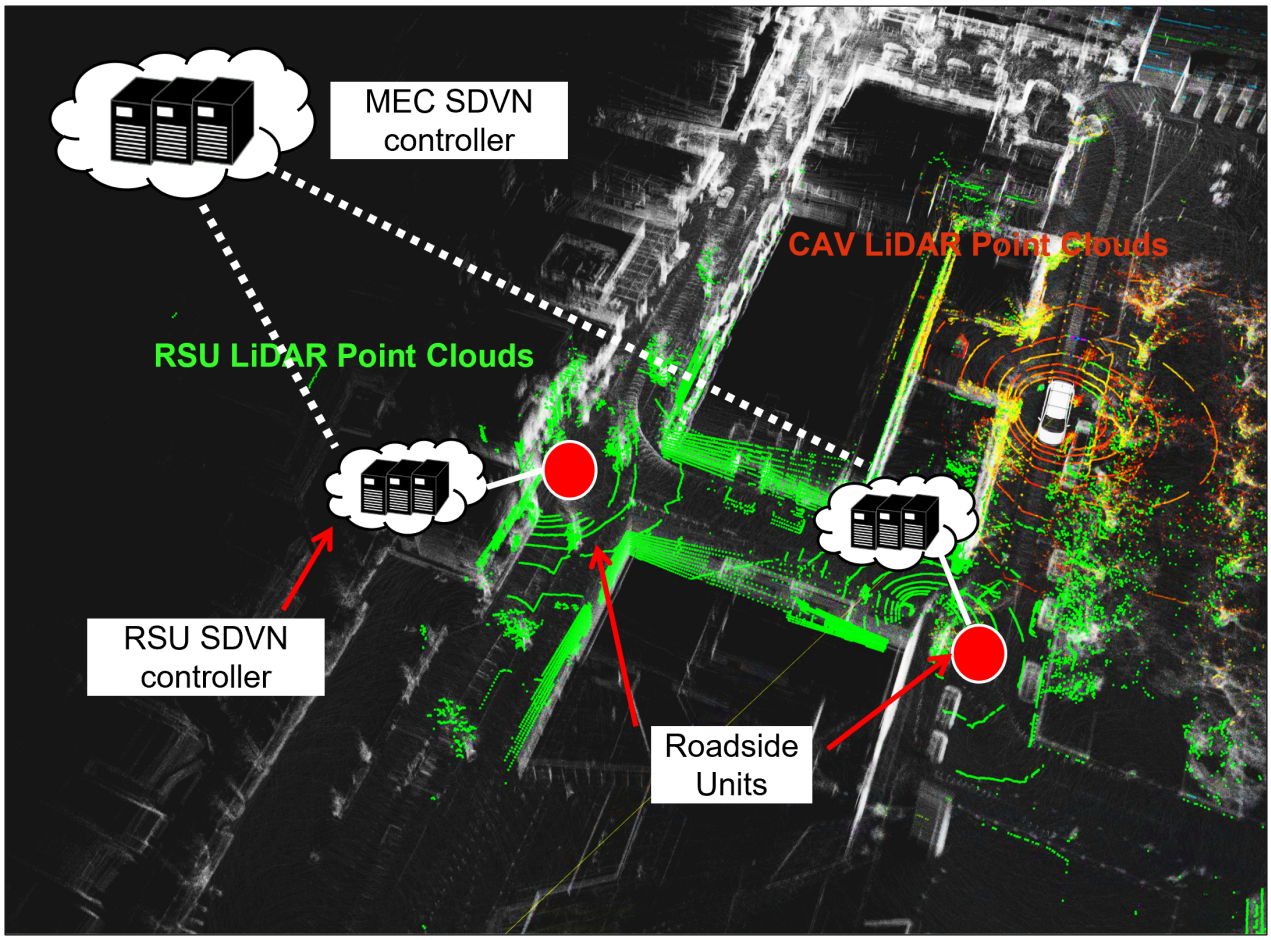

Figure 4.8: Cooperative perception under higher-layer orchestration.

master accurate information about the exact timing of each CAV when their safety needs are met by cooperative perception, it is possible to take the most effective sensor ON/OFF strategy to save power. This information can be reported by CAVs actively or notified by the upper-layer orchestrator after prediction according to historical data.

Scalability: Our ultimate target is to promote this framework system to be deployed in every RSU of society. To that end, scalability is an indispensable requirement. The software part can be developed in containers for convenient migration to RSU operating systems. Moreover, to manage those distributed RSU systems jointly, we can rely on upper-layer orchestrator, such as the global SDVN controller introduced in Sect. 3.2.1. Figure 4.8 shows an example of how SDVN controller in MEC/Cloud can contribute to the RSU cooperative perception. When the CAV velocity is extremely fast or the road scenario is extremely complex, the CAV may require more sensor data for safety. In this case, MEC SDVN controller will notify the critical RSUs along the course of the CAV and issue routing policies to them. Finally, the sensor data originated from multiple RSUs can be relayed via backhaul networks and reach the target CAV via V2X. Obviously, a single RSU system cannot perform such a large-scale coordination.

4.4 Proof of concept of Het-SDVN

4.4.1 Experimental topology

To simplify the experimental topology without losing hierarchical mechanisms, the scenario that a vehicle benefits from cooperative perception (CP) in the current local sub-SDVN network and requests CP from another sub-SDVN network is considered, as shown in Fig. 4.9. In this scenario, Vehicle1 runs CP for safety. The nearest CP server at RSU1 handles the CP request containing an accurate vehicle position. Sensing data from RSU1 is then delivered to Vehicle1 in its demanded format (detected objects, raw data) through a V2X network organized by the local SDVN controller. For the purpose of efficiency, Vehicle1 also needs perceptual information of RSU2, which exceeds the charge area of RSU1. Hence, this type of CP request goes to the CP server at MEC or Cloud. The global SDVN controller is responsible for sensing data routing across these two sub-SDVN networks.

In this topology, D-plane consists of two parts: the local SDVN D-plane within RSU1 coverage and the global D-plane connecting the two sub-SDVN networks. The former D-

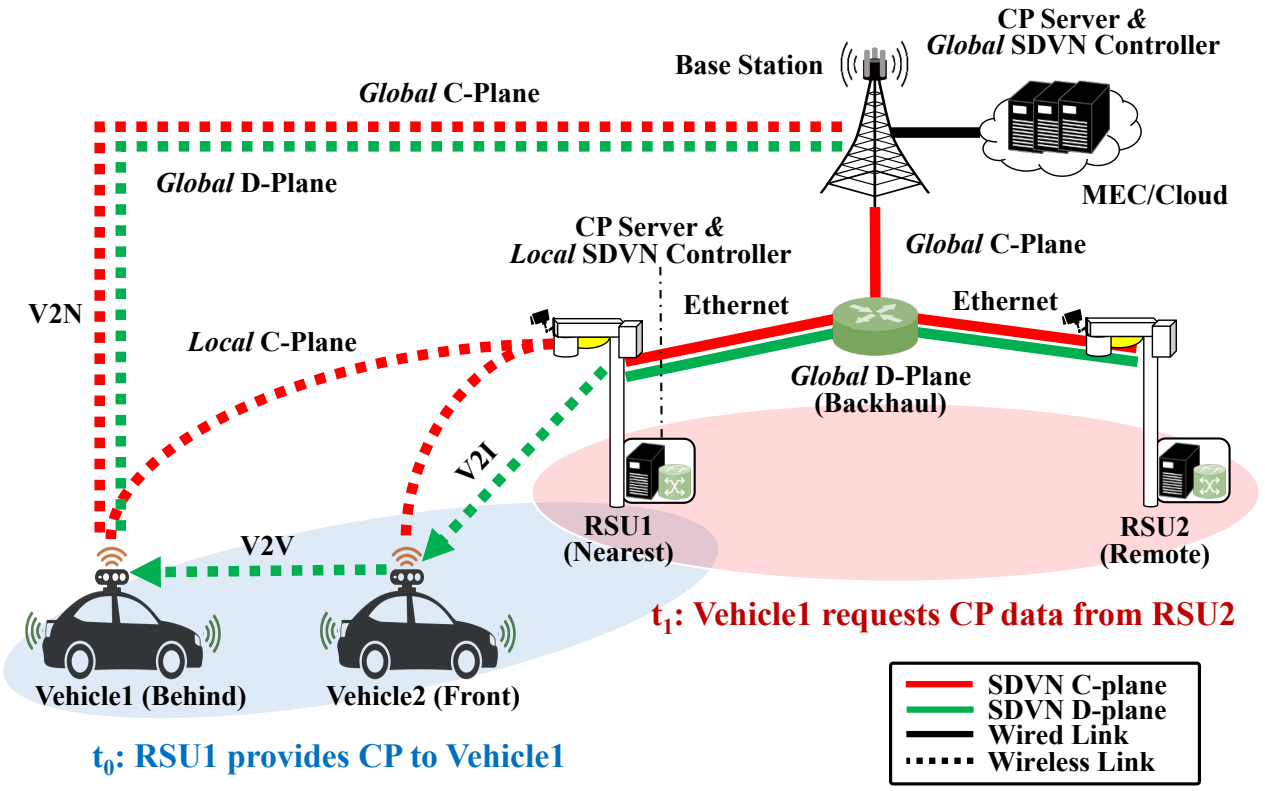

Figure 4.9: Experimental topology for Het-SDVN demonstration.

plane includes three nodes, two vehicles and one RSU, as well as multiple V2V/V2I links to forward sensing data. The latter D-plane are mainly wired networks, where sensing data needs to pass through large amounts of backhaul switches and Ethernet links in between.

As for C-plane, the described CP relies on the local SDVN C-plane of RSU1 and the global SDVN C-plane to schedule network resources. These two C-planes require different coverage. The former C-plane only needs to cover a target region, like an intersection with high accident probability where RSU1 can locate for safety, while the latter C-plane must be ubiquitous to mitigate the risk of local SDVN controller failures and provide CP even in RSU-less areas.

4.4.2 Environment setup

The smart mobility field for the proof of concept is placed at Tokyo Institute of Technology, Ōokayama campus [6]. This field includes smart vehicles and RSUs for automated driving and V2X-related tests. The proof-of-concept environment is shown in Fig. 4.10. It is seen that hardware equipment for sensing, communication, and computation is installed on the

exploited vehicles and RSUs. Table 4.2 reveals the details about the equipment. Here, LiDARs are used to monitor dynamic 3D objects. Therefore, the dense pointclouds become major data sources of CP. The 32-laser LiDARs and 80-laser LiDARs are deployed on vehicles and RSUs, respectively.

For D-plane implementation, Wi-Fi (IEEE 802.11a/n/ac) at 5 GHz and WiGig (IEEE 802.11ad) at 60 GHz are two options for the local SDVN D-plane. To support the WiGig, directional antennas are installed on RSUs and the rooftop of vehicles so that mmWave V2I and V2V are enabled. The global SDVN D-plane directly uses campus Ethernet, but a backup could be 4G LTE. Pocket LTE devices are put on vehicles to provide access to the global SDVN C-plane. As for the local SDVN C-plane, Wi-Fi (IEEE 802.11b/g/n) at 2.4 GHz is adopted. These Wi-Fi APs are set up on RSUs.

In addition, computation devices with customized capabilities are supplied in order to perform CP and the functions of SDVN controllers on vehicles, RSUs, and the MEC server.

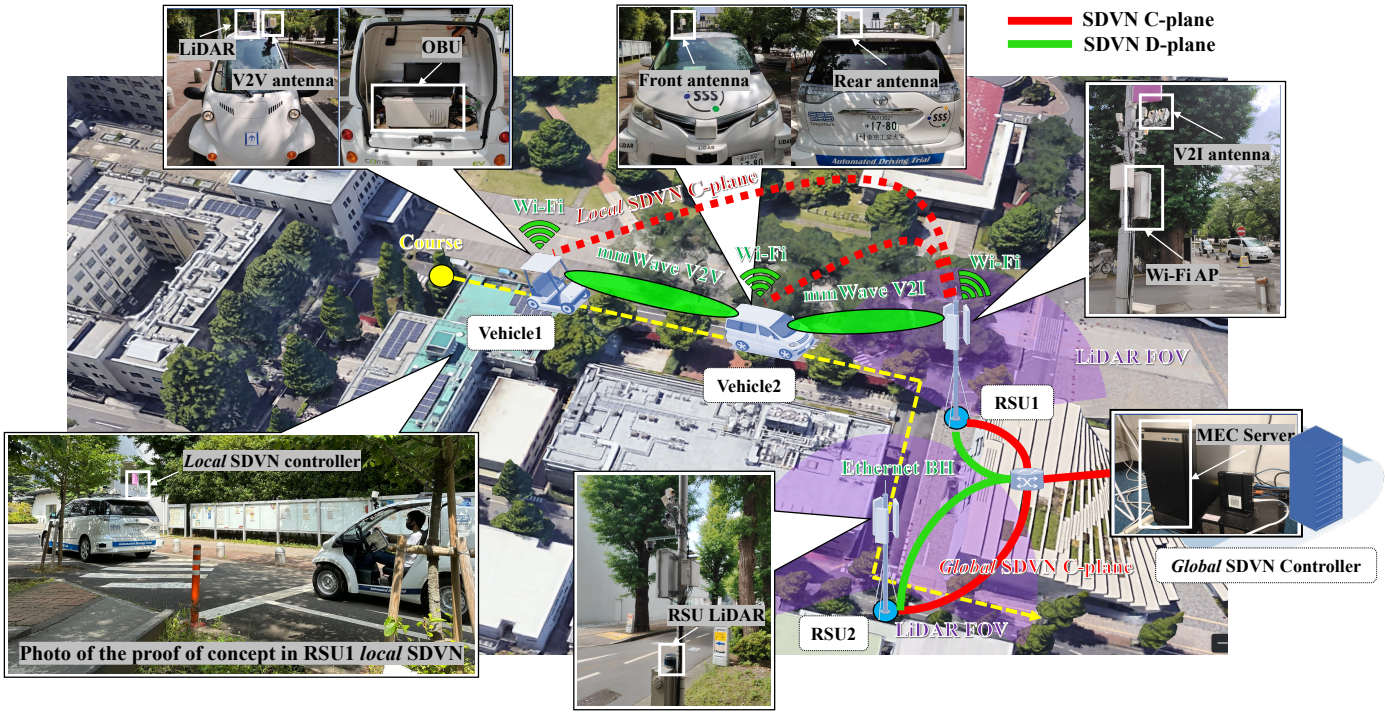

Figure 4.10: Proof-of-concept environment.

Table 4.2: Proof-of-concept hardware

Category	Purpose	Specifications
Sensor	RSU LiDAR	Number of lasers: 80 Frame rate: 10/20 Hz Output: 44.982 Mbps (UDP packets)
	Vehicle LiDAR	Number of lasers: 32 Frame rate: 5/10/20 Hz Output: 15.6 Mbps (UDP packets)
AP	Local D-Plane	Standard: IEEE 802.11ad Frequency: 60 GHz (2.16 GHz BW) Data rate: 385 Mbps - 2.5 Gbps
		Standard: IEEE 802.11a/n/ac Frequency: 5 GHz (20 MHz BW) Data rate: 6 Mbps - 173.3 Mbps
	Global C-Plane	Standard: 4G LTE Frequency: 2.5 GHz (20 MHz BW) Coverage: Up to 12 km
	Local C-Plane	Standard: IEEE 802.11b/g/n Frequency: 2.4 GHz (20 MHz BW) Coverage: Up to 400 m
Computer	Vehicle PC	Model: Mouse DAIV 7N (32 GB) CPU: 8-core Intel Core i9-11900K GPU: NVIDIA GeForce RTX 3080
	RSU PC	Model: Jetson AGX Orin (32 GB) CPU: 12-core Arm Cortex-A78AE GPU: 2048-core NVIDIA Ampere
	MEC Server	Model: Precision Tower 7920 (64 GB) CPU: 10-core Intel Xeon Silver 4210 GPU: NVIDIA Quadro RTX 5000

4.4.3 Network orchestration

The design of network orchestration in this proof of concept showcases the hierarchy and heterogeneity principles of the proposed Het-SDVN architecture. Figure 4.11 explicitly draws the application, networking, and data sequences when Vehicle1 runs CP and claims for various data formats.

In Fig. 4.11(a) and (b), the CP client on Vehicle1 broadcasts CP requests, indicating a region of interest (ROI) and format preference, which are received by the nearest local CP server on RSU1. As shown in Fig. 4.11(a), when Vehicle1 specifies the format as detected objects and the ROI as the current sub-SDVN, the local CP server on RSU1 sends a request to the local SDVN controller and performs LiDAR detection. The local SDVN controller on RSU1 creates OpenFlow tables and installs them on the Open vSwitches of Vehicle1 and RSU1, respectively. The OpenFlow table for RSU1 is used to broadcast the detected objects of RSU1 via UDP over 5 GHz Wi-Fi. When the ROI changes to the RSU2 sub-SDVN, the local CP server on RSU1 notifies the global CP server on MEC and requests the local SDVN controller to enable broadcast-based networking. The global CP server forwards the Vehicle1 request to RSU2 and simultaneously sends a request to the global SDVN controller for routing the detected-object data over the backhaul networks.

The sequence is almost the same when raw LiDAR data becomes the preferred format, as shown in Fig. 4.11(b). The major difference lies in the local SDVN. The large data size of LiDAR pointcloud makes it intractable for broadcasting. Therefore, the local SDVN controller on RSU1 installs new flow tables on Vehicle1, Vehicle2, and RSU1. The OpenFlow table for Vehicle2 is used to relay the raw data to Vehicle1 through a V2I and a V2V link of 60 GHz WiGig.

In this proof of concept, both the CP client and servers are implemented as ROS2 nodes [69], leveraging the detection algorithm (CenterPoint) in autoware.universe [70], a ROS2-based open-source framework for automated driving. Besides, a Python-written SDN controller framework called Ryu is used to realize the local and global SDVN functions [71]. Ryu provides OpenFlow components and well-defined API. For the development of various interfaces (i.e., the CP client-server interface, CP server-to-SDVN controller interface, and SDVN local-to-global interface), Python sockets and Python Flask are utilized. Flask enables the creation of HTTP-based RESTful APIs, which are widely used by web applications and as northbound interfaces of SDN controllers.

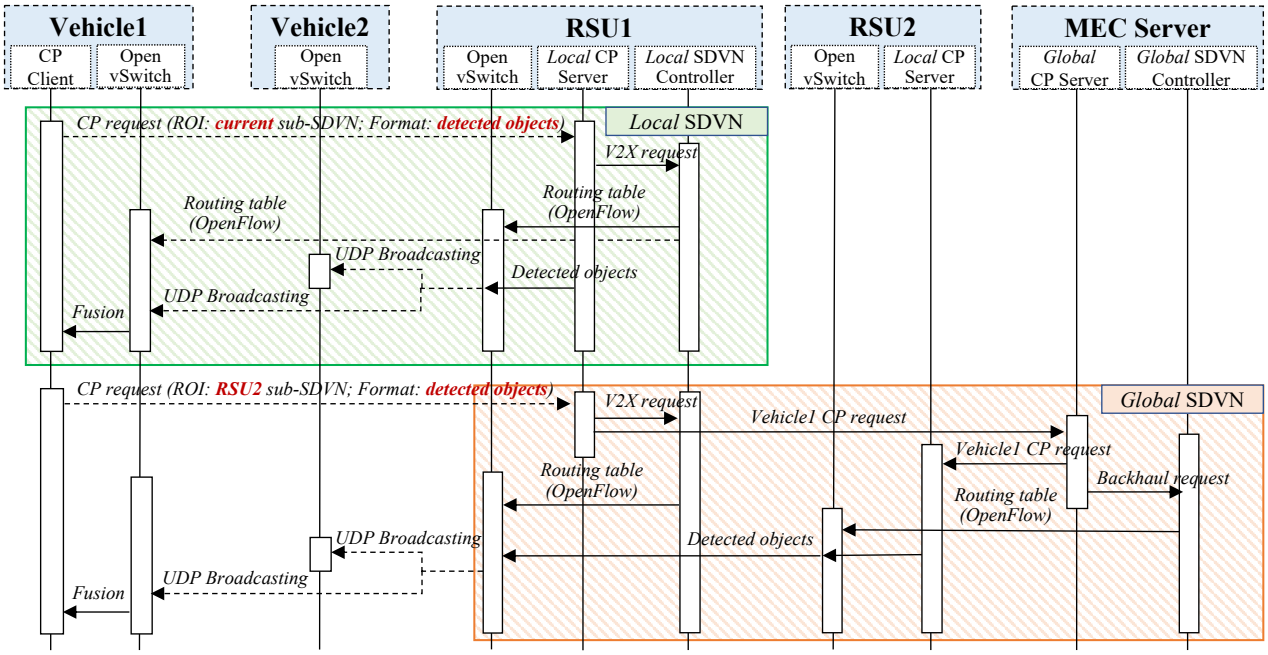

(a) Vehicle1 requests CP in a detected-object format

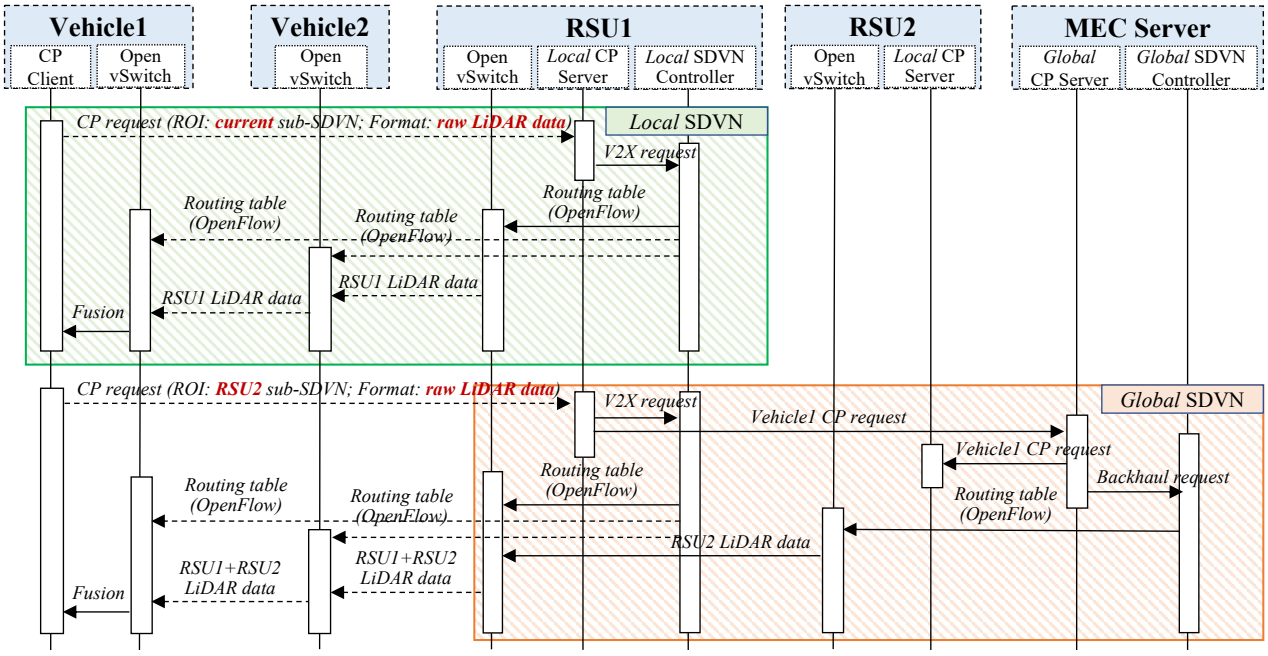

(b) Vehicle1 requests CP in a raw-data format

Figure 4.11: Sequence diagrams of Het-SDVN for CP. (a). Detected object-based CP. (b). Raw LiDAR data-based CP.

4.4.4 Evaluation and discussion

Proof-of-concept results are discussed from three aspects: the required data rate for two different types of CP, the performance of the deployed local SDVN network and the overall performance including the backhaul performance (global D-plane), controller reaction delay and the visualization of CP.

4.4.4.1 Required data rate

Table 4.3: Average data rate (raw LiDAR data, detected objects).

Pointcloud Data Rate RSU LiDAR	Detection Data Rate RSU1	Detection Data Rate RSU2
46.5 Mbps	2.84 Mbps	1.39 Mbps

Table 4.3 shows the practical output data rate of RSU1/RSU2 LiDAR and the data rates of detected objects on RSU1 and RSU2, respectively. The former value depends on the LiDAR specification. RoboSense 80-laser LiDAR Ruby-Lite is used by RSU1 and RSU2. The measured average data rate is 46.5 Mbps, about 3 times that of the RoboSense 32-laser LiDAR used by Vehicle1. It makes sense because RSU LiDARs are supposed to monitor more precisely to ensure road safety. The latter values are affected by the surrounding object number, the detected object number, the used detection algorithm, the message format, etc. In this measurement, object detection is done by the ROS2 node `lidar_centerpoint` of autoware.universe. It publishes detected objects in ROS2 message format `DetectedObjects`, which are transferred via UDP. In 10 minutes, the average detection data rates of RSU1 and RSU2 are 2.84 Mbps and 1.39 Mbps, respectively.

Comparing the measured data rates, it shows that sharing raw LiDAR data for CP poses greater challenges to network performances, especially to the throughput (about 20 times higher than the detected objects with only one LiDAR). It is crucial to consider different radio access technologies and transmission modes of V2X in the local SDVN network.

4.4.4.2 Local SDVN performance

Vehicle1 receives CP data within the local SDVN of RSU1. Therefore, key performance metrics like the C-plane coverage and D-plane throughputs should be evaluated.

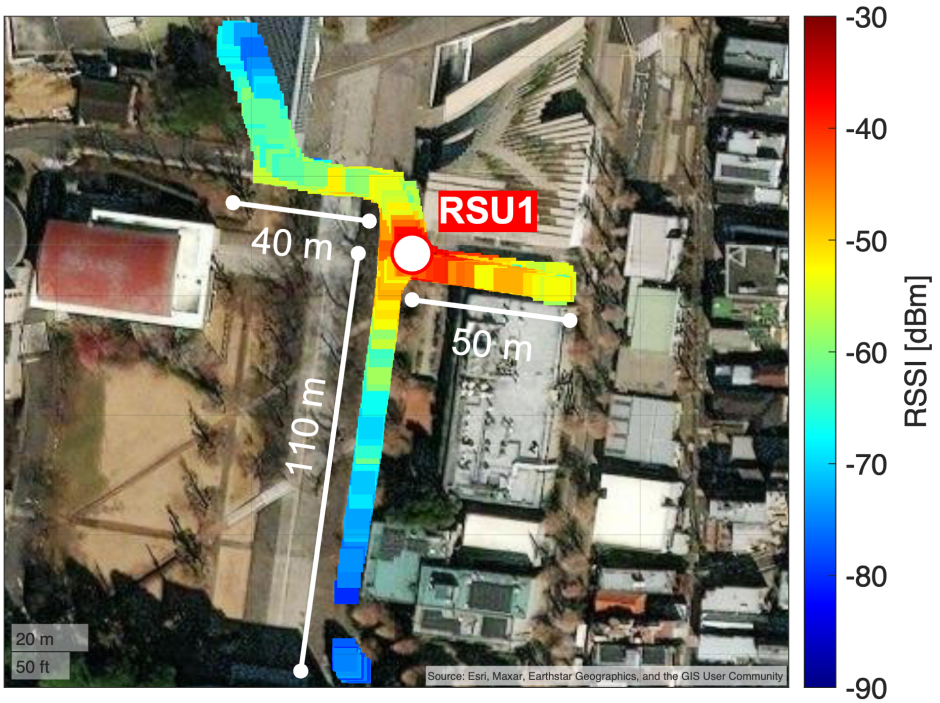

(a) *Local* C-plane over 2.4 GHz Wi-Fi

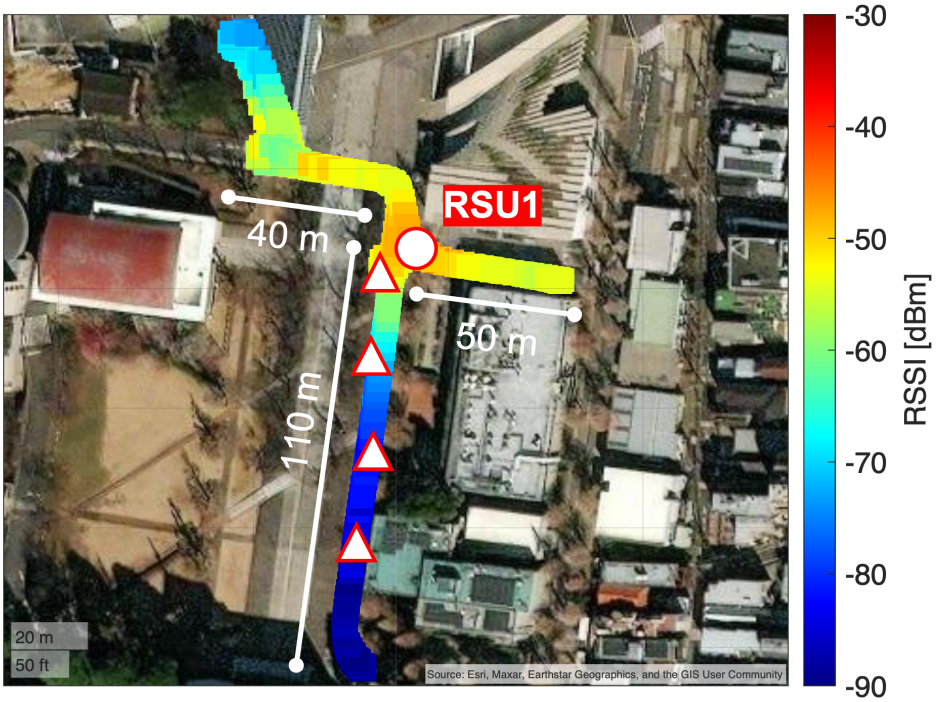

(b) *Local* D-plane over 5 GHz Wi-Fi

Figure 4.12: RSSI maps of the SDVN WiFi C/D-planes.

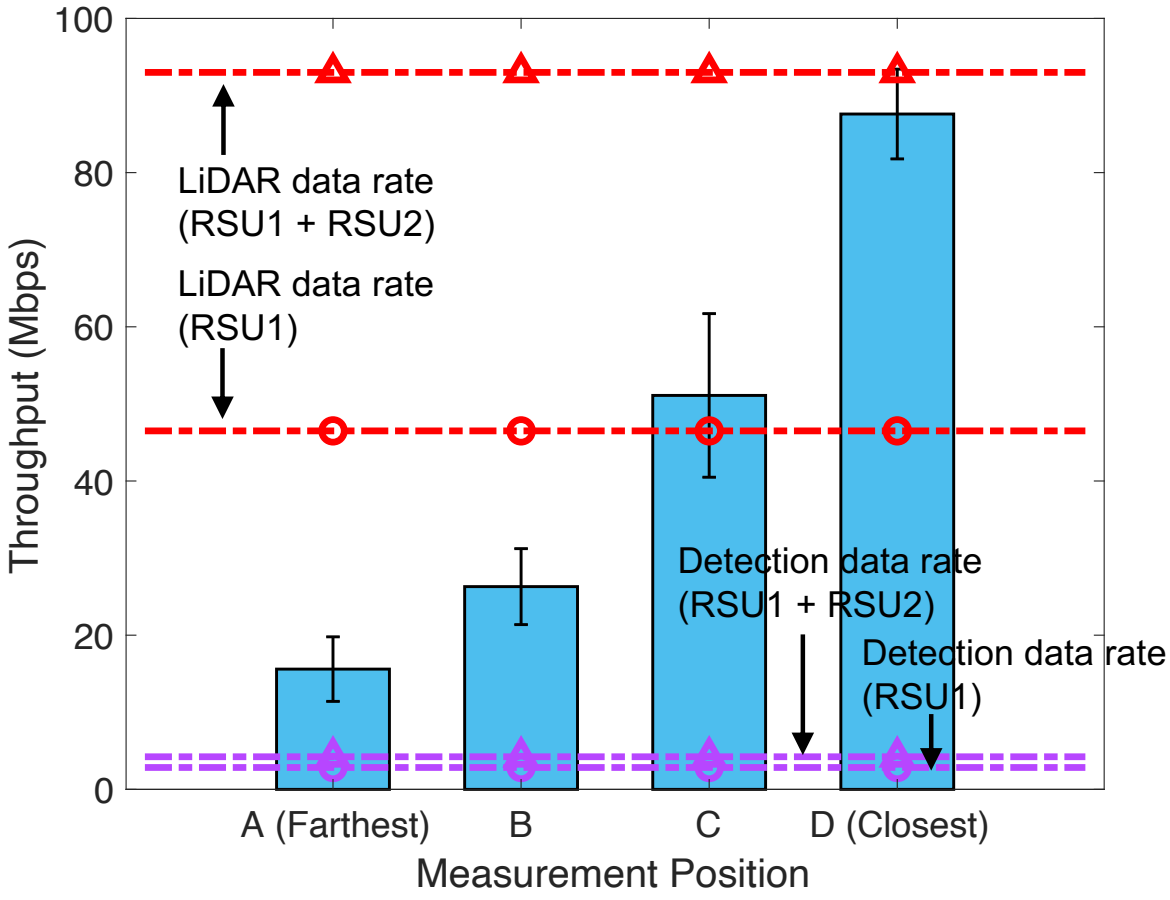

Figure 4.13: Throughputs of Wi-Fi as local SDVN D-plane.

Figure 4.12 showcases the received signal strength indicator (RSSI) maps of RSU1 Wi-Fi as the local C/D-planes. As shown in Fig. 4.12(a), RSU1 is located at a T-type intersection (red circle). Since the RSSI values are measured under the condition that the Wi-Fi association is available, it demonstrates that using 2.4 GHz Wi-Fi as the local C-plane on RSU1 can cover all three main roads to the intersection. So does the 5 GHz Wi-Fi D-plane, as shown in Fig. 4.12(b). Four red triangles are marked along the experimental course (from bottom to top: A→B→C→D), which indicate the positions where Wi-Fi D-plane throughputs are recorded.

Figure 4.13 plots the average Wi-Fi D-plane throughputs. The error bars represent standard deviations and the dash lines indicate the required data rates under four processes depicted in Fig. 4.11. It is seen that the practical throughput of 5 GHz Wi-Fi outdoors degrades as the distance from RSU1 increases. When it comes to point B, this D-plane has failed to support the broadcasting of RSU1 LiDAR data. Even at the closest point D, the

throughput improves, which, however, is still far from the requirement of transmitting both RSU1 and RSU2 LiDAR data. It demonstrates that the 5 GHz Wi-Fi D-plane is only capable of detected object-based CP. Heterogeneous V2X, especially high-frequency V2X like mmWave is necessary in order to enable raw data-based CP.

In contrast, the 60 GHz WiGig as another choice of local SDVN D-plane has extraordinary throughput performance. The peak throughput observed on one WiGig V2I/V2V link reaches 2.20 Gbps. Due to the directivity of WiGig antennas, this performance is only sustained in line-of-sight communications. In addition, when multi-hop mmWave V2X occurs on a straight lane/road, like the topology of this proof of concept (RSU1→Vehicle2→Vehicle1), interference is non-negligible. This impact has been studied in [72], where the authors proposed to configure mmWave antennas as ZigZag to mitigate inter-vehicle interference. In this work, channel management is implemented as a function of the local SDVN controller to relax interference. In Fig. 4.10, Ch2 (60.48 GHz) and Ch3 (62.64 GHz) are allocated to the mmWave V2I and V2V links, respectively. Table 4.4 compares the throughputs and packet delivery ratios (PDR) of mmWave D-plane with and without such channel control. It is shown that by applying channel control, the average D-plane throughput increases from 602.1 Mbps to 1.84 Gbps and the PDR also improves from 66.33% to 99.99%.

Table 4.4: Throughput and PDR of mmWave (WiGig) D-plane.

	mmWave D-Plane w/o Channel Control	mmWave D-Plane w Channel Control
Throughput	602.1 Mbps	1.84 Gbps
PDR	66.33 %	99.99 %

4.4.4.3 Overall performance

This proof of concept aims to effectively integrate the local and global SDVN networks. To examine network operations, the data rates of mmWave and backhaul interfaces on Vehicle1, Vehicle2 and RSU1 are recored using Wireshark after synchronization. Figure 4.14 shows the data rate variation when SDVN controllers are requested to orchestrate the network for CP following the sequence of Fig. 4.11(b). It is seen that the mmWave V2I and V2V links start to carry raw LiDAR data (from RSU1) after the local SDVN controller responds. When Vehicle1 demands raw LiDAR data from RSU2, the global SDVN controller successfully arranges the

backhaul network, which can be observed from the significant growth of backhaul data rates. Meanwhile, the data rates on mmWave V2I and V2V links double, which implies that RSU2 LiDAR data get properly transmitted over the local SDVN network.

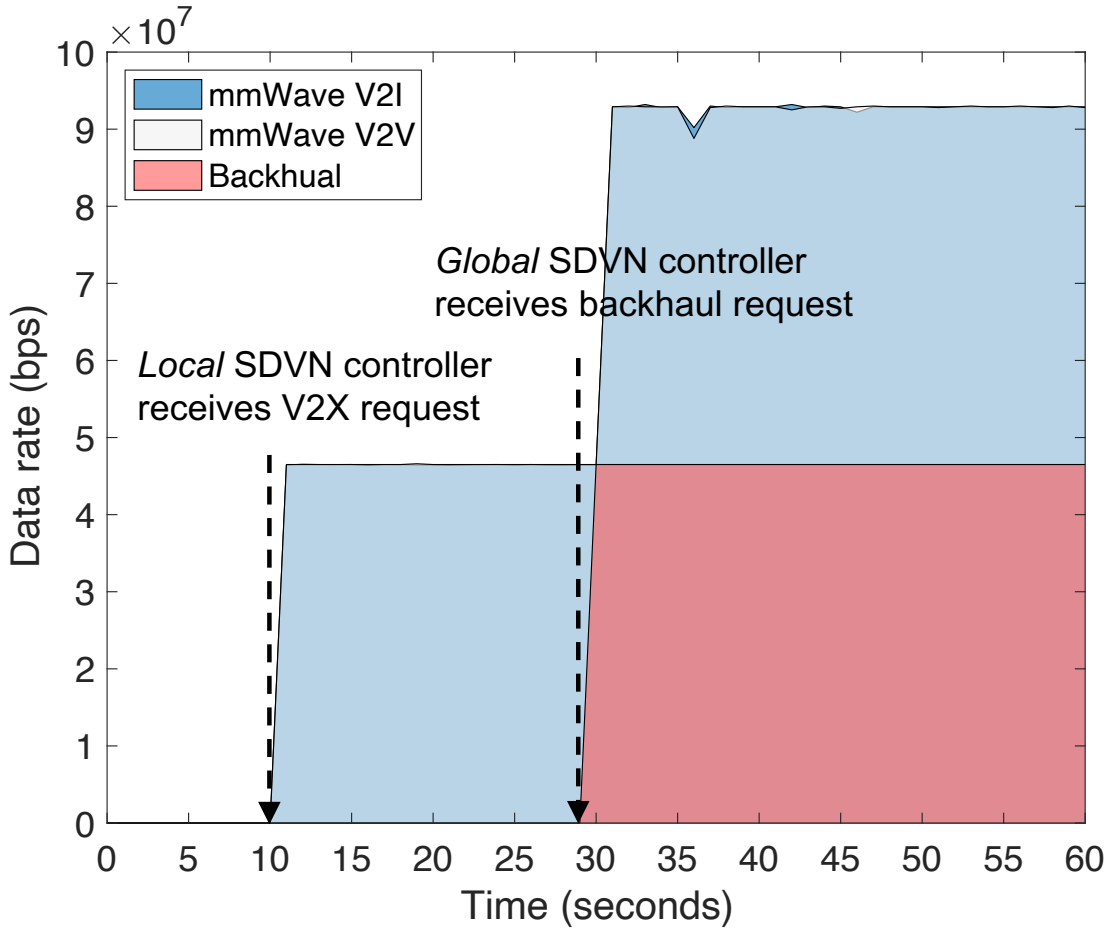

Figure 4.14: Variation of link data rates under SDVN controller orchestrations.

The local and global C-planes use heterogeneous networks (2.4 GHz Wi-Fi and Ethernet). It is necessary to evaluate their HTTP latency and flow installation latency separately. Table 4.5 presents the test results. The HTTP latency over Wi-Fi C-plane is slightly larger and more unstable than that over Ethernet, probably due to the outdoor wireless interference. Nevertheless, if the global CP server is deployed on Cloud, instead of the MEC server in this proof of concept. The HTTP latency can range from tens to hundreds of milliseconds. Therefore, safety-critical requests need to be firstly processed by the local CP server. As for flow installation latency, it is measured by CBench [58], one of the benchmarking tools for SDN controllers. The CBench emulates one OpenFlow switch (connecting to the Ryu

controllers) and calculates the number of flow modifications per second. The number of test iterations is set to 20. Other parameters keep default and the same. It is seen that the local and global SDVN controllers present similar flow installation efficiency regardless of network types. Since the network flow can be configured within 3 ms, it is likely to support advanced V2X applications which require an end-to-end latency of less than 10 ms.

Table 4.5: Latency performance of CP and SDVN controllers.

CP Client-Local CP Server HTTP Latency	Local CP Server-Global CP Server HTTP Latency
3.307 ms	2.539 ms

Local SDVN Controller Flow Installation Latency	Global SDVN Controller Flow Installation Latency
1.796 ms	2.693 ms

On Vehicle1 PC, the received CP data are visualized using the ROS2 tool Rviz, as shown in Fig. 4.15. Figure 4.15(a) reflects the detected objects from RSU1 and RSU2 as colored bounding boxes with motion vectors, representing their categories, sizes, and mobility. These attributes are extracted from raw LiDAR data using the detection method CenterPoint, which significantly reduces the data size so that legacy V2X is still capable of broadcasting detected objects. Although sharing raw data is resource-consuming, demanding high-frequency V2X and additional bandwidth allocation, the LiDAR pointcloud data from RSU1 and RSU2, as shown in Fig. 4.15(b), are imperative for high-level automated driving in terms of reliability and liability. Regarding reliability, these raw data complement the pointcloud density of Vehicle1 LiDAR and light up the vacancy spots along the driving course, which can increase maneuvering agility and the tolerable time for safe maneuvering [20,21]. As for liability, automated vehicles share higher portions of liability for incidents as the levels of autonomy upgrade, because they gradually take over the driving responsibility from human drivers [73]. RSUs, however, share very limited liability when they don't control vehicles directly. Therefore, Vehicle1 has the obligation to identify the trustworthiness of detection results from RSU1 and RSU2 if their authentication information (e.g., detection capability) is incomplete. With raw data at hand, Vehicle1 can perform detection by itself, as shown in Fig. 4.15(c), so the safety-critical decisions (brake, deceleration) can be double-checked. The visualization results

clearly demonstrate the capability of the proposed Het-SDVN in managing heterogeneous V2X resources to enable diverse CP effectively.

4.4.4.4 Discussions on scalability

The Het-SDVN introduces hierarchical C-planes and D-planes. In the proof of concept, the global C-plane is through the LTE at 2.5 GHz and Ethernet. The LTE capacity here is equal to the WiMAX capacity in Chapter 3, which supports the collection of mobility information from 1171 vehicles. For both the global C-plane and global D-plane, the Ethernet network is extensible and has enough capacity to connect a large number of RSUs. As for the local C-plane, since the 2.4 GHz Wi-Fi (IEEE 802.11b/g/n) is used, its capacity is 11 - 72.2 Mbps in coverage, which allows 171 - 1128 vehicles to upload their mobility information at 10 Hz. The local D-plane has two different RATs, the 5 GHz Wi-Fi (IEEE 802.11a/n/ac) and 60 GHz WiGig, for sharing detected objects and raw LiDAR data, respectively. The former takes around 2.84 Mbps bandwidth, while the latter costs about 46.5 Mbps bandwidth with the 80-laser LiDAR (Ruby Lite). Accordingly, the Wi-Fi D-plane has a capacity of 6 - 173.3 Mbps, and the WiGig D-plane has a capacity of up to 2.5 Gbps. Their supported number of D-plane units (vehicles or RSUs) is 2 - 61 and 53, respectively. By improving the hardware, this number can be further increased. Moreover, the local SDVN framework for RSUs adopts the Ryu controller. In the benchmark evaluation [58], the flow installation of the Ryu controller only delayed 2.32 ms when the number of OpenFlow switches increased from 2 to 128, which reflected the good scalability of the deployed local SDVN controller in the proof of concept.

4.5 Conclusion

The emergence of advanced V2X applications facilitates the advancement of V2X communications and the innovation on traditional vehicular networks. In order to effectively support various types of cooperative perception (CP) and ensure this safety-critical V2X application is deliverable to vehicles anywhere and anytime, this chapter proposed Het-SDVN, an SDN-based V2X network architecture, consisting of hierarchical C-planes, geographically distributed but logically centralized sub-SDVNs, and heterogeneous V2X. The network roles were clearly defined. For CP in local SDVNs, communications are orchestrated by RSUs with local SDVN controllers; for CP in other SDVNs or infrastructure-rare regions, communications for crossing sub-SDVNs are orchestrated by global SDVN controllers at MEC/Cloud servers. To

empower the RSUs with SDVN functions, this chapter presented a framework that integrates ROS, Ryu, and OVS and adds customized functional components for application, network, and sensor management. This framework was deployed and tested, showing that a maximum power saving ratio of 60% was achieved with the CAM-triggered sensor ON/OFF strategy, and the delay for CP preparation was less than 30 ms. Eventually, the holistic Het-SDVN was set up in Tokyo Institute of Technology, and its support for CP has been demonstrated via a proof of concept. Evaluation results validated the feasibility of Wi-Fi as local C-planes and stressed the importance of mmWave and the necessity of interference management when performing raw sensor data sharing. Moreover, no significant difference in flow installation performance was observed between the local and global SDVN controllers over different networks. They were all under 3 ms, showing the potential to meet the latency requirement (less than 10 ms) of advanced V2X applications [7].

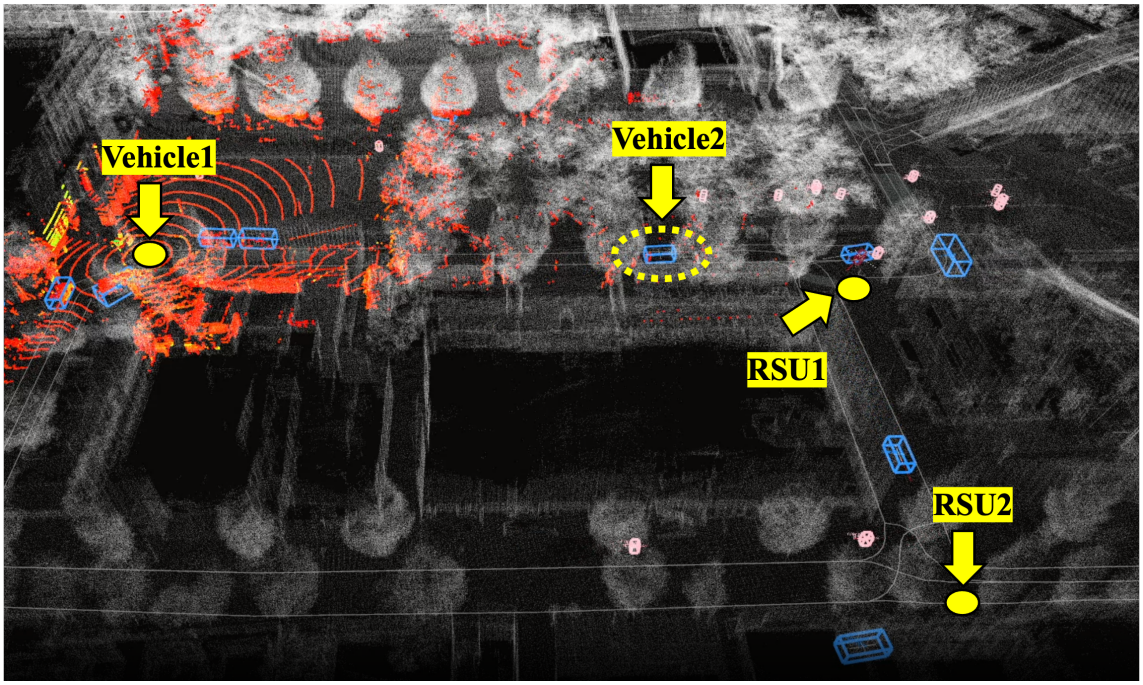

(a) Detected object-based CP.

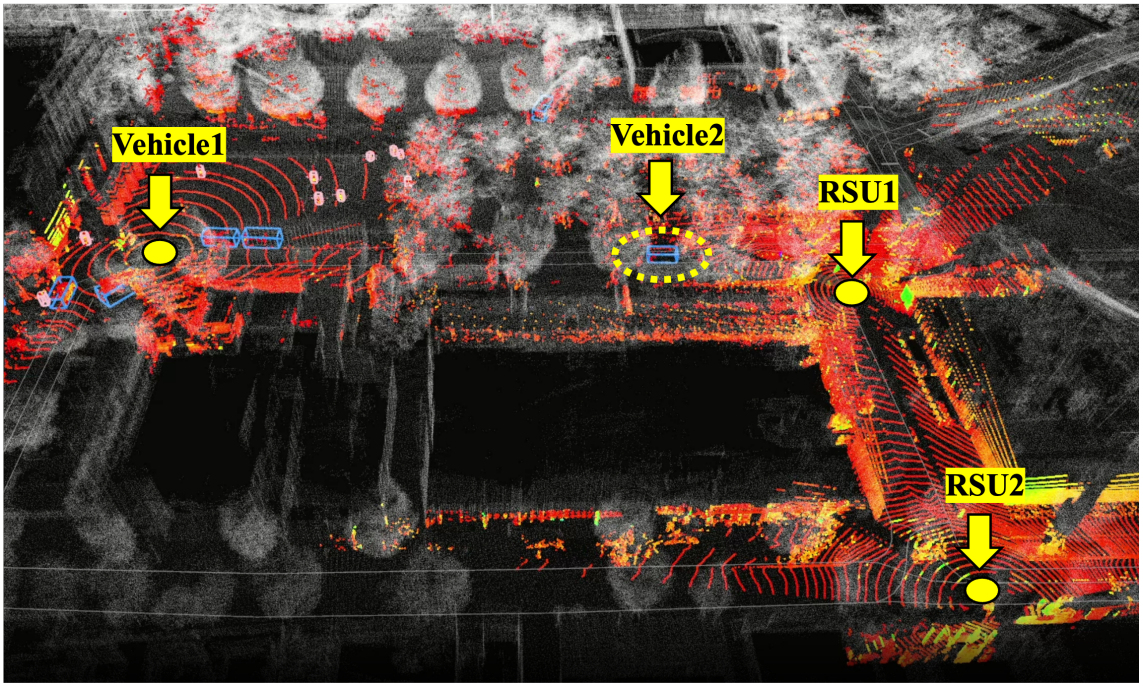

(b) Raw LiDAR data-based CP.

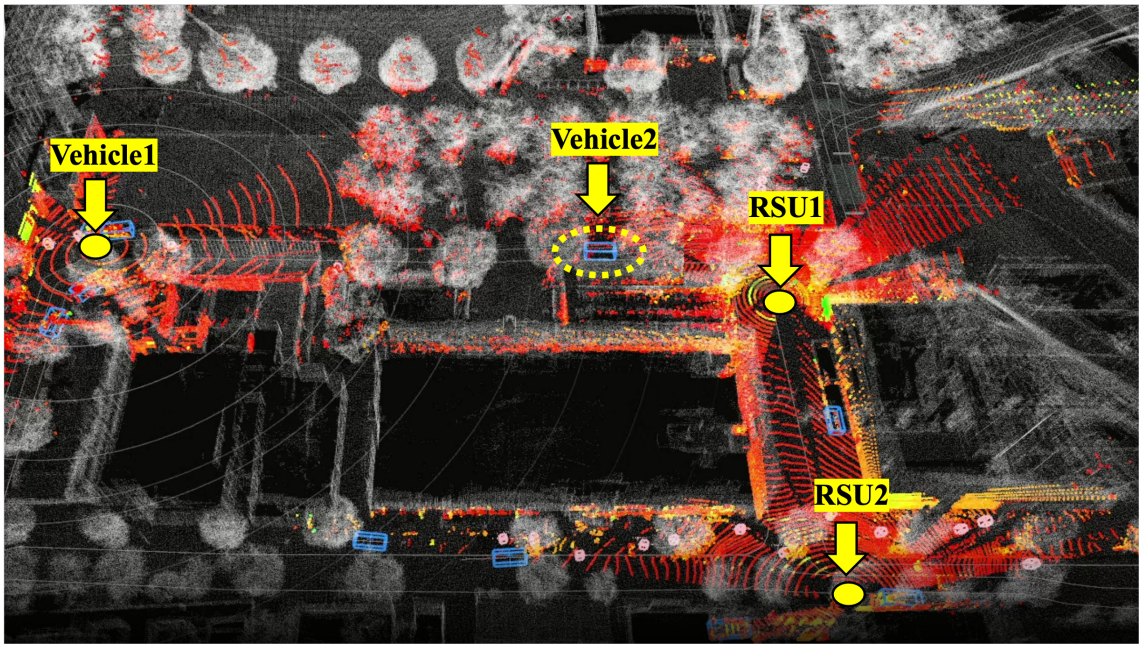

(c) Detection performed with raw LiDAR data from CP.

Figure 4.15: Visualization of received CP data on Vehicle1 PC. (a). RSU1 and RSU2 send detected objects. (b) RSU1 and RSU2 send raw LiDAR data. (c) Vehicle1 performs detection with raw LiDAR data from CP.

Chapter 5

Orchestration of Mobility-Aware HD Map Distribution in Het-SDVN

In Chapter 4, a hierarchical SDVN architecture with heterogeneous V2X (Het-SDVN) has been proposed and demonstrated. Through dynamic collaborations between vehicles and two layers of C-planes/SDVN controllers at RSUs and MEC/Cloud, respectively, cooperative perception (CP), the safety-critical V2X application which also adopts a three-layer architecture (CP client, local CP server, global CP server), are effectively enabled. High-definition (HD) map distribution can be regarded as an extension of CP. HD maps play an essential role in automated driving systems. The 3D pointcloud data they include, contribute to precise localization at a centimeter level, environmental awareness beyond the field of view (FOV), and safe maneuvering based on transient information like traffic signs and landmarks. The current dilemma is that vehicles cannot store an entire end-to-end map due to the overwhelming data size. These maps are expected to be partitioned to reduce their size and distributed to moving vehicles over the air. Existing methods simply evenly cut map tiles and distribute them via legacy Wi-Fi. From the author's perspective, map partitioning and distribution need a more intricate design that takes into account the vehicle's speed and the network's performance. In this chapter, the author states the necessary conditions for map partition and proposes a strategy to guarantee an overlap between partitions and optimize the overlap's length to avoid localization failure. To take advantage of Het-SDVN, the author develops a vehicle context-based millimeter-wave (mmWave) map distribution system with roadside units (RSU) under edge/cloud orchestration. The proposed system has been demonstrated by road tests with automated vehicles and Het-SDVN network infrastructures.

5.1 Motivation

The development of automated driving technologies is at a crucial moment. Consumers are not merely satisfied with the Advanced Driver-Assistance Systems (ADAS). They pursue higher-level, Level 3-5, automated driving systems as laid out by the Society of Automotive Engineers (SAE) International [1]. To that end, an increasing number of sensors including global navigation satellite system (GNSS) antennas, radars, cameras, light detection and ranging (LiDAR), etc, are being mounted on vehicles to enhance different capabilities. The creation of high-definition (HD) maps is one of the major functions enabled by this improved vehicular sensing system.

HD maps are 3D maps that contain spatial and semantic information about the roadway environment. These maps play a significant role in automated driving. It helps automated vehicles (AV) achieve centimeter-level localization accuracy, perform fine-grained path planning, and mitigate the difficulty of contextual perception [74]. As shown in Fig. 5.1, the spatial information is presented in form of pointclouds measured by LiDARs, while the semantic information (e.g., road markings) is denoted by vector elements, a.k.a. vector maps. In contrast to HD maps, navigational maps for human drivers are of meter-level accuracy and mainly comprise semantic information [75], it is possible to download a city or state-wide map at once over cellular networks (e.g., 221.4 MB for Tokyo [76]). However, the tremendous amount of pointcloud data in HD maps can easily overwhelm the storage capacity of AVs. It is reported that the total data volume of an HD map collected for one hour is about 1 TB [54].

Therefore, updating these maps, after partitioning, over air interfaces during automated driving seems to be a means to unleash the issue of storage. This also paves the way for more advanced vehicle-to-everything (V2X) communications to support ultra-fast map distribution. However, existing V2X technologies have well-known limitations in data rates. The dedicated short range communications (DSRC) at 5.9 GHz only supports a peak data rate of 27 Mbps, which further degrades to 6 Mbps with high vehicle densities [47]. Although the long term evolution (LTE) V2X makes certain improvements, its achievable data rate is still below 28.8 Mbps [17]. In 2020, new radio (NR) V2X was standardized in 3GPP Rel-16 to enhance the communication performance [77] but its commercialization schedule is hard to predict.

In this chapter, the author addresses the challenges above from two fronts: 1) Section 3.1 proposes an adaptive strategy in map partition to retain overlap to avoid localization failure

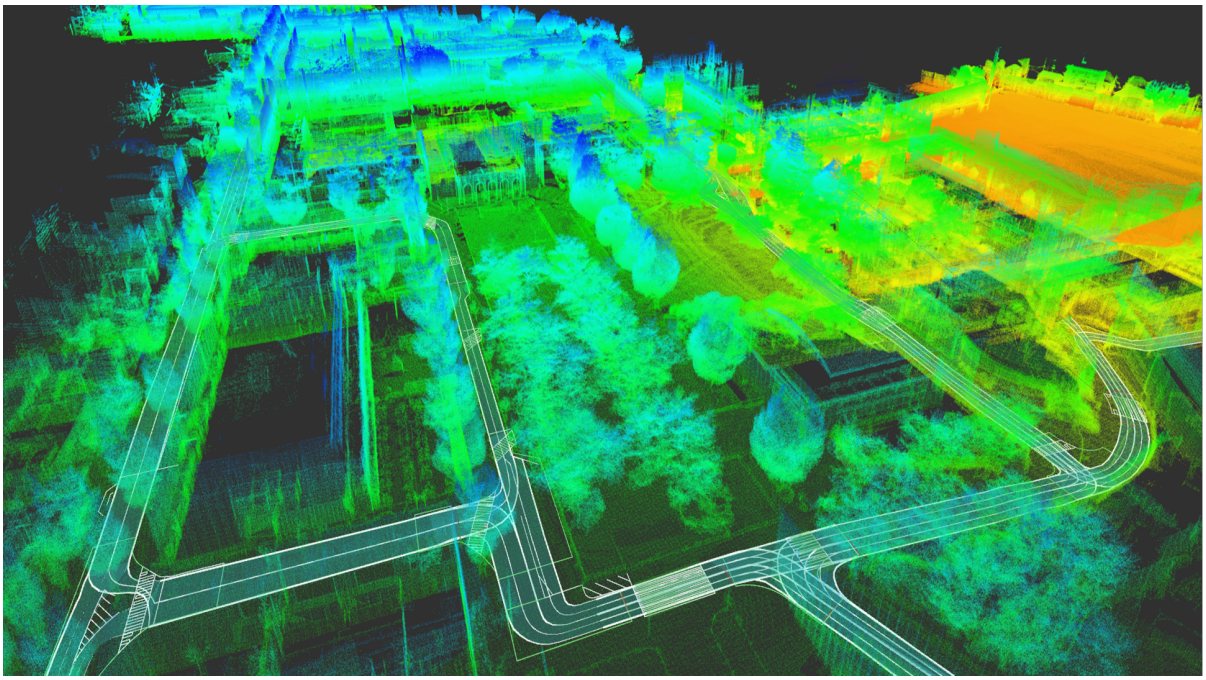

Figure 5.1: An example HD map containing pointcloud data and semantic information.

at boundaries due to the network delay and optimize map extents; 2) Section 3.2 designs an efficient map distribution system using millimeter wave (mmWave) under the orchestration of edge/cloud servers. In addition, proof-of-concept trials in real driving scenarios are presented in Section 3.3. The performances of the proposed system are comprehensively evaluated.

5.2 Design of mobility-aware map partition

In addition to existing map partition considerations, such as software file size limitations and pointcloud density standards, this section will be introducing considerations for the proposed inclusion of a strategy to make sure that there is an overlap between partitioned HD maps and optimize its roadway length. The guarantee of overlap is crucial. It works as a safety feature to avoid localization failure, when utilizing scan matching, at map boundaries caused by network delay. Meanwhile, optimizing the overlap's roadway length further extends the reach of the partitioned HD maps. Both of these measures ensure that the automated vehicle will always have an HD map throughout its trip. To realize this, the proposed map partition takes the vehicle's speed and its relationship with two factors: the time it takes to connect and download the HD map from the RSU into account.

5.2.1 Connection time

Beamforming (BF) is now widely applied in wireless communications to compensate for the severe path loss between the transmitter and the receiver. Meanwhile, this technology introduces non-negligible overhead in the initial access to the networks. It needs to perform an exhaustive search to locate a suitable communication path between the vehicles and RSUs. The high mobility of vehicles would complicate this process and cause a connection delay after entering the RSU coverage. This delay in connection with the RSU coupled with the vehicle's speed becomes the initial distance consideration to determine if there remains sufficient overlap and how long the boundaries of the partitioned map could be extended.

5.2.2 Download time

After connecting to the network, the vehicle would be able to download the map partition. The speed at which it can download the map depends on the practical throughput/data rate of the RSU. The time it takes to fully download the HD map together with the vehicle's speed is an additional consideration in determining overlap length sufficiency and the partitioned map's roadway length.

5.2.3 Overlap optimization

Figure 5.2 illustrates the necessity of overlap optimization between contiguous map partitions. The vehicle's capacity to store or load HD maps for automated driving is still highly constrained, due to either hardware limitations or legacy issues of the software. Assuming that the vehicle can store an HD map with a length of l, when updating maps near the boundary, a part of the new map has to be reserved to create an overlapping area for stable localization. Conventionally, the overlap starts at the edge of the RSU coverage, i.e., the initial access point when the vehicle's speed is equal to 0. Such a method of delineating overlap occupies a considerable part of the new map and confines its reach because of the limits of vehicle storage.

Hence, it is imperative to save the overlap area by taking the connection time (t_1) and download time (t_2) into account. If the vehicle's speed v_0 is known, the saved length from overlapping in the new map can be represented as

$$l_{saved} = l_c + l_d + \sigma_1 + \sigma_2 \tag{5.1}$$

where $l_c = d_1 = v_0 t_1$ indicates the passing distance for V2X connection after entering RSU coverage, $l_d = d_2 - d_1$ indicates the passing distance for map downloading which is inversely proportional to V2X data rates. σ_1 and σ_2 denote the standard deviations of d_1 and d_2 respectively. A minimum overlapping length of $\sigma_1 + \sigma_2$ can be reserved to keep redundancy and enhance the system robustness. In this way overlap creation becomes adaptive to the vehicle's speed and V2X performance, saving overlapping areas and extending the reach of the new map.

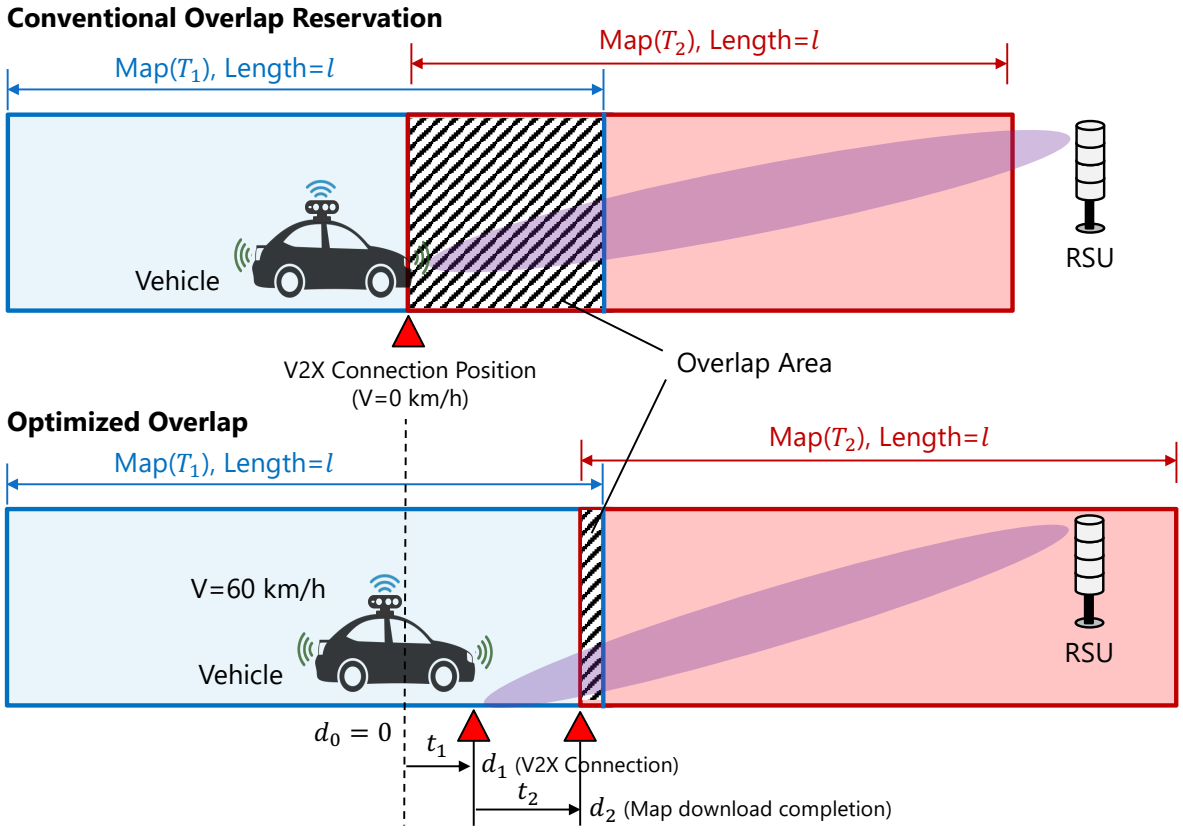

Figure 5.2: Illustration of overlap optimization.

5.3 Design of mmWave map distribution system

5.3.1 Prior arts

5.3.1.1 Map distribution system

The wireless distribution of HD maps, especially the part of point cloud data (PCD) maps, is challenging considering the limitations of current mobile services and traditional V2X technologies. Shimada et al. categorized the elements of HD maps into four layers: 1) permanent static data (map data); 2) transient static data (roadside infrastructure); 3) transient dynamic data (congestion, signal phase); 4) highly dynamic data (vehicles, pedestrians) [78]. Of the four layers, PCD maps belong to the first layer.

From top to bottom, the data volume and required data rate for transmission largely increase. As such, existing works mostly focus on the distribution of higher-layer map data in a manner called cooperative perception through V2X communications. These data are embedded in light V2X messages (e.g., CAM, DENM) and broadcasted by vehicles or roadside units (RSUs) at a low data rate using DSRC technologies. The typical systems include Tsukada et. al's Proxy CAM [79], AutoC2X [4] and Miucic et.al's prototype system employing BSM-based cooperative perception [80]. In the works of Mizutani et al, they have evaluated the distribution of PCD maps during automated driving [81] by showing that the vehicle successfully downloaded PCD maps over Wi-Fi at 60 Mbps in 1.16 s. However, the downloaded maps were highly downsampled which can be ineffective for localization under extreme conditions. Besides, PCD maps need to assist other automated driving functions, such as semantic segmentation, road boundary detection, etc, which require much higher resolutions. Hence, new V2X technologies are being pursued to meet the demanding requirements for such map distribution.

5.3.1.2 mmWave V2X networks

The mmWave, as a promising technology for 5G and beyond, has been incorporated into the frequency range of 5G NR (FR2: 24.5 GHz - 52.6 GHz). Owing to the rich unexploited spectrum resource, mmWave can realize the new features of 5G systems including the ultra-reliable and low latency communications (URLLC), enhanced mobile broadband (eMBB), and massive machine type communication (mMTC). More so, commercialized mmWave technologies have shown their great potential for access and backhaul networks [82]. For example,

IEEE 802.11ad (a.k.a WiGig) operating in the unlicensed 60 GHz band can allocate 2.16 GHz bandwidth for communications, which corresponds to a data rate of 6.75 Gbps [83]. Its follow-up standard IEEE 802.11ay supports channel bonding and adds MIMO, thus the peak data rate can go up to 176 Gbps [84].

As a result, mmWave has countless applications in this data-hungry era. One of them is V2X networks, which is an important application scenario considering the huge market scale of the automotive industry. In V2X, mmWave is mainly applied to the safety applications [17]. Particularly for cooperative perception, mmWave empowers the exchanging of raw sensory data among vehicles [85,86,87], between vehicles and road infrastructures [88,89,90], or between vehicles and networks [91]. In super smart society, the deployment of RSUs with mmWave V2X capabilities is accelerating. Examples of relevant projects include the Lightpole Site by Ericsson/Philipps [92], the LuxTurrim5G project in Finland [93] and the Super Smart Society (SSS) project in Tokyo Tech [6]. Therefore, it is evident that mmWave can contribute to smooth automated driving by ultra-fast and low-latency distribution of HD maps over V2X, which is not possible in previous efforts.

5.3.2 System design

The overview of the system is shown in Fig. 5.3. An intact HD map covering the end-to-end traveling of automated vehicles is partitioned into regional maps. Excluding extreme conditions (e.g., in mountains or jungles), we assume that most of these regions have infrastructures that provide wireless connectivity between vehicles and the network. During automated driving, the vehicle proactively reports context information to remote map servers over cellular networks. The context information includes the real-time position, velocity, destination, etc. Remote servers then analyze this information to determine the parameters of map partition and select the most appropriate roadside unit (RSU) to cache the partitioned maps. The vehicle will be notified with the map uniform resource locator (URL) and description of the selected RSU. Finally, the RSU opens the service port for access. Remote servers keep monitoring the mmWave association between the vehicle and RSU to ensure successful map distribution.

There are three major participants in this system. Each of them shall satisfy certain functionalities to fulfill their tasks.

1) Automated vehicles: A complex, integrated and intelligent software system is the basis for automated driving. Typically, there are five subsystems, i.e., sensing, localization, per-

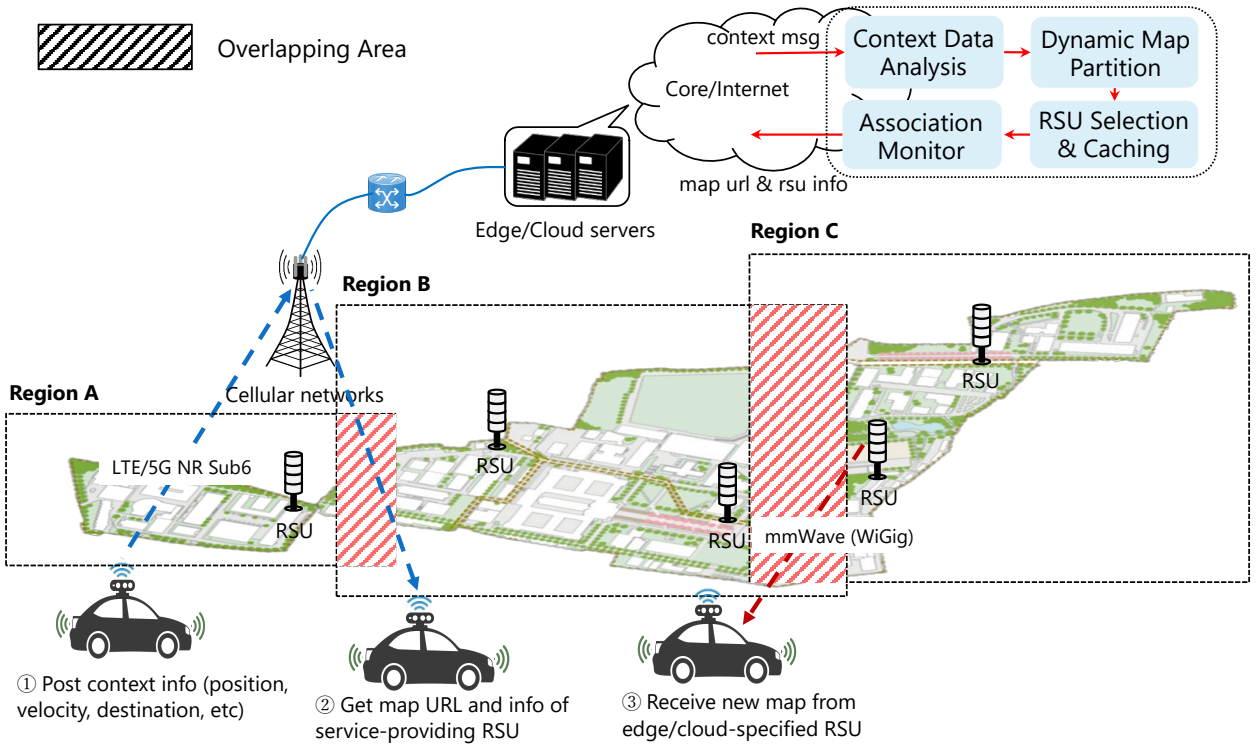

Figure 5.3: System overview.

ception, planning, and control. Localization heavily relies on LiDAR scan matching with HD maps, especially in urban canyons where the performance of GNSS severely degrades due to non-line of sight (NLOS). In this design, vehicle context information is uploaded to remote servers, for which a proxy application is needed to organize sensor data and set up communication. To separate communications between the control plane and data plane, each vehicle shall have two types of wireless interfaces. For the control plane which exchanges context and response messages, cellular interfaces (LTE/5G NR Sub6) are applicable due to their wide coverage. For the data plane that transmits HD maps with ultra-low latency, it is believed that the mmWave interface is a must. In addition, an efficient database/file system is necessary for HD map updates.

2) Edge/Cloud servers: In this system, map servers manage the service centrally. There are a variety of options to deploy these servers on the cloud, such as Amazon AWS [94], Microsoft Azure [95], Google Cloud [96], etc. Recently, activities on configuring mobile edge computing (MEC) in the vicinity of base stations are growing [97,98,99,100]. It's an alternative to bringing map servers to the edge which is closer to vehicles. As such, not only is the

uncertain delay that occurs in the backbone avoidable, the enormous service requests to the cloud can be offloaded. Nonetheless, regardless of locations, map servers need to accomplish their duties, as depicted in Fig. 5.3. Received context messages shall be parsed in Context Data Analysis, and sent to Dynamic Map Partition as key references. Map servers must be aware of the local RSU topology for RSU Selection & Caching. Association Monitor serves a security purpose, recording the status/statistics of map distribution through mmWave.

3) Roadside units: Existing standards have not clarified the physical image of an RSU, although it is no longer a novel concept in the ITS. Therefore, any stationary infrastructure entity (street lights, base stations, etc) can potentially become an RSU as long as they equip sensing, computing, and communication capabilities. To fulfill the requirements of this system, RSUs must enable mmWave for V2X communications. Corresponding software shall support large file transmission. To cache partitioned HD maps from edge/cloud servers, there shall be enough storage and a high-speed backhaul, for which both optical fiber and mmWave are applicable. It is also expected that RSUs can have a high penetration rate in future society to improve the quality-of-service (QoS) of HD map delivery.

5.3.3 System implementation

Table 5.1: System hardware.

Purpose	**Hardware**	**Specifications**
Test Vehicle	Robocar MV2	$V_{max} \leq 60$ km/h
	Garmin GPS 18x USB	$ACC < 3$ m, 95%
	RoboSense RS-LiDAR-32	Laser: 32 channels, $ACC \pm 5$ cm
Edge Server	Tsukumo Workstation WA9J-H200/XT	Intel Core i9-10980XE, NVIDIA RTX 3090, MEM 128 GB, SSD 4 TB, Ubuntu 18.04 LTS
RSU	Intel NUC 11 Pro Mini PC	Intel Core i5-1145G7, MEM 8 GB, SSD 500 GB, Ubuntu 16.04 LTS

A full-fledged proof-of-concept system consisting of a test vehicle, an edge server, and

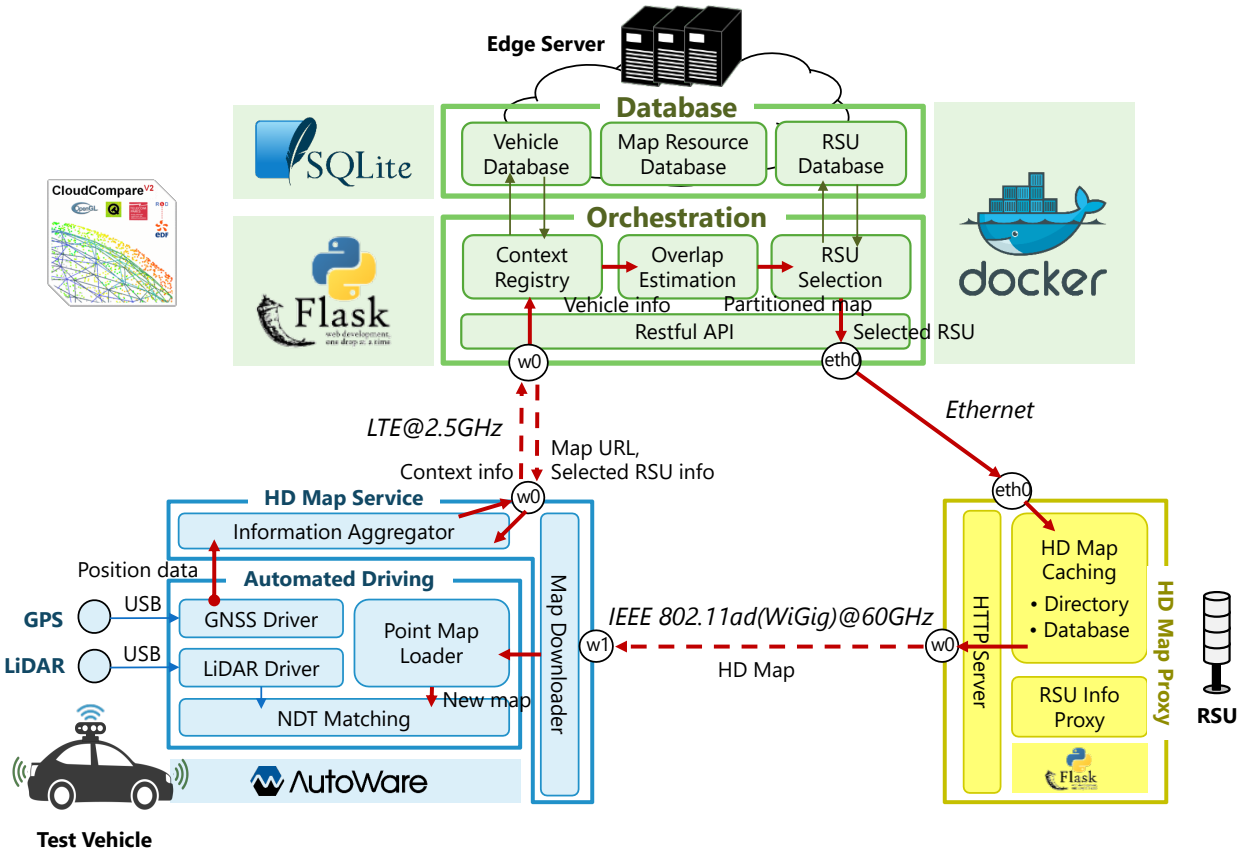

Figure 5.4: System implementation.

several RSUs has been implemented. Most of the hardware is commercial-off-the-shelf (COTS) products. For instance, the test vehicle RoboCar MV2 [101] is a product of ZMP. The edge server adopts Tsukomo's workstation WA9J-H200/XT [102], built with state-of-the-art GPU (NVIDIA Geforce RTX 3090) and extensive storage (Memory 128 GB, SSD 4 TB). In addition, Intel mini-PC NUC 11 Pro [103] is installed in RSUs as the processing unit. To localize the test vehicle, a GPS receiver (GPS 18x USB [104]) and a 3D LiDAR (RS-LiDAR-32 [105]) are mounted on its rooftop. The hardware mentioned above has been summarized in Table 5.1.

Figure 5.4 reveals the functional components for the system implementation. Some of them are based on open-source projects (Autoware [106], SQLite [107], Docker [108]) and commonly used Python frameworks (Flask [109], HTTP [110]).

1) Context registry: This component receives context information from the test vehicle via designed RESTful APIs and registers it into the vehicle database. Beforehand, vehicle position is read from the GPS receiver and formatted by the GNSS driver provided in Autoware, which

is the world's first open-source automated driving project. This position data is published at a frequency of 10 Hz. The information aggregator component adds other meta information including the vehicle ID, velocity, and destination to the context and posts them to the Flask server launched at the edge via the 2.5 GHz LTE.

2) Overlap estimation: This component calculates the size of roadway length that can be saved to extend the boundaries of partitioned maps and makes sure that there remains an overlap in between, as discussed in Section III. The vehicle velocity from the context registry and the network status of RSUs are important inputs. Our ultimate target is to do the partitioning online, however, for simplicity, we have made a partition set M with regular parameter pairs (V_i, R_j), where V_i is the velocities between $0 - 60$ km/h with $\Delta v = 10$ km/h, while R_j is the achievable data rates referring to the modulation and coding scheme (MCS) table of the commercialized mmWave communication standard IEEE 802.11ad/WiGig in the unlicensed 60 GHz band [111]. As such, from the real-time inputs (V_t, R_t), the desired partition can be obtained by $\underset{M_{(i,j)}}{argmin}(\|(V_t, R_t) - (V_i, R_j)\|)$. The tool that has been used to partition the HD maps for this work is CloudCompare [112], free and open-source software for 3D point cloud processing.

3) RSU selection: This component selects the most suitable RSU to cache and delivers new HD maps to the test vehicle. To master the physical and logical topology of local RSUs, the edge server periodically sends inquiry messages to them over Ethernet networks. RSU info proxy helps RSUs to respond to their status/statistics, which is also implemented by Flask. The collected RSU information is stored as a graph with metadata in the RSU database. For simplicity, this implementation selects the closest RSU near the region boundary along the driving course for new map delivery. The new map is cached to the selected RSU using the HTTP service.

4) Map distribution: The map distribution is managed by HTTP servers in RSUs. The HTTP server maintains the cached HD maps and corresponding URLs. mmWave is used as the transmission medium between the test vehicle and RSUs. For this implementation, IEEE 802.11ad/WiGig is the best choice because there have been plenty of mature antenna products compliant with this mmWave standard. The antennas we used are fabricated by Panasonic, which supports beamforming and MCS up to 9, indicating a maximum data rate of 2.5 Gbps.

After the map downloader in the test vehicle completes its task, the point map loader of Autoware will load the new map to replace the current map without disturbing the local-

ization, and continue automated driving smoothly. Furthermore, an outdoor experiment is conducted to demonstrate these functionalities.

5.4 Proof of concept and evaluation

5.4.1 mmWave ITS testbed

As shown in Fig. 5.5, a mmWave ITS testbed consisting of the described components in our designed system is established in the Ookayama Area of Tokyo Institute of Technology. We consider a scenario where the test vehicle equipped with LiDAR and mmWave antennas is performing automated driving toward the target area (Midorigaoka Area). Along the course, a RSU capable of mmWave V2X is deployed near the boundary between the two areas. The edge server which manages the HD map distribution is located in one of the buildings in the university, and is connected to the RSUs through the high-speed campus LAN and mmWave backhaul networks.

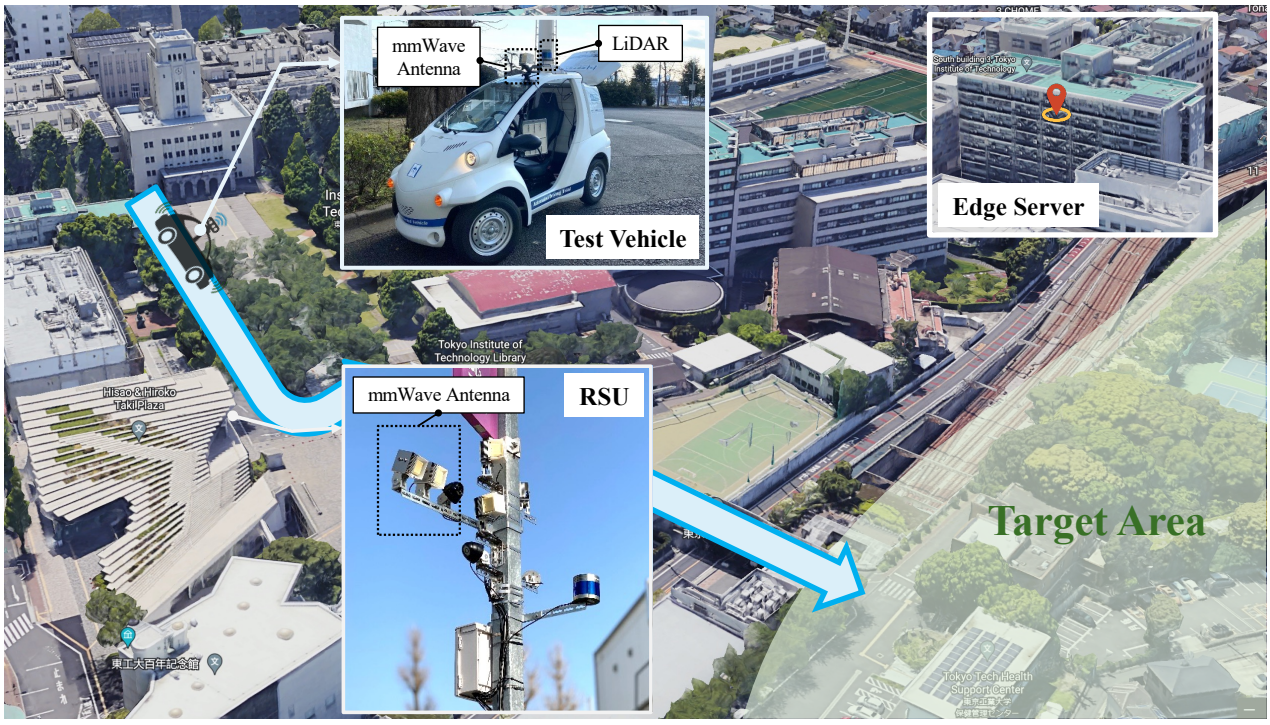

Figure 5.5: Proof-of-concept scenario and testbed setup (overlaid on Google Earth Image (Mar. 13, 2019), Tokyo Tech, Japan).

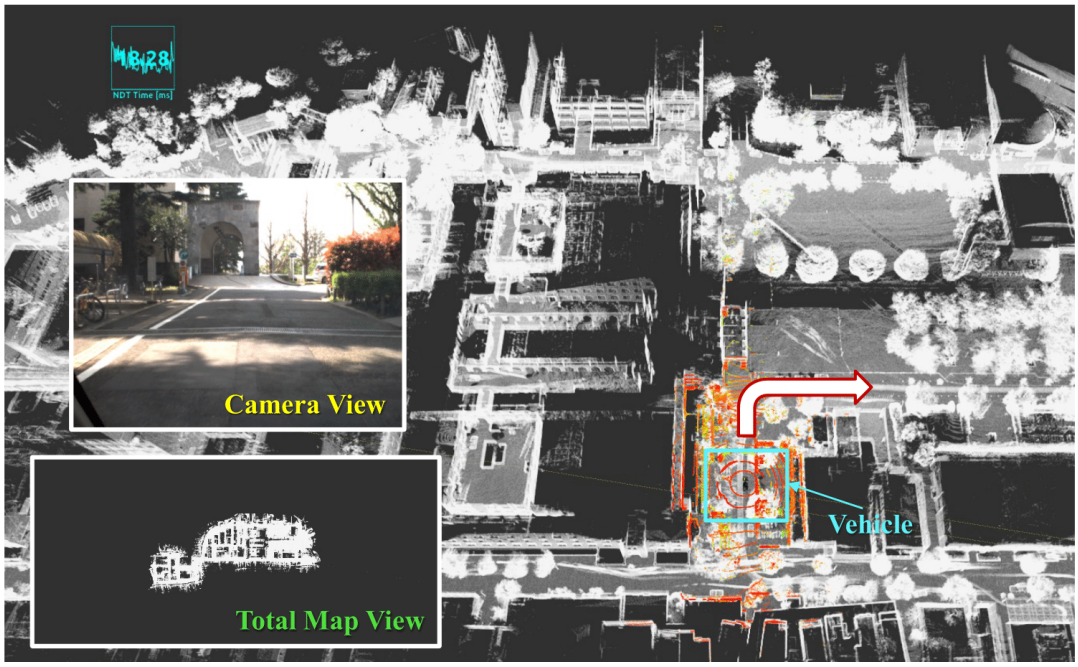

(a) Navigation in Ookayama Area.

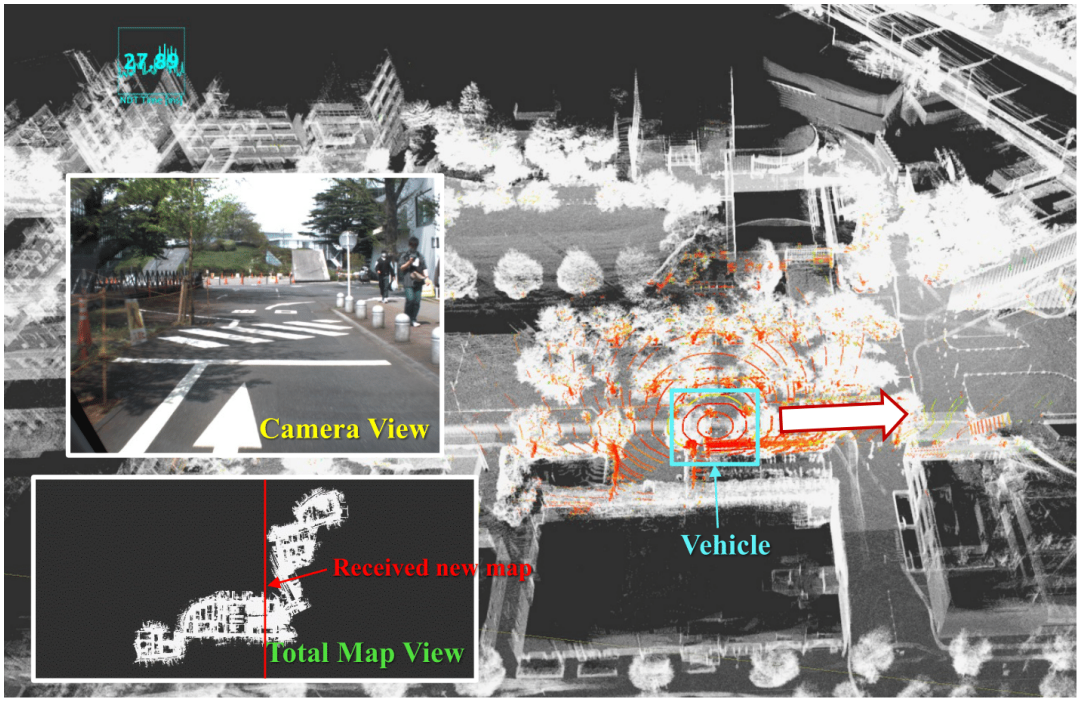

(b) Download New (Partitioned) Map.

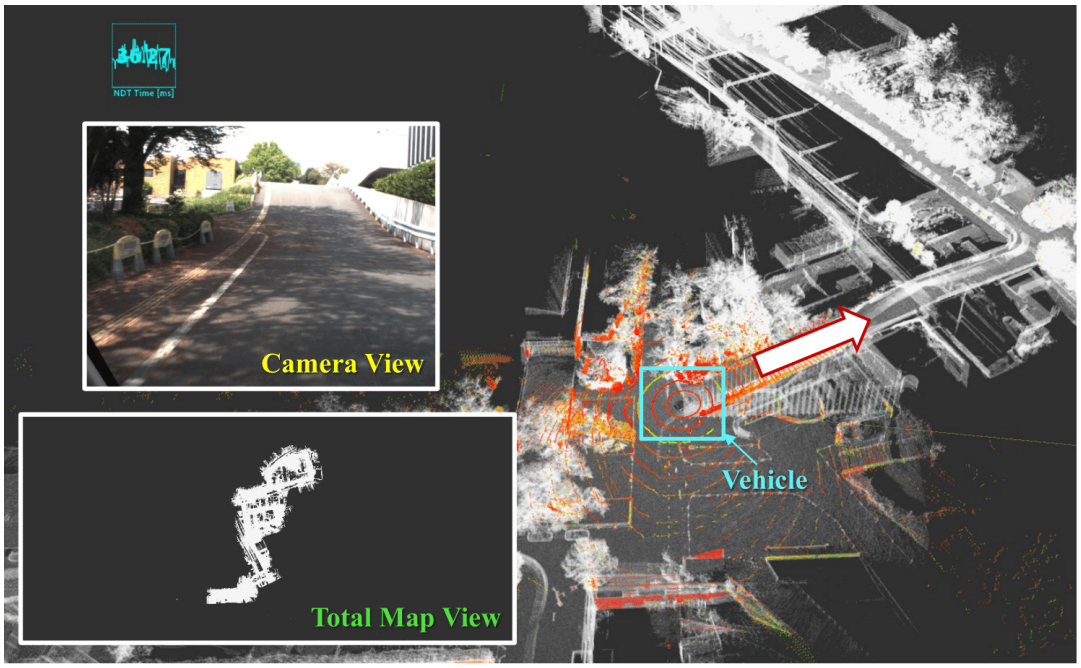

(c) Navigation in Midorigaoka Area.

Figure 5.6: Functionality verification through real driving tests (vehicle velocity: 20 km/h, map size of Midorigaoka area: 267 MB).

5.4.2 Verification

The system functionalities are verified by real driving tests heading to the Midorigaoka Area from the Ookayama Area. Figure 5.6 shows the vehicle driving process visualized in RViz, a convenient tool of Autoware for topic visualization in the 3D space. The grey point clouds represent the loaded PCD map, and the red point clouds represent the point clouds that are generated from real-time LiDAR scanning. These two point clouds are used by the normal distributions transform (NDT) algorithm, an efficient localization method for smooth automated driving. The vehicle's velocity for this test is 20 km/h which complies with the allowable speed limit at the university. From (a) to (c), we are able to demonstrate that the test vehicle was able to move smoothly while successfully receiving the new partitioned map over mmWave without localization failure and releasing space by deleting the old map from storage. Note that the map used for the distribution test had a size of 267 MB. This selection is brought on by Autoware's limit of loading PCD maps with a size up to 1 GB. The system becomes slower as the map size increases, an issue that can be resolved by improving hardware performance.

5.4.3 Evaluation

In this subsection, the system performance is evaluated from the following three aspects based on the results of field tests.

1) Optimized overlap length: As discussed in Section II, if the system is mobility-aware and has good knowledge of the network status (from real-time or experience data), we can optimize the length of overlaps while keeping the automated driving robust. Table 5.2 summarizes the results obtained from multiple measurements. The three velocities we have tested, i.e., 10 km/h, 20 km/h, and 30 km/h, follow the speed limit in the region. They are often regarded as the common velocities in urban areas. It is found that the average connection time ($t_1 = 0.941$ s, 1.052 s, 0.857 s) is almost the same regardless of the vehicle's velocity. Hence, the connection distance is simply proportional to their speed. The average download time (t_2) depends on the network performance, which needs to be jointly considered with the vehicle's speed to calculate the download distance. From the results, there is a clear trend that the optimized overlap length is increasing as the vehicle's speed rises, compared with which the increment of the minimum overlapping length ($\sigma_1 + \sigma_2$) is insignificant.

Table 5.2: Overlap optimization results.

Velocity (km/h)	Average Connection Distance (m)	Average Download Distance (m)	Optimized Length (m)
10	2.61	5.47	8.08 ± 0.74
20	5.84	10.50	16.34 ± 2.57
30	7.14	16.41	23.55 ± 4.54

2) Map distribution data rate: The IEEE 802.11ad/WiGig has good robustness against mobility impact [17]. Figure 5.7(a) presents the experimental data rates when the vehicle moves at 10 km/h, 20 km/h, and 30 km/h respectively. The average data rates at these velocities are all approximately equal to 1.1 Gbps. The velocity of 0 km/h means that the vehicle is stopped at the edge of RSU coverage to download the HD map where the data rate becomes relatively lower (565 Mbps on average). Theoretical data rates complying with IEEE 802.11ad/WiGig mmWave standard are also drawn in the figure. Since the MCS supported by the installed mmWave antennas is $[1, 9]$, the minimum data rate is supposed to be 350 Mbps, while the maximum data rate can reach 2.5 Gbps. Comparing theoretical values with the experimental results shows that even if there is a gap in the peak data rate, performance

has still far surpassed the legacy WLAN and traditional V2X technologies.

3) Map distribution latency: The previous study uses Wi-Fi for HD map distribution [81]. To highlight the superiority of mmWave, we compare three types of radio access technologies: 2.4 GHz Wi-Fi, 5 GHz Wi-Fi, and 60 GHz mmWave, in terms of map download latency from the RSU. The map used has a file size of 267 MB. Figure 5.7(b) shows the results. The 2.4 GHz Wi-Fi takes the longest time to finish downloading (around 24 s) and an improvement is observed in the performance of 5 GHz Wi-Fi, which shortens the time by about 5 s. But, in comparison to the two Wi-Fis, the 60 GHz mmWave has shown an overwhelming advantage. As in most of our trials, it can distribute the map within less than 2 seconds. Therefore, it is critical to apply mmWave. The more efficient the map distribution system becomes, the smoother and safer the automated driving will be.

5.5 Conclusion

With Het-SDVN, we can brighten a future where automated vehicles can perform safe and smooth end-to-end travel and enjoy HD map services with edge/cloud connectivity and resource orchestration. Before that, two questions are waiting to be answered: 1) how to make appropriate map partitions under storage limitations and safety constraints, and 2) how to facilitate map distribution with state-of-the-art communication technologies? For the former, this chapter investigated two key factors in map partition and proposed an adaptive strategy to retain an optimized overlap for successful localization at the boundary between maps. As for the latter, this chapter introduced mmWave to the map distribution system and presented our implementation process. This system successfully delivered the required HD map to the vehicle in field trials. The experimental results revealed that the effectiveness of our overlap optimization becomes more significant as the vehicle's velocity increases. It was also proved that mmWave has overwhelming advantages in map distribution (data rate over 1 Gbps, and latency of less than 2 s for a map of 267 MB) versus legacy Wi-Fi and traditional V2X technologies. Future efforts on this topic will focus on improving the scalability of this map distribution system, for which experiments will be carried out with diverse vehicle densities, at higher vehicle velocities, and in various ITS environments (e.g., RSU layout).

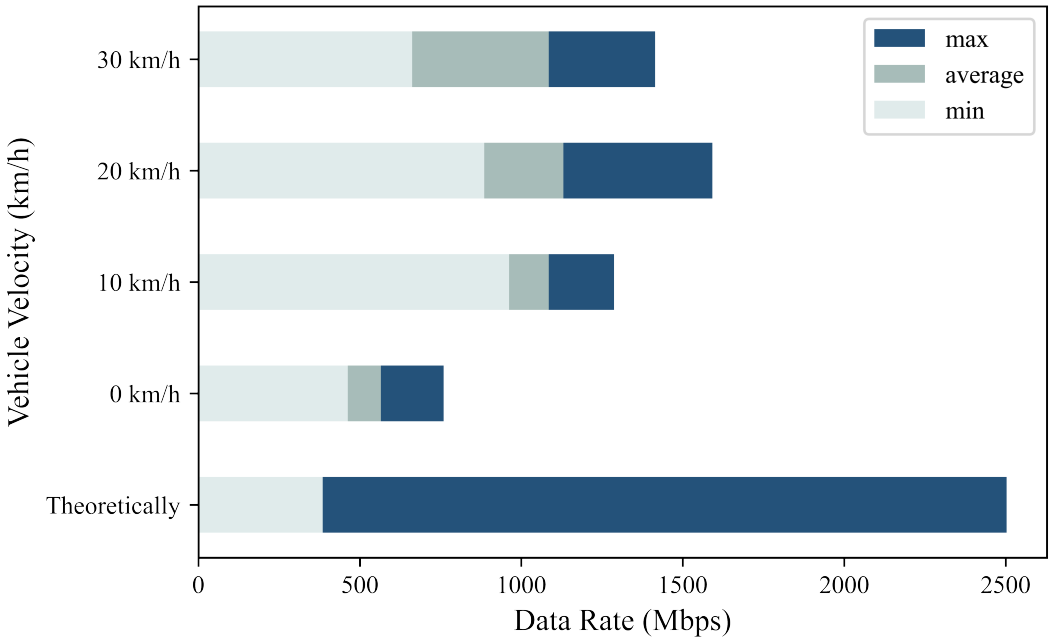

(a) Experimental data rate (mmWave) v.s. vehicle velocity

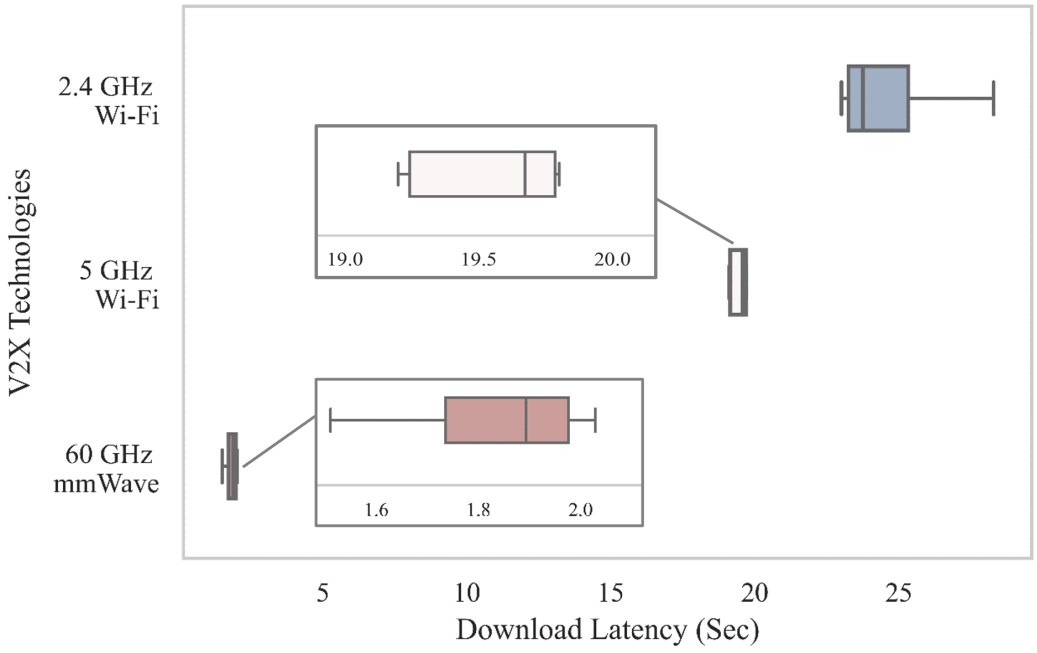

(b) Comparison of map download latency v.s. legacy Wi-Fi

Figure 5.7: Evaluation results of mmWave map distribution system.

Chapter 6

Final Remarks and Future Work

6.1 Summary of the thesis

- Chapter 1: It highlighted the significance of V2X in ITS and automated driving and showcased advanced V2X applications that have not yet been commercialized. After revealing the research target "cooperative perception", it underscored the limitations of existing V2X technologies and current vehicular networks. At the end, it summarized the author's efforts and contributions towards the research target.

- Chapter 2: It provided a comprehensive overview about cooperative perception including the classification and fusion techniques. It presented an in-depth discussion on data type selection for cooperative perception, emphasizing the values of raw data sharing. In the second part, it introduced the concept and principles of SDN, showing the great benefits that SDN can potentially bring to the vehicular network. Finally, it pointed out the challenges ahead of the successful transition from SDN to SDVN.

- Chapter 3: It discussed the required performances for the enhanced vehicular network in order to achieve safe automated driving. Based on the discussion, a software-defined dynamic mmWave V2X network was proposed for cooperative perception. Then, it established prototype systems with commercialized hardware equipment and open-sourced software frameworks for indoor and outdoor proofs of concept (PoCs). In the indoor PoC, the two modes of software-defined cooperative perception were implemented over mmWave V2V/V2I communications, showing that the indoor prototype system can achieve the network functions of the proposed architecture. By replacing some equip-

ment, the outdoor PoC was carried out in a real road environment. Under the dynamic management of SDN controller, the cooperative perception, which distributed raw LiDAR pointcloud data from RSUs to the vehicle over mmWave in a U-bend turning scenario, was realized. These PoCs verified mmWave performance, the feasibility of the proposed network architecture, and the safety benefit of cooperative perception.

- Chapter 4: In order to effectively support various types of cooperative perception (CP) and ensure this safety-critical V2X application is deliverable to vehicles anywhere and anytime, it proposed Het-SDVN, an SDN-based V2X network architecture, consisting of hierarchical C-planes, geographically distributed but logically centralized sub-SDVNs, and heterogeneous V2X. The network roles were clearly defined. For CP in local SDVNs, communications are orchestrated by RSUs with local SDVN controllers; for CP in other SDVNs or infrastructure-rare regions, communications for crossing sub-SDVNs are orchestrated by global SDVN controllers at MEC/Cloud servers. To empower the RSUs with SDVN functions, it presented a framework that integrates ROS, Ryu, and OVS and adds customized functional components for application, network, and sensor management. This framework was deployed and tested, showing that a maximum power saving ratio of 60% was achieved with the CAM-triggered sensor ON/OFF strategy, and the delay for CP preparation was less than 30 ms. Eventually, the holistic Het-SDVN was set up in Tokyo Institute of Technology, and its support for CP has been demonstrated via a proof of concept. Evaluation results validated the feasibility of Wi-Fi as local C-planes and stressed the importance of mmWave and the necessity of interference management when performing raw sensor data sharing. Moreover, no significant difference in flow installation performance was observed between the local and global SDVN controllers over different networks. They were all under 3 ms, showing the potential to meet the latency requirement (less than 10 ms) of advanced V2X applications [7].

- Chapter 5: It created a new service of HD map distribution for future fully automated vehicles by taking advantage of the designed Het-SDVN architecture. With the global C-plane, the map distribution was mobility-aware, and the HD map could be properly partitioned to optimize the size of overlap. To facilitate the map distribution, according to the vehicle position, the partitioned map was cached to the nearest RSU and then downloaded by the vehicle through the mmWave V2X network. The field trial showed that the vehicle, MEC/Cloud server, and RSUs formed an interactive and collaborative

system that successfully delivered the demanded map to the vehicle without disturbing its localization. This implementation also demonstrated the capability of the proposed Het-SDVN to foster novel V2X applications other than cooperative perception.

Moreover, the unique contributions and added values of Chapter 3 and Chapter 4 works, compared to the existing SDVN implementation and cooperative perception studies, can be showcased through Table 6.1 and Table 6.2.

Table 6.1: Comparisons with existing SDVN implementation studies.

State of the art	Ref. [113]	Ref. [28]	Ref. [29]	Ref. [30]	**Chapter 3**	**Chapter 4**
Architecture	Fully centralized	Fully centralized	Fully centralized	Hierarchical	Fully centralized	Hierarchical
D-plane RAT	IEEE 802.11p	LTE & Wi-Fi	Wi-Fi	Wi-Fi	WiGig	WiGig & Wi-Fi
Target V2X service	Basic [12]	Basic [12]	Basic [12]	Basic [12]	Advanced [7]	Advanced & Basic [12,7]
Controller function	Load balance	RAT & Mobility mgmt.	Access mgmt.	Mobility mgmt.	Context, access, routing mgmt.	Context, access, routing, RAT mgmt.
Evaluation method	Small-scale emulation	Small-scale emulation	Small-scale testbed	Small-scale testbed	Large-scale test field	Large-scale test field
Tool	NS-3 SUMO	Mininet-WiFi	Raspberry Pi	Zodiac FX	Vehicles & RSUs	Vehicles & RSUs

Table 6.2: Comparisons with existing cooperative perception studies.

State of the art	Ref. [114]	Ref. [90]	Ref. [85]	Ref. [86]	**Chapter 3**	**Chapter 4**
Data type	Objects	Objects	Features	Point clouds	Point clouds	Point clouds & Objects
Data rate requirement	Low	Low	Middle	High	High	High
Implemented RAT	IEEE 802.11p	IEEE 802.11p	WiGig	N/A	WiGig	WiGig & Wi-Fi
Transmission mode	Broadcast	Broadcast	Broadcast	N/A	Relay	Relay & Broadcast
Communication method	V2I	V2I	V2V	N/A	V2I & V2N	V2V, V2I, V2N
Network controller	None	None	None	None	SDVN controller	SDVN controller
Contribution	System	Fusion	Fusion	Detection	System & Network solution	System & Network solution

6.2 Suggested future works

In the future, large-scale simulations and evaluations are needed to fill in the remaining gaps between the proposals and experiments. Moreover, the proposed systems and technologies have the potential to make significant contributions to several promising fields. We plan to make some explorations in the following fields.

6.2.1 Het-SDVN for construction of mobility digital twin

Digital twin (DT) is considered a key application of beyond 5G and 6G. Constructing a mobility DT needs to collect a huge amount of sensing information from the massive sensors distributed in the environment to the DT server located at MEC/Cloud. It is similar to the requirement of cooperative perception, which collects the sensing data to the vehicle. Hence, the proposed Het-SDVN provides flexibility and programmability for establishing various mobility DT, including car sharing, smart intersections, etc. In addition to the radio resource management we mainly focused on in Chapter 3 and 4, the capability of SDVN controllers can be further extended to manage the computing and storage resources distributed in the vehicular network. For instance, to quickly construct a mobility DT and provide the DT service, the global SDVN controller in Het-SDVN can select an edge server to host the DT, and then work with local SDVN controllers to route the required sensing data to that server.

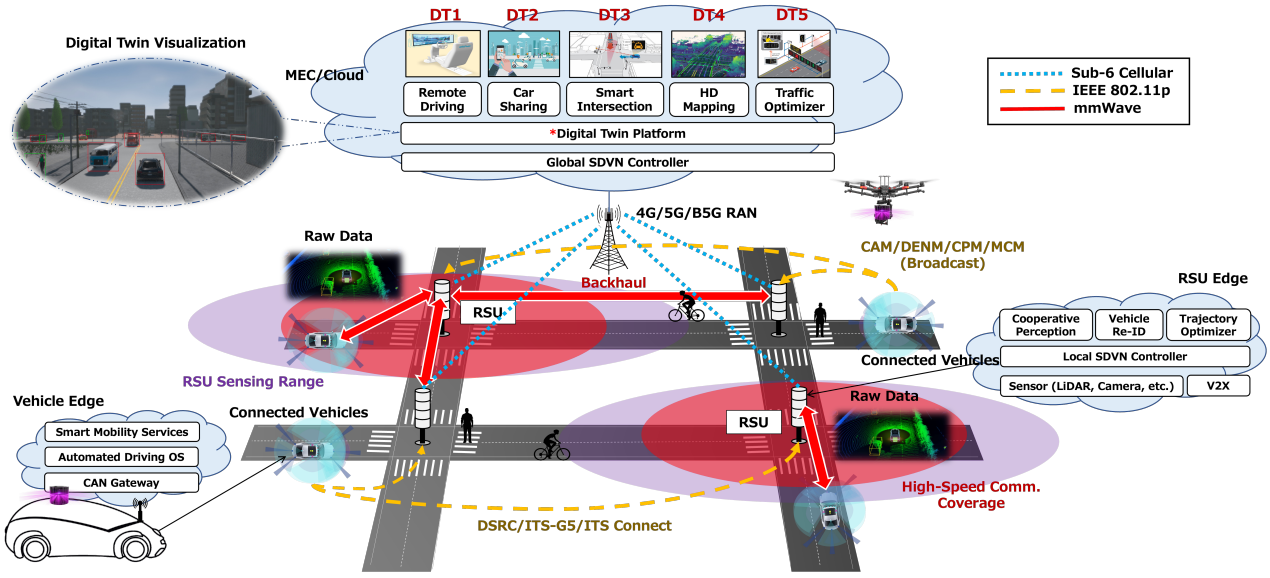

Figure 6.1: Het-SDVN for constructing mobility digital twins.

6.2.2 Het-SDVN for scalable and dynamic HD map distribution

In Chapter 5, we demonstrated the application of mobility-aware HD map distribution in the Het-SDVN. Although the mmWave V2I achieved ultra-fast map delivery from the RSU to the vehicle and ensured the vehicle's stable localization, however, if the vehicle number continuously increases, the allocated bandwidth for each vehicle will reduce, resulting in a

higher HD map download latency and affecting the localization performance. To overcome this challenge, we will investigate the clustering strategy for vehicles that request the same map. We will also need to select the optimal vehicle in the cluster as the head, to receive the HD map from the RSU first, then distribute the map within the cluster via mmWave V2V communications, as shown in Fig. 6.2. The clustering function can be deployed at the Het-SDVN local C-plane. We can also study other issues that relate to this HD map distribution system, such as inter-vehicle interference control, RAT handover, etc.

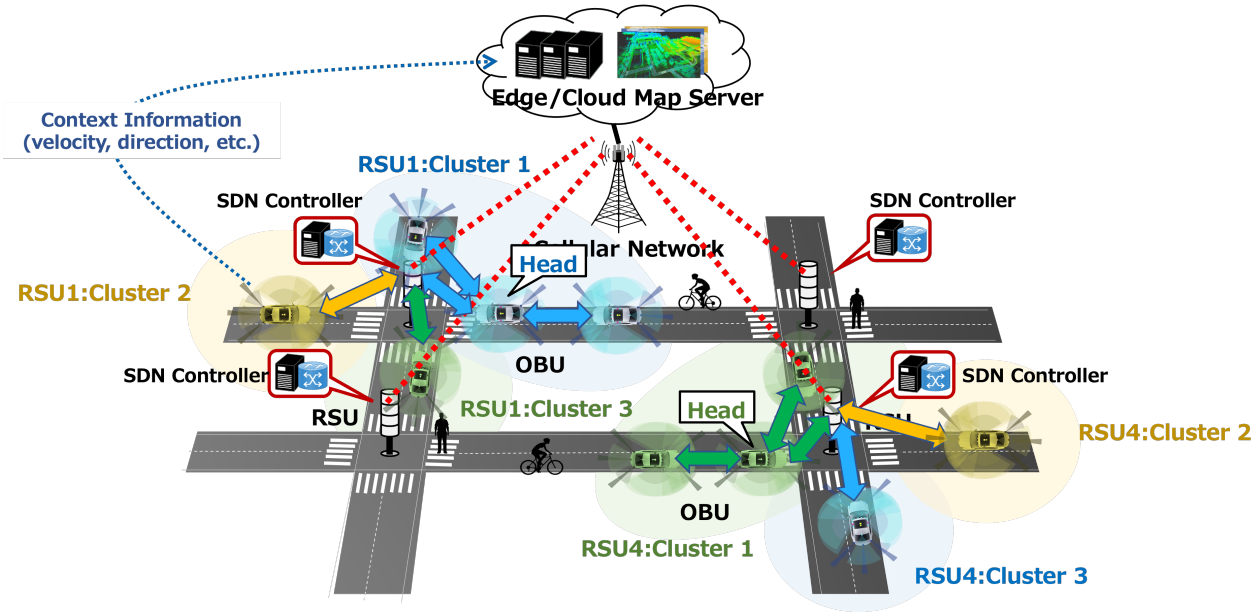

Figure 6.2: Het-SDVN-based HD map distribution system.

6.2.3 Path planning assisted by cooperative perception

With the proposed Het-SDVN, cooperative perception can be extensively supported. As we indicated in Sect. 1.2, many other applications will benefit from the cooperative perception data. Figure 6.3 shows our imagined future path-planning system. The vehicle's path planning consists of two phases: global path planning and local path planning. Before the global path planning, with the help of the global SDVN controller, the detected traffic of RSUs can be sent to the vehicle in the form of CPM for analysis and generating an optimal route. When the vehicle performs local planning in a sub-SDVN network, the local SDVN controller can coordinate the transmission of raw sensor data for fine-grained maneuvering and trajectory

control. It will increase the safety and efficiency of traditional path planning without V2X information. Proofs of concept should be conducted to demonstrate this system.

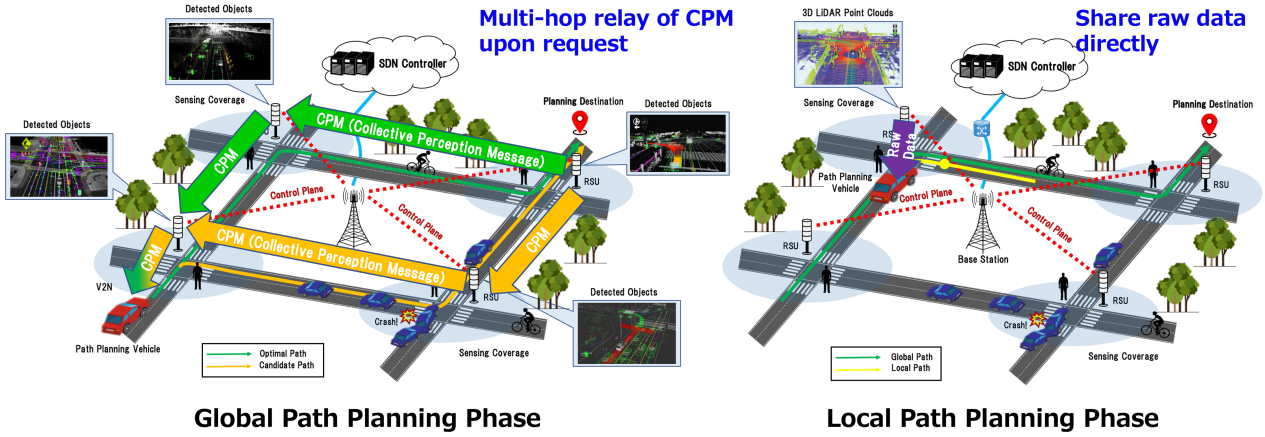

Figure 6.3: Cooperative perception-assisted path planning system.

Appendix I

List of Publications

I.1 Journal papers

- Z. Li, T. Yu, R. Fukatsu, G. K. Tran and K. Sakaguchi, "Towards Safe Automated Driving: Design of Software-Defined Dynamic MmWave V2X Networks and PoC Implementation," in IEEE Open Journal of Vehicular Technology, vol. 2, pp. 78-93, 2021.
- Z. Li, K. Wang, T. Yu and K. Sakaguchi, "Het-SDVN: SDN-Based Radio Resource Management of Heterogeneous V2X for Cooperative Perception," in IEEE Access, vol. 11, pp. 76255-76268, 2023.

I.2 Journal papers not related to this thesis

- J. Nakazato, M. Nakamura, T. Yu, Z. Li, K. Maruta, G. K. Tran and K. Sakaguchi, "Market Analysis of MEC-Assisted Beyond 5G Ecosystem," in IEEE Access, vol. 9, pp. 53996-54008, 2021.
- Y. Yin, H. Chen, Z. Li, T. Yu and K. Sakaguchi. "ZigZag Antenna Configuration for MmWave V2V with Relay in Typical Road Scenarios: Design, Analysis and Experiment." IEICE Transactions on Communications, vol. E104-B, no.10, pp.1307-1317, Oct. 2021.
- J. Nakazato, Z. Li, K. Maruta, K. Kubota, T. Yu, G. K. Tran, K. Sakaguchi and S. Masuko. “MEC/Cloud Orchestrator to Facilitate Private/Local Beyond 5G with MEC and Proof-of-Concept Implementation,” MPDI Sensors, Vol. 22, No. 14, July 2022.

I.3 International conferences

- Z. Li, T. Yu, R. Fukatsu, G. K. Tran and K. Sakaguchi, "Proof-of-Concept of a SDN Based mmWave V2X Network for Safe Automated Driving," 2019 IEEE Global Communications Conference (GLOBECOM), Waikoloa, HI, USA, pp. 1-6, 2019.
- Z. Li, M. L. R. Lagahit, M. Matsuoka and K. Sakaguchi, "Design of Mobility-Aware Map Partition and Distribution System for Smooth Automated Driving," 2022 IEEE 33rd Annual International Symposium on Personal, Indoor and Mobile Radio Communications (PIMRC), Kyoto, Japan, pp. 628-634, 2022.
- Z. Li, T. Yu, T. Suzuki and K. Sakaguchi, "Building an SDVN Framework for RSU-Centric Cooperative Perception with Heterogeneous V2X," 2023 IEEE 20th Consumer Communications & Networking Conference (CCNC), Las Vegas, NV, USA, pp. 1-7, 2023.

I.4 International conferences not related to this thesis

- J. Nakazato, M. Nakamura, T. Yu, Z. Li, G. K. Tran and K. Sakaguchi, "Design of MEC 5G Cellular Networks: Viewpoints from Telecom Operators and Backhaul Owners," 2020 IEEE International Conference on Communications Workshops (ICC Workshops), Dublin, Ireland, pp. 1-6, 2020.
- Y. Yin, H. Chen, Z. Li, R. Fukatsu, T. Yu and K. Sakaguchi, "Design of Antenna Configuration for Interference Control in MmWave V2V Communication Systems," 2020 IEEE 92nd Vehicular Technology Conference (VTC2020-Fall), Victoria, BC, Canada, pp. 1-5, 2020.
- K. Maruta, M. Takizawa, R. Fukatsu, Y. Wang, Z. Li and K. Sakaguchi, "Blind-Spot Visualization via AR Glasses using Millimeter-Wave V2X for Safe Driving," 2021 IEEE 94th Vehicular Technology Conference (VTC2021-Fall), Norman, OK, USA, pp. 1-5, 2021.
- K. Wang, Z. Li, T. Yu and K. Sakaguchi, "Smart Mobility Digital Twin for Automated Driving: Design and Proof-of-Concept," 2023 IEEE 97th Vehicular Technology Conference (VTC2023-Spring), Florence, Italy, pp. 1-6, 2023.

- M. L. R. Lagahit, Z. Li, K. Sakaguchi and and M. Matsuoka, "Exploring Ground Segmentation From LiDAR Scanning-Derived Images Using Convolutional Neural Networks," Int. Arch. Photogramm. Remote Sens. Spatial Inf. Sci., XLVIII-1/W1-2023, 221–226, 2023.

I.5 Domestic conferences

- J. Nakazato, M. Nakamura, T. Yu, Z. Li, G. K. Tran and K. Sakaguchi, “Design of MEC Cellular Networks: Viewpoints from Telecom Operator and Backhaul Owner,” IEICE RCS Technical Report, Dec. 2019.
- J. Nakazato, Z. Li, K. Maruta and K. Sakaguchi, “Viewpoint from Local Telecom Operators and Cloud Owners,” IEICE Technical Report, RCS, Mar. 2021.
- Z. Li, T. Yu, T. Suzuki and K. Sakaguchi, "Building an SDVN Framework for RSU-Centric Cooperative Perception with Heterogeneous V2X," 2023 RCS Mobile Communication Workshop, pp. 1-7, Mar. 2023.

Appendix II

Abbreviations

3GPP	3rd Generation Partnership Project
IEEE	Institute of Electrical and Electronics Engineers
ETSI	European Telecommunications Standards Institute
SAE	Society of Automotive Engineers
ISO	International Organization for Standardization
ITS	Intelligent Transportation System
ONF	Open Network Foundation
EEBL	Electronic Emergency Brake Light
FCW	Foward Collision Warning
BSW/LCW	Blind Spot Warning/Lane Change Warning
GLOSA	Green Light Optimal Speed Advisory
EVW	Emergency Vehicle Warning
VNFP	Vehicle Near-Field Payment
ETC	Electronic Toll collection
IVI	In-Vehicle Infotainment
V2X	Vehicle-to-Everything Communication
V2V	Vehicle-to-Vehicle Communication
V2I	Vehicle-to-Infrastructure Communication
V2P	Vehicle-to-Pedestrian Communication
V2N	Vehicle-to-Network Communication
CDA	Cooperative Driving Automation
QoS	Quality of Service

CP	Cooperative Perception/Collective Perception
CAM	Cooperative Awareness Message
CPM	Collective Perception Message
DENM	Decentralized Environmental Notification Message
MCM	Maneuver Coordination Message
DSRC	Dedicated short-range communications
LTE	Long-Term Evolution
NR	New Radio
mmWave	Millimeter Wave
THz	Terahertz
VLC	Visible Light Communication
WAVE	Wireless Access in Vehicular Environments
MIMO	Multiple-Input and Multiple-Output
OFDM	Orthogonal Frequency Division Multiplexing
OCB	Outside of the Context of BS
EDCA	Enhanced Distributed Channel Access
HARQ	Hybrid Automatic Repeat Request
LDPC	Low-Density Parity-Check
VRU	Vulnerable Road User
RSU	Roadside Unit
OBU	Onboard Unit
CAV	Connected and Automated Vehicle
VANET	Vehicular Ad-Hoc Network
C-V2X	Cellular Vehicle-to-Everything Communication
SDN	Software Defined Networking
SDWN/SWMN	Software Defined Wireless Network/Software Defined Mobile Network
SDVN	Software Defined Vehicular Network
C-plane	Control Plane
D-plane	D-Plane
NBI	Northbound Interface
SBI	Southbound Interface
WBI/EBI	Westbound Interface/Eastbound Interface
MEC	Multi-Access Edge Computing

NFV	Network Functions Virtualization
RAT	Radio Access Technology
RAN	Radio Access Network
RRM	Radio Resource Management
GNSS	Global Navigation Satellite System
GPS	Global Positioning System
IMU	Inertial Measurement Unit
LiDAR	Light Detection and Ranging
FoV	Field of View
LOS/NLOS	Line-Of-Sight/Non-Line-Of-Sight
RSSI	Radio Signal Strength Indicator
RTT	Round-Trip Time
TCP	Transmission Control Protocol
UDP	User Datagram Protocol
HTTP	Hypertext Transfer Protocol
PoC	Proof of Concept
COTS	Commercial Off-The-Shelf
ROS	Robot Operating System
OVS	Open Virtual Switch
ODL	OpenDaylight
SLAM	Simultaneous Localization and Mapping
NDT	Normal Distributions Transform
HD	High Definition
WLAN	Wireless Local Area Network
DT	Digital Twin

References

[1] SAE J3016. Taxonomy and Definitions for Terms Related to On-Road Motor Vehicle Automated Driving Systems. Jun. 2018.

[2] SAE J3216. Taxonomy and Definitions for Terms Related to Cooperative Driving Automation for On-Road Motor Vehicles. Jul. 2021.

[3] ETSI TR 103-562 (V2.1.1). Intelligent Transport Systems (ITS); Vehicular Communications; Basic Set of Applications; Analysis of the Collective Perception Service (CPS); Release 2, Dec. 2019.

[4] Manabu Tsukada, Takaharu Oi, Akihide Ito, Mai Hirata, and Hiroshi Esaki. AutoC2X: Open-source software to realize V2X cooperative perception among autonomous vehicles. In *2020 IEEE 92nd Vehicular Technology Conference (VTC2020-Fall)*, pp. 1–6, 2020.

[5] RS-LiDAR-32 User Manual. `https://www.robosense.ai/en/rslidar/RS-LiDAR-32`.

[6] SSS Promotion Consortium. `https://www.sss.e.titech.ac.jp/`.

[7] 3GPP TR 22.886 (V16.2.0). Study on enhancement of 3GPP support for 5G V2X services, Dec. 2018.

[8] ISO/TC 204. ITS Standardization Activities of ISO/TC 204, Oct. 2019.

[9] SAE J2945/1. On-Board Minimum Performance Requirements for V2V Safety Systems, Mar. 2016.

[10] China SAE T/China SAE 53-2017. Cooperative Intelligent Transportation System; Vehicular Communication; Application Layer Specification and Data Exchange Standard, Sept. 2017.

[11] ETSI TR 102 638 (V1.1.1). Intelligent Transport Systems (ITS); Vehicular Communications; Basic Set of Applications; Definitions, Jun. 2009.

[12] 3GPP TR 22.885 (V14.0.0). Study on LTE support for Vehicle-to-Everything (V2X) services, Dec. 2015.

[13] ETSI TR 103 578 (0.0.12 Draft). Intelligent Transport Systems (ITS); Vehicular Communications; Basic Set of Applications; Definitions, Jun. 2023.

[14] ETSI TS 103 324 (V2.1.1). Intelligent Transport System (ITS); Vehicular Communications; Basic Set of Applications; Collective Perception Service; Release 2, Jun. 2023.

[15] ETSI TS 102 637-2 (V1.2.1). Intelligent Transport Systems (ITS); Vehicular Communications; Basic Set of Applications; Part 2: Specification of Cooperative Awareness Basic Service, Mar. 2011.

[16] ETSI TS 102 637-3 (V1.1.1). Intelligent Transport Systems (ITS); Vehicular Communications; Basic Set of Applications; Part 3: Specifications of Decentralized Environmental Notification Basic Service, Sept. 2010.

[17] Kei Sakaguchi, Ryuichi Fukatsu, Tao Yu, Eisuke Fukuda, Kim Mahler, Robert Heath, Takeo Fujii, Kazuaki Takahashi, Alexey Khoryaev, Satoshi Nagata, and Takayuki Shimizu. Towards mmWave V2X in 5G and Beyond to Support Automated Driving. *IEICE Transactions on Communications*, Vol. advpub, p. 2020EBI0001, 2020.

[18] Kazuki Maruta, Miyuu Takizawa, Ryuichi Fukatsu, Yue Wang, Zongdian Li, and Kei Sakaguchi. Blind-Spot Visualization via AR Glasses using Millimeter-Wave V2X for Safe Driving. In *2021 IEEE 94th Vehicular Technology Conference (VTC2021-Fall)*, pp. 1–5, 2021.

[19] ETSI TS 102 636-4-2 (V1.4.1). Intelligent Transport Systems (ITS); Vehicular Communications; GeoNetworking; Part 4: Geographical addressing and forwarding for point-to-point and point-to-multipoint communications; Sub-part 2: Media-dependent functionalities for ITS-G5, Feb. 2021.

[20] Ryuichi Fukatsu and Kei Sakaguchi. Automated Driving with Cooperative Perception Using Millimeter-Wave V2V Communications for Safe Overtaking. *Sensors*, Vol. 21, No. 8, 2021.

[21] Ryuichi Fukatsu and Kei Sakaguchi. Automated Driving with Cooperative Perception Based on CVFH and Millimeter-Wave V2I Communications for Safe and Efficient Passing through Intersections. *Sensors*, Vol. 21, No. 17, 2021.

[22] Song Wang, Jingqi Huang, and Xinyu Zhang. Demystifying Millimeter-Wave V2X: Towards Robust and Efficient Directional Connectivity under High Mobility. In *Proceedings of the 26th Annual International Conference on Mobile Computing and Networking*, MobiCom '20, New York, NY, USA, 2020. Association for Computing Machinery.

[23] Junhyeong Kim, You-Jun Choi, Gosan Noh, and Heesang Chung. On the feasibility of remote driving applications over mmwave 5g vehicular communications: Implementation and demonstration. *IEEE Transactions on Vehicular Technology*, Vol. 72, No. 2, pp. 2009–2023, 2023.

[24] Yue Yin, Tao Yu, Kazuki Maruta, and Kei Sakaguchi. Distributed and Scalable Radio Resource Management for mmWave V2V Relays towards Safe Automated Driving. *Sensors*, Vol. 22, No. 1, 2022.

[25] Nelson Cardona, Estefanía Coronado, Steven Latré, Roberto Riggio, and Johann M. Marquez-Barja. Software-Defined Vehicular Networking: Opportunities and Challenges. *IEEE Access*, Vol. 8, pp. 219971–219995, 2020.

[26] Xiaohu Ge, Zipeng Li, and Shikuan Li. 5G Software Defined Vehicular Networks. *IEEE Communications Magazine*, Vol. 55, No. 7, pp. 87–93, 2017.

[27] Zongjian He, Jiannong Cao, and Xuefeng Liu. SDVN: enabling rapid network innovation for heterogeneous vehicular communication. *IEEE Network*, Vol. 30, No. 4, pp. 10–15, 2016.

[28] Ramon Dos Reis Fontes, Claudia Campolo, Christian Esteve Rothenberg, and Antonella Molinaro. From Theory to Experimental Evaluation: Resource Management in Software-Defined Vehicular Networks. *IEEE Access*, Vol. 5, pp. 3069–3076, 2017.

[29] Gokhan Secinti, Berk Canberk, Trung Q. Duong, and Lei Shu. Software Defined Architecture for VANET: A Testbed Implementation with Wireless Access Management. *IEEE Communications Magazine*, Vol. 55, No. 7, pp. 135–141, 2017.

[30] Ousmane Sadio, Ibrahima Ngom, and Claude Lishou. Design and Prototyping of a Software Defined Vehicular Networking. *IEEE Transactions on Vehicular Technology*, Vol. 69, No. 1, pp. 842–850, 2020.

[31] Michael Aeberhard and Nico Kaempchen. High-level sensor data fusion architecture for vehicle surround environment perception. In *Proceedings of the 8th International Workshop on Intelligent Transportation*, pp. 1–6, Mar. 2011.

[32] Tomoya Kitazato, Manabu Tsukada, Hideya Ochiai, and Hiroshi Esaki. Proxy cooperative awareness message: an infrastructure-assisted V2V messaging. In *2016 Ninth International Conference on Mobile Computing and Ubiquitous Networking (ICMU)*, pp. 1–6, 2016.

[33] Qi Chen, Xu Ma, Sihai Tang, Jingda Guo, Qing Yang, and Song Fu. F-cooper: Feature based cooperative perception for autonomous vehicle edge computing system using 3d point clouds. In *Proceedings of the 4th ACM/IEEE Symposium on Edge Computing*, SEC '19, p. 88–100, New York, NY, USA, 2019. Association for Computing Machinery.

[34] Yue Hu, Shaoheng Fang, Zixing Lei, Yiqi Zhong, and Siheng Chen. Where2comm: Communication-Efficient Collaborative Perception via Spatial Confidence Maps. In *Neurips 2022*, pp. 1–6, Nov. 2022.

[35] Eduardo Arnold, Mehrdad Dianati, Robert de Temple, and Saber Fallah. Cooperative perception for 3d object detection in driving scenarios using infrastructure sensors. *IEEE Transactions on Intelligent Transportation Systems*, Vol. 23, No. 3, pp. 1852–1864, 2022.

[36] Xumiao Zhang, Anlan Zhang, Jiachen Sun, Xiao Zhu, Y. Ethan Guo, Feng Qian, and Z. Morley Mao. Emp: Edge-assisted multi-vehicle perception. MobiCom '21, p. 545–558, New York, NY, USA, 2021. Association for Computing Machinery.

[37] Seong-Woo Kim, Baoxing Qin, Zhuang Jie Chong, Xiaotong Shen, Wei Liu, Marcelo H. Ang, Emilio Frazzoli, and Daniela Rus. Multivehicle cooperative driving using cooperative perception: Design and experimental validation. *IEEE Transactions on Intelligent Transportation Systems*, Vol. 16, No. 2, pp. 663–680, 2015.

[38] Nick McKeown, Tom Anderson, Hari Balakrishnan, Guru Parulkar, Larry Peterson, Jennifer Rexford, Scott Shenker, and Jonathan Turner. Openflow: Enabling innovation in campus networks. Vol. 38, No. 2, p. 69–74, mar 2008.

[39] Open Network Foundation (ONF). Software-Defined Networking: The New Norm for Networks, Apr. 2012.

[40] Salvatore Costanzo, Laura Galluccio, Giacomo Morabito, and Sergio Palazzo. Software defined wireless networks: Unbridling sdns. In *2012 European Workshop on Software Defined Networking*, pp. 1–6, 2012.

[41] Tao Chen, Marja Matinmikko, Xianfu Chen, Xuan Zhou, and Petri Ahokangas. Software defined mobile networks: concept, survey, and research directions. *IEEE Communications Magazine*, Vol. 53, No. 11, pp. 126–133, 2015.

[42] Gia Khanh Tran, Ricardo Santos, Hiroaki Ogawa, Makoto Nakamura, Kei Sakaguchi, and Andreas Kassler. Context-based dynamic meshed backhaul construction for 5g heterogeneous networks. *Journal of Sensor and Actuator Networks*, Vol. 7, No. 4, 2018.

[43] D. Wakabayashi. Self-Driving Uber Car Kills Pedestrian in Arizona, Where Robots Roam. *The New York Times*, Mar. 2018.

[44] Mate Boban, Apostolos Kousaridas, Konstantinos Manolakis, Josef Eichinger, and Wen Xu. Connected Roads of the Future: Use Cases, Requirements, and Design Considerations for Vehicle-to-Everything Communications. *IEEE Vehicular Technology Magazine*, Vol. 13, No. 3, pp. 110–123, 2018.

[45] Cisco. Cisco Visual Networking Index: Global Mobile Data Traffic Forecast Update, 2016-2021. White Paper, Feb. 2017.

[46] ETSI EN 302 663 (V1.2.0). Intelligent Transport Systems (ITS); Access layer specification for Intelligent Transport Systems operating in the 5 GHz frequency band, Nov. 2012.

[47] John B. Kenney. Dedicated Short-Range Communications (DSRC) Standards in the United States. *Proceedings of the IEEE*, Vol. 99, No. 7, pp. 1162–1182, 2011.

[48] 3GPP TR 21.914 (V14.0.0). Summary of Rel-14 Work Items: Vehicle-to-Everything (V2X) related item, May 2018.

[49] Elisabeth Uhlemann. Connected-Vehicles Applications Are Emerging [Connected Vehicles]. *IEEE Vehicular Technology Magazine*, Vol. 11, No. 1, pp. 25–96, 2016.

[50] Gaurang Naik, Biplav Choudhury, and Jung-Min Park. IEEE 802.11bd & 5G NR V2X: Evolution of Radio Access Technologies for V2X Communications. *IEEE Access*, Vol. 7, pp. 70169–70184, 2019.

[51] Ammara Anjum Khan, Mehran Abolhasan, and Wei Ni. 5G next generation VANETs using SDN and fog computing framework. In *2018 15th IEEE Annual Consumer Communications & Networking Conference (CCNC)*, pp. 1–6, 2018.

[52] Lionel Nkenyereye, Lewis Nkenyereye, S. M. Riazul Islam, Chaker Abdelaziz Kerrache, M. Abdullah-Al-Wadud, and Atif Alamri. Software Defined Network-Based Multi-Access Edge Framework for Vehicular Networks. *IEEE Access*, Vol. 8, pp. 4220–4234, 2020.

[53] Ramon R. Fontes, Samira Afzal, Samuel H. B. Brito, Mateus A. S. Santos, and Christian Esteve Rothenberg. Mininet-WiFi: Emulating software-defined wireless networks. In *2015 11th International Conference on Network and Service Management (CNSM)*, pp. 384–389, 2015.

[54] Heiko G. Seif and Xiaolong Hu. Autonomous Driving in the iCity—HD Maps as a Key Challenge of the Automotive Industry. *ELSEVIER, Engineering*, Vol. 2, No. 2, pp. 159–162, 2016.

[55] Ryuichi Fukatsu and Kei Sakaguchi. Millimeter-Wave V2V Communications with Cooperative Perception for Automated Driving. In *2019 IEEE 89th Vehicular Technology Conference (VTC2019-Spring)*, pp. 1–5, 2019.

[56] Swetank Kumar Saha, Hany Assasa, Adrian Loch, Naveen Muralidhar Prakash, Roshan Shyamsunder, Shivang Aggarwal, Daniel Steinmetzer, Dimitrios Koutsonikolas, Joerg Widmer, and Matthias Hollick. Fast and Infuriating: Performance and Pitfalls of 60 GHz WLANs Based on Consumer-Grade Hardware. In *2018 15th Annual IEEE International Conference on Sensing, Communication, and Networking (SECON)*, pp. 1–9, 2018.

[57] 3GPP TS 21.886 (V16.2.0). Enhancement of 3GPP support for V2X scenarios, Jun. 2019.

[58] Liehuang Zhu, Md M. Karim, Kashif Sharif, Chang Xu, Fan Li, Xiaojiang Du, and Mohsen Guizani. Sdn controllers: A comprehensive analysis and performance evaluation study. *ACM Comput. Surv.*, Vol. 53, No. 6, dec 2020.

[59] Md. Noor-A-Rahim, Zilong Liu, Haeyoung Lee, Mohammad Omar Khyam, Jianhua He, Dirk Pesch, Klaus Moessner, Walid Saad, and H. Vincent Poor. 6G for Vehicle-to-Everything (V2X) Communications: Enabling Technologies, Challenges, and Opportunities. *Proceedings of the IEEE*, Vol. 110, No. 6, pp. 712–734, 2022.

[60] Daniele Pirrone, Antonio Ferraro, Dimitrios C. Zografopoulos, Walter Fuscaldo, Pascal Szriftgiser, Guillaume Ducournau, and Romeo Beccherelli. Metasurface-Based Filters for High Data Rate THz Wireless Communication: Experimental Validation of a 14 Gbps OOK and 104 Gbps QAM-16 Wireless Link in the 300 GHz Band. *IEEE Transactions on Wireless Communications*, Vol. 21, No. 10, pp. 8688–8697, 2022.

[61] Yuki Goto, Isamu Takai, Takaya Yamazato, Hiraku Okada, Toshiaki Fujii, Shoji Kawahito, Shintaro Arai, Tomohiro Yendo, and Koji Kamakura. A New Automotive VLC System Using Optical Communication Image Sensor. *IEEE Photonics Journal*, Vol. 8, No. 3, pp. 1–17, 2016.

[62] Starlink Specifications - Mobile Service Plan. `https://www.starlink.com/legal/documents/DOC-1002-69942-69`.

[63] Cohda MK6 RSU. `https://www.cohdawireless.com/solutions/hardware/mk6-rsu/`.

[64] Moyukh Laha and Raja Datta. Intelligent On/Off Switching of mmRSUs in Urban Vehicular Networks: A Deep Q-Learning Approach. In *2022 National Conference on Communications (NCC)*, pp. 221–226, 2022.

[65] Buffalo WAPM-1266WDPR Specification. `https://www.buffalo.jp/product/detail/wapm-1266wdpr.html`.

[66] Sven Laux, Gurjashan Singh Pannu, Stefan Schneider, Jan Tiemann, Florian Klingler, Christoph Sommer, and Falko Dressler. Demo: OpenC2X — An open source experimental and prototyping platform supporting ETSI ITS-G5. In *2016 IEEE Vehicular Networking Conference (VNC)*, pp. 1–2, 2016.

[67] RoboCar MV2. https://www.zmp.co.jp/products/robocar/robocar-mv2.

[68] Autoware Fundation. https://www.autoware.org/.

[69] ROS2 Foxy. https://docs.ros.org/en/foxy/.

[70] Autoware Universe Document - lidar_centerpoint. https://autowarefoundation.github.io/autoware.universe/main/perception/lidar_centerpoint/.

[71] Ryu SDN Framework. https://ryu.readthedocs.io/en/latest/.

[72] Yue Yin, Haoze Chen, Zongdian Li, Tao Yu, and Kei Sakaguchi. Zigzag antenna configuration for mmWave v2v with relay in typical road scenarios: Design, analysis and experiment. *IEICE Transactions on Communications*, Vol. 104, pp. 1307–1317, 2021.

[73] James M. Anderson, Nidhi Kalra, Karlyn D. Stanley, Paul Sorensen, Constantine Samaras, and Tobi A. Oluwatola. *Autonomous Vehicle Technology: A Guide for Policymakers*. RAND Corporation, Santa Monica, CA, 2016.

[74] J. Tang and S. Liu. Edge High-Precise Map Service for Autonomous Driving. *ZTE Technology Journal*, Vol. 25, No. 3, Jun. 2019.

[75] Google Maps. https://cloud.google.com/.

[76] OpenStreetMap: Japan. https://download.geofabrik.de/asia/japan.html.

[77] Mario H. Castañeda Garcia, Alejandro Molina-Galan, Mate Boban, Javier Gozalvez, Baldomero Coll-Perales, Taylan Şahin, and Apostolos Kousaridas. A Tutorial on 5G NR V2X Communications. *IEEE Communications Surveys Tutorials*, Vol. 23, No. 3, pp. 1972–2026, 2021.

[78] Hideki Shimada, Akihiro Yamaguchi, Hiroaki Takada, and Kenya Sato. Implementation and Evaluation of Local Dynamic Map in Safety Driving Systems. *Journal of Transportation Technologies*, Vol. 5, pp. 102–112, 2015.

[79] Tomoya Kitazato, Manabu Tsukada, Hideya Ochiai, and Hiroshi Esaki. Proxy cooperative awareness message: an infrastructure-assisted V2V messaging. In *2016 Ninth International Conference on Mobile Computing and Ubiquitous Networking (ICMU)*, pp. 1–6, 2016.

[80] Radovan Miucic, Ashish Sheikh, Zeljko Medenica, and Raju Kunde. V2X Applications Using Collaborative Perception. In *2018 IEEE 88th Vehicular Technology Conference (VTC-Fall)*, pp. 1–6, 2018.

[81] Masaya Mizutani, Manabu Tsukada, Yuki Iida, and Hiroshi Esaki. 3D maps distribution of self-driving vehicles using roadside edges. In *2020 Eighth International Symposium on Computing and Networking Workshops (CANDARW)*, pp. 40–45, 2020.

[82] Makoto Nakamura, Hiroaki Nishiuchi, Jin Nakazato, Konstantin Koslowski, Julian Daube, Ricardo Santos, Gia Khanh Tran, and Kei Sakaguchi. Experimental Verification of SDN/NFV in Integrated mmWave Access and Mesh Backhaul Networks. *IEICE Transactions on Communications*, Vol. advpub, p. 2020NVP0002, 2020.

[83] IEEE Standard for Information technology–Telecommunications and information exchange between systems–Local and metropolitan area networks–Specific requirements-Part 11: Wireless LAN Medium Access Control (MAC) and Physical Layer (PHY) Specifications Amendment 3: Enhancements for Very High Throughput in the 60 GHz Band. *IEEE Std 802.11ad-2012 (Amendment to IEEE Std 802.11-2012, as amended by IEEE Std 802.11ae-2012 and IEEE Std 802.11aa-2012)*, pp. 1–628, 2012.

[84] IEEE Standard for Information Technology–Telecommunications and Information Exchange between Systems Local and Metropolitan Area Networks–Specific Requirements Part 11: Wireless LAN Medium Access Control (MAC) and Physical Layer (PHY) Specifications Amendment 2: Enhanced Throughput for Operation in License-exempt Bands above 45 GHz. *IEEE Std 802.11ay-2021 (Amendment to IEEE Std 802.11-2020 as amendment by IEEE Std 802.11ax-2021)*, pp. 1–768, 2021.

[85] Hang Qiu, Fawad Ahmad, Fan Bai, Marco Gruteser, and Ramesh Govindan. AVR: Augmented Vehicular Reality. MobiSys '18, p. 81–95, New York, NY, USA, 2018. Association for Computing Machinery.

[86] Q. Chen, S. Tang, Q. Yang, and S. Fu. Cooper: Cooperative Perception for Connected Autonomous Vehicles Based on 3D Point Clouds. In *2019 IEEE 39th International Conference on Distributed Computing Systems (ICDCS)*, pp. 514–524, Los Alamitos, CA, USA, Jun. 2019. IEEE Computer Society.

[87] Chang-Heng Wang, Takayuki Shimizu, Haritha Muralidharan, and Akihiko Yamamuro. Demo: A Real-Time High-Definition Vehicular Sensor Data Sharing System using Millimeter Wave V2V Communications. In *2020 IEEE Vehicular Networking Conference (VNC)*, pp. 1–2, 2020.

[88] Zongdian Li, Tao Yu, Ryuichi Fukatsu, Gia Khanh Tran, and Kei Sakaguchi. Towards Safe Automated Driving: Design of Software-Defined Dynamic MmWave V2X Networks and PoC Implementation. *IEEE Open Journal of Vehicular Technology*, Vol. 2, pp. 78–93, 2021.

[89] Eduardo Arnold, Mehrdad Dianati, Robert de Temple, and Saber Fallah. Cooperative Perception for 3D Object Detection in Driving Scenarios Using Infrastructure Sensors. *IEEE Transactions on Intelligent Transportation Systems*, Vol. 23, No. 3, pp. 1852–1864, 2022.

[90] Mao Shan, Karan Narula, Yung Fei Wong, Stewart Worrall, Malik Khan, Paul Alexander, and Eduardo Nebot. Demonstrations of Cooperative Perception: Safety and Robustness in Connected and Automated Vehicle Operations. *Sensors*, Vol. 21, No. 1, 2021.

[91] Xumiao Zhang, Anlan Zhang, Jiachen Sun, Xiao Zhu, Y. Ethan Guo, Feng Qian, and Z. Morley Mao. EMP: Edge-Assisted Multi-Vehicle Perception. In *Proceedings of the 27th Annual International Conference on Mobile Computing and Networking*, MobiCom '21, p. 545–558, New York, NY, USA, 2021. Association for Computing Machinery.

[92] Ericsson Network Lightpole Product (2017): "Ericsson Lightpole Site". `https://www.ericsson.com/en/portfolio/networks?nav=fgb_101_0561%7Cfgb_101_0516%7Cfgb_101_0526`.

[93] LuxTurrim5G project. `https://www.luxturrim5g.com/`.

[94] Amazon Web Services. `https://aws.amazon.com/`.

[95] Microsoft Azure. `https://azure.microsoft.com/`.

[96] Google Cloud. `https://cloud.google.com/`.

[97] Makoto Nakamura, Hiroaki Nishiuchi, Konstantin Koslowski, Julian Daube, Ricardo Santos, Gia Khanh Tran, and Kei Sakaguchi. Performance Evaluation of Prefetching Algorithm for Real-Time Edge Content Delivery in 5G System. In *2019 IEEE 90th Vehicular Technology Conference (VTC2019-Fall)*, pp. 1–5, 2019.

[98] Jun Zhang and Khaled B. Letaief. Mobile Edge Intelligence and Computing for the Internet of Vehicles. *Proceedings of the IEEE*, Vol. 108, No. 2, pp. 246–261, 2020.

[99] Huisheng Ma, Shufang Li, Erqing Zhang, Zhengnan Lv, Jing Hu, and Xinlei Wei. Cooperative Autonomous Driving Oriented MEC-Aided 5G-V2X: Prototype System Design, Field Tests and AI-Based Optimization Tools. *IEEE Access*, Vol. 8, pp. 54288–54302, 2020.

[100] Francesco Spinelli and Vincenzo Mancuso. Toward Enabled Industrial Verticals in 5G: A Survey on MEC-Based Approaches to Provisioning and Flexibility. *IEEE Communications Surveys Tutorials*, Vol. 23, No. 1, pp. 596–630, 2021.

[101] RoboCar MV2. `https://www.zmp.co.jp/products/robocar/robocar-mv2`.

[102] Tsukumo Model WA9J-H200/XT. `https://www.tsukumo.co.jp/bto/pc/workstation/2020/WA9J-H200XT.html`.

[103] Intel NUC 11 Pro. `https://www.intel.com/content/www/us/en/products/sku/205600/intel-nuc-11-pro-mini-pc-nuc11tnkv5/specifications.html`.

[104] Garmin GPS 18x USB. `https://www.garmin.com/en-US/p/27594`.

[105] RoboSense RS-LiDAR-32. `https://www.robosense.ai/en/rslidar/RS-LiDAR-32`.

[106] Autoware Fundation. `https://www.autoware.org/`.

[107] SQLite. `https://www.sqlite.org/index.html`.

[108] Docker. `https://www.docker.com/`.

[109] Python Flask. `https://flask.palletsprojects.com/`.

[110] HTTP servers. `https://docs.python.org/3/library/http.server.html`.

[111] Rohde & Schwarz. 802.11ad - WLAN at 60 GHz A Technology Introduction. *White Paper*, pp. 23–24, Nov. 2017.

[112] CloudCompare. `https://www.danielgm.net/cc/`.

[113] Guiyang Luo, Haibo Zhou, Nan Cheng, Quan Yuan, Jinglin Li, Fangchun Yang, and Xuemin Shen. Software-defined cooperative data sharing in edge computing assisted 5g-vanet. *IEEE Transactions on Mobile Computing*, Vol. 20, No. 3, pp. 1212–1229, 2021.

[114] Manabu Tsukada, Takaharu Oi, Masahiro Kitazawa, and Hiroshi Esaki. Networked roadside perception units for autonomous driving. *Sensors*, Vol. 20, No. 18, 2020.